March 10, 1965

To the Graduate Council:

I am submitting herewith a thesis written by James Ross Waggoner entitled "Stripping Rates of Carbon Dioxide from Water in Spray Type Liquid-Gas Contactors." I recommend that it be accepted for eighteen quarter hours of credit in partial fulfillment of the requirements of the degree of Master of Science, with a major in Chemical Engineering.

D M Pickett
Major Professor

We have read this thesis and
recommend its acceptance:

H Johnson

L. H. Turner

D C Bogue

Accepted for the Council:

Hilton A. Smith
Dean of the Graduate School

STRIPPING RATES OF CARBON DIOXIDE FROM WATER IN SPRAY TYPE LIQUID-GAS CONTACTORS

A Thesis

Presented to

the Graduate Council of

The University of Tennessee

In Partial Fulfillment

of the Requirements for the Degree

Master of Science

---

by

James Ross Waggoner

March 1965

ACKNOWLEDGEMENT

The author is grateful for the opportunity to continue his education toward a Master of Science degree made possible through assistantships presented by the Department of Chemical and Metallurgical Engineering and the Engineering Mechanics Department. Financial aid given by the Oak Ridge National Laboratory is also greatly appreciated.

Dr. F. N. Peebles, who supervised the research, gave invaluable assistance toward the solving of theoretical problems and the interpretation of experimental results and his effort is certainly admired and appreciated. The enthusiasm, patience and timely experimental suggestions offered by Earl Rosenbalm, together with his many superlative skills, were extremely helpful to the author. Experimental assistance given by personnel in the Chemical Engineering Shop and the University of Tennessee Experiment Station is also appreciated. Typing of the thesis was accomplished by Mrs. Sylvia Ross and her concern and work deserves a special note of appreciation.

The author extends a special thanks to his Mother and Father whose sharing of the financial burden and whose unceasing encouragement were most beneficial toward completing the required work.

ABSTRACT

Stripping rates of carbon dioxide from water with air were determined for two spray type liquid-gas contactors proposed for use at Oak Ridge National Laboratory in the Molten Salt Reactor Experiment pump bowl. Carbonated water was circulated through the spray chamber in the form of droplets flowing from one of two sprinkler heads and contacted with a sweep air stream until the stripping process reached air-water equilibrium.

The over-all liquid-phase stripping rate was defined from mathematical models, devised to represent the mass transfer conditions in the test equipment. The over-all stripping coefficient appeared as the parameter in theoretical equations relating carbon dioxide liquid concentration as a function of stripping time. Desired stripping coefficients were obtained by choosing the value of the parameter which gave the "best fit" of theoretical results to experimental liquid concentration data.

Experimental liquid concentration data were obtained using a ph technique that determined the amount of carbonic acid in the aqueous solution. Carbon dioxide concentrations in the exit gas stream were also measured using a thermal conductivity gas analyzer. No effort was made to analyze this data in a manner similar to the analysis of liquid data, since the theoretical gas concentration equations were essentially invariant with values of the stripping rate parameter.

Stripping rate coefficients were evaluated for both liquid-gas

contactors at liquid flow rates ranging from 15 GPM to 64 GPM and a sweep air flow rate of 3 CFM. The over-all liquid-phase coefficients ranged from 0.19 minutes^{-1} at the low liquid flow rate to 1.85 minutes^{-1} at the highest liquid flow rate. These results agree within 67 per cent of mass transfer coefficients obtained from similar investigations with packed towers reported in the literature.

A plot of reciprocal over-all stripping rate versus reciprocal liquid flow rate for both stripping systems revealed that each system was controlled by resistance in the liquid-phase.

Raschig rings were inserted into the spray chamber of one of the stripping systems in an attempt to increase stripping effectiveness. No beneficial effect on the rate of desorption was achieved for the conditions of this investigation.

TABLE OF CONTENTS

LIST OF TABLES

LIST OF FIGURES

FIGURE PAGE

FIGURE PAGE

CHAPTER I

INTRODUCTION

The Oak Ridge National Laboratory has instigated research at The University of Tennessee to better understand the dynamics of mass transfer operations involving radioactive gases dissolved in molten salts. In particular, mass transfer data were desired for desorption of xenon gas from a molten uranium fluoride solution with helium under liquid-gas contact conditions to be employed in the Molten Salt Reactor Experiment (MSRE) pump bowl.

To simulate reactor facilities a gas-liquid stripping system was constructed at Oak Ridge and transferred to the University. This system included a cylindrical Plexiglas reservoir and two stainless steel spray rings or sprinkler heads which, when mounted inside the reservoir with their respective network of baffles, constituted two different methods of liquid-gas contacting.

With the purpose in mind of later paralleling experimental results with actual reactor conditions, a carbon dioxide-air-water system was chosen for study. To objectively analyze experimental data on the effectiveness of each of the two methods of stripping, mathematical models were constructed to simulate mass transfer conditions. From these models mass transfer coefficients or, to be more descriptive, stripping rate coefficients were defined to provide a basis of comparison between the two experimental systems and to provide possible projection to actual

reactor conditions. Stripping rate values were determined by fitting experimental liquid concentration data with theoretical results derived from the mathematical models. The stripping coefficient was contained as a parameter in equations relating carbon dioxide liquid concentration as a function of stripping time, and a "best fit" of experimental results depended on the value of the parameter. The resulting stripping coefficients were put in a common form of presenting mass transfer data according to Foust (2), where the reciprocal over-all mass transfer rate is the sum of individual gas-phase and liquid-phase resistances. Previous work with carbon dioxide-air-water systems indicate that the liquid-phase resistance approximates the total resistance to mass transfer. Therefore, the over-all liquid-phase stripping coefficient was obtained as a function of liquid flow rate.

Other experimental objectives included breaking down the over-all liquid-phase mass transfer coefficient in an attempt to determine the individual liquid-phase and gas-phase coefficients. Substantiation of the theory of negligible gas-phase resistance for these carbon dioxide-air-water stripping systems was an added motive in this work.

Additional objectives include ways to increase stripping effectiveness which were brought to mind through an analysis of the dynamic behavior of the liquid and gas contained in the stripping tank. Physical parameters such as entrappment of gas bubbles in the liquid reservoir and stagnated gas volumes above the liquid have pronounced effect on stripping rates.

Experimentally, carbonated water contained in the Plexiglas reser-

voir was circulated through the spray ring mounted inside the tank, contacted with a sweep air stream and returned to the reservoir. Desorption of carbon dioxide from water was measured using a ph technique and carbon dioxide concentrations in the air stream after stripping were determined with a thermal conductivity gas analyzer.

Investigations were carried out at room temperature and atmospheric pressure with water flow rates ranging from 15 GPM. to 64 GPM. The sweep air flow rate was set at 3 CFM. at 70^{o}F. and one atmosphere pressure for stripping determinations. Stripping experiments were also undertaken at sweep air flow rates of 10 Liters/Min.

CHAPTER II

THEORY

I. MATHEMATICAL MODELS TO DESCRIBE GAS-LIQUID CONTACTORS

Figures 1 and 2 depict the essential features of the liquid-gas contactors investigated in this study. The stripping system shown in Figure 1 is identified as the "small spray ring" system and the contacting system in Figure 2 is referred to as the "large spray ring" system.

Two separate mathematical representations were needed to describe the response of these two spray chambers. Following are presentations of the theory employed in analysis of the experimental data obtained.

Mathematical Model for Small Spray Ring Contactor

An accurate analysis of any experimental system is largely dependent upon the selection of a mathematical model which best describes the system. To choose an appropriate model, one which fits the system but yet is not too complicated to give desired results, experimental work was carried out to learn how the stripping system behaved under certain dynamic conditions. Most attention was given to the behavior of the gas space above the water reservoir during stripping. This work was particularly important for an analysis of the small spray ring and its system of guide and splash baffles.

Due to the arrangement of baffles mounted under this spray ring, the outer gas pool, defined in Figure 1, was found to be a fairly stagnant gas space. Experimental results showed that 5.6 residence times

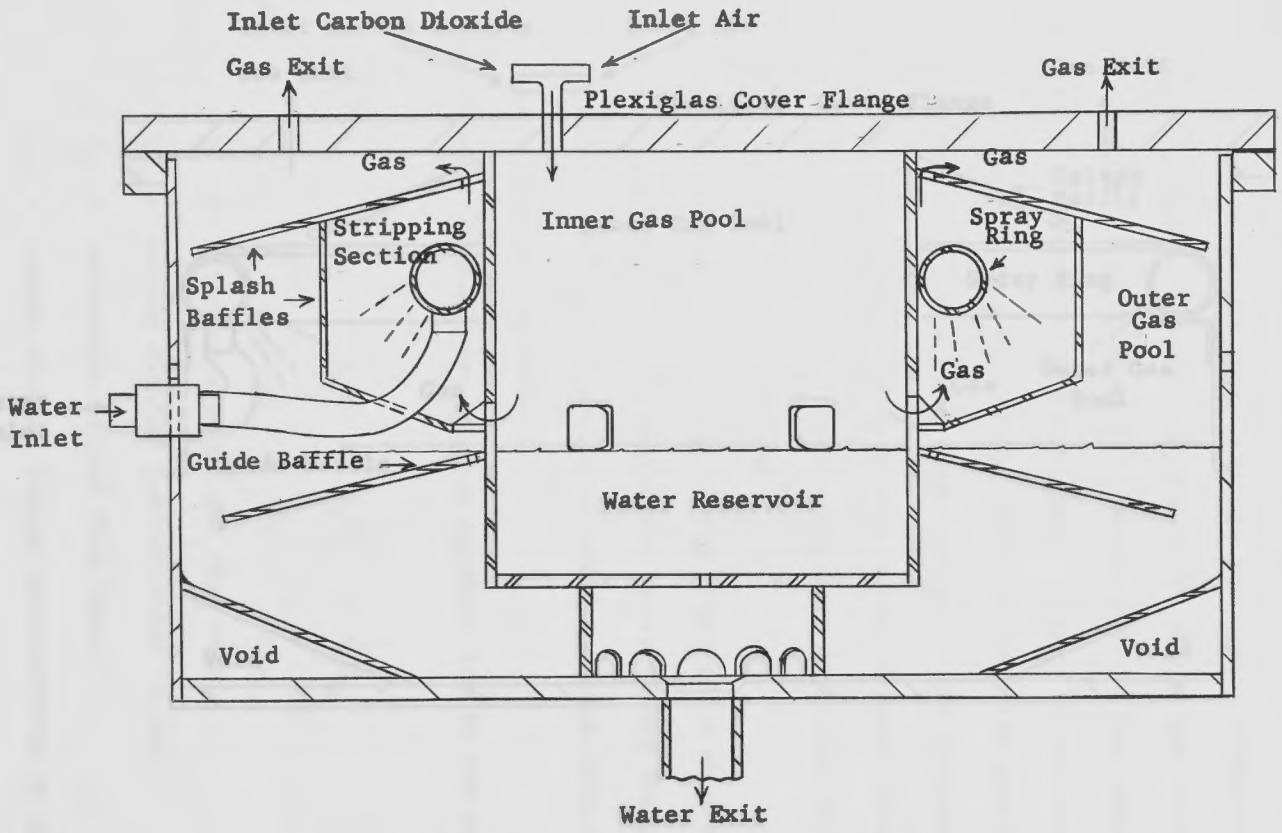

Figure 1. Splash Baffle and Guide Baffle Assembly for Small Spray Ring, in a Cross-Sectional View of the Storage Tank.

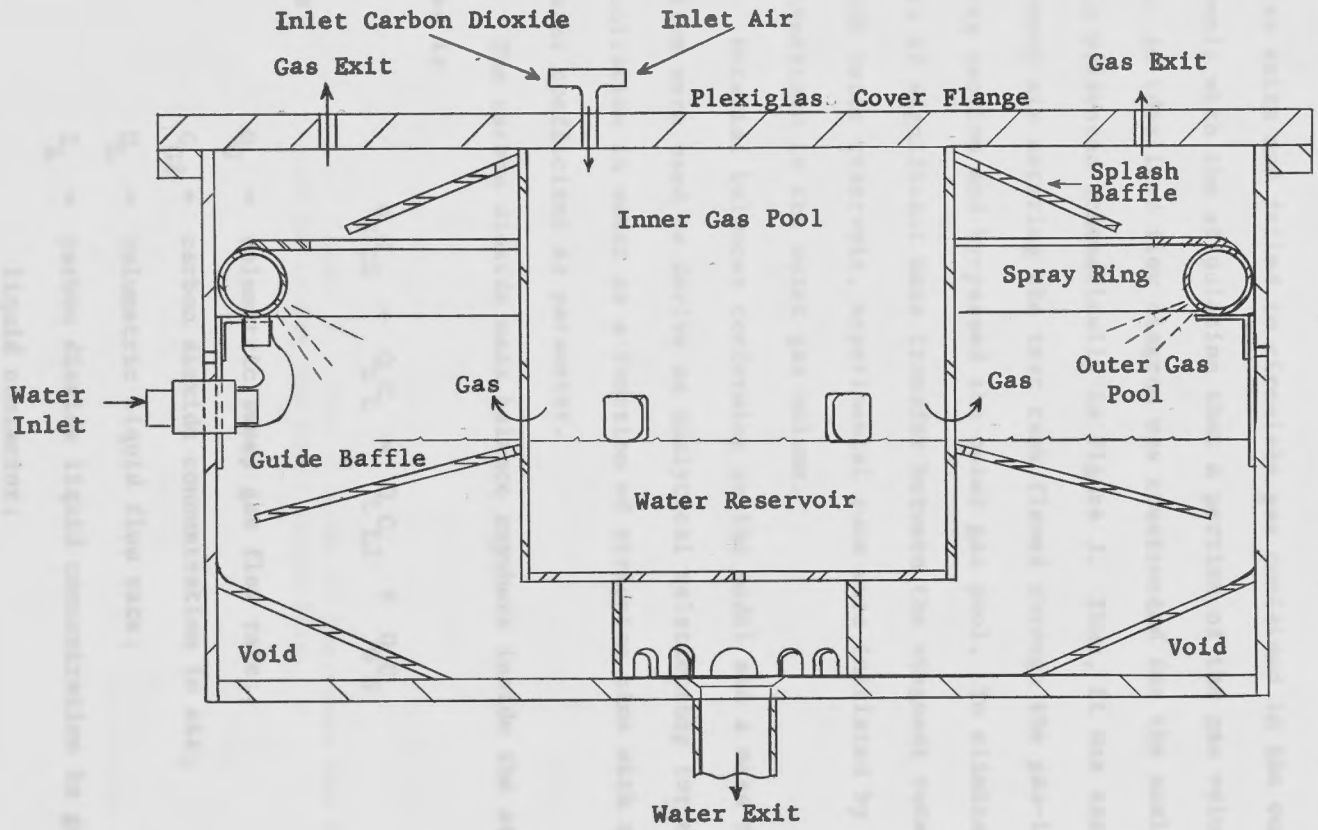

Figure 2. Splash Baffle and Guide Baffle Assembly for the Large Spray Ring in a Cross-Sectional View of the Storage Tank.

were required to displace carbon dioxide with air in this outer gas volume, a residence time being the volume divided by flow rate. Thus, a large fraction of the sweep air flowed through the stripping section to the gas exits and failed to circulate gas contained in the outer pool. To comply with the stipulation that a portion of the gas volume was stagnated, an idealized flow diagram was constructed for the small spray ring and is presented schematically in Figure 3. Thus, it was assumed that all sweep air entering the test tank flowed through the gas-liquid contacting section and by-passed the outer gas pool. To eliminate the possibility of significant mass transfer between the stagnant outer gas space and the water reservoir, experimental runs were initiated by having just air contained in the outer gas volume.

Material balances conforming to the model and a mass transfer rate equation were used to derive an analytical relationship for carbon dioxide concentration in water as a function of stripping time with the mass transfer coefficient as parameter.

The carbon dioxide mass balance anywhere inside the stripping system is

$$Q_G C_{G2} + Q_L C_L = Q_L C_{L2} + Q_G C_G \qquad (1)$$

where:

Q_G = volumetric sweep gas flow rate;

C_{G2} = carbon dioxide concentration in air;

Q_L = volumetric liquid flow rate;

C_L = carbon dioxide liquid concentration in gas-liquid contactor;

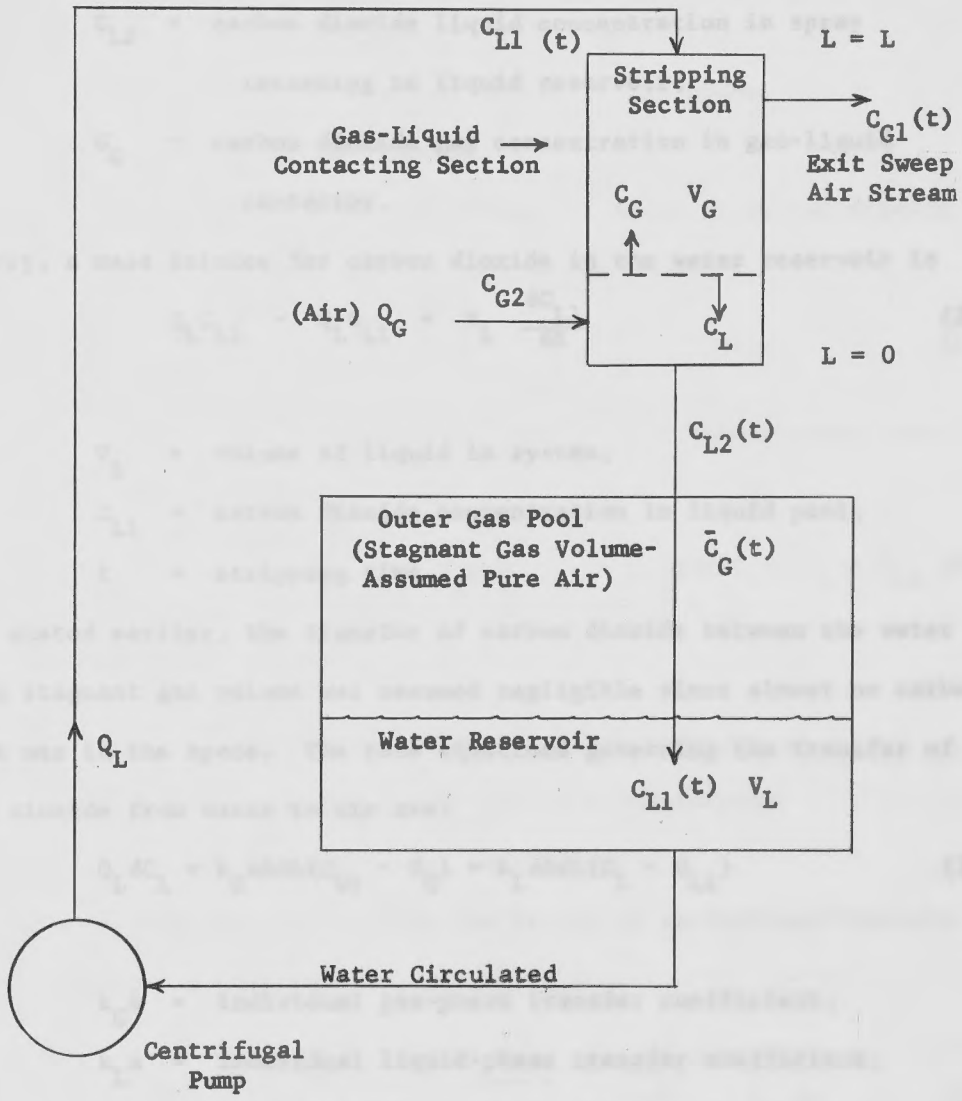

Figure 3. Flow Diagram to Represent the Stripping System Employing the Small Spray Ring.

C_{L2} = carbon dioxide liquid concentration in spray returning to liquid reservoir;

C_G = carbon dioxide gas concentration in gas-liquid contactor.

Similarly, a mass balance for carbon dioxide in the water reservoir is

$$Q_L C_{L2} - Q_L C_{L1} = V_L \frac{dC_{L1}}{dt} \quad (2)$$

where:

V_L = volume of liquid in system;

C_{L1} = carbon dioxide concentration in liquid pool;

t = stripping time.

As was stated earlier, the transfer of carbon dioxide between the water and the stagnant gas volume was assumed negligible since almost no carbon dioxide was in the space. The rate equations governing the transfer of carbon dioxide from water to air are:

$$Q_L dC_L = k_G aAdL(C_{Gi} - C_G) = k_L aAdL(C_L - C_{Li}) \quad (3)$$

where:

$k_G a$ = individual gas-phase transfer coefficient;

$k_L a$ = individual liquid-phase transfer coefficient;

C_{Gi}, C_{Li} = interfacial gas and liquid concentrations;

AdL = differential stripping volume.

At room temperature and atmospheric pressure Henry's law,

$$P = H C_L \quad (4)$$

provides the general phase-equilibrium relation which holds for dilute solutions of carbon dioxide in water (8),

where:

P = partial pressure of solute in gas-phase;

H = Henry's law constant.

Assuming the ideal gas law holds for dilute solutions of carbon dioxide in air and combining it with Henry's law, we can obtain :

$$C_{Gi} = \frac{H}{R\,T_{avg}}\, C_{Li} \quad . \tag{5}$$

To eliminate interfacial concentrations, the gas and liquid-phase rate equations are added to give

$$\left(\frac{R\,T_{avg}}{Hk_G a} + \frac{1}{k_L a} \right) \frac{Q_L}{A} \frac{dC_L}{dL} = \frac{R\,T_{avg}}{H}\, C_{Gi} - \frac{R\,T_{avg}}{H}\, C_G + C_L - C_{Li} \tag{6}$$

where:

$\left(\frac{R\,T_{avg}}{Hk_G a} + \frac{1}{k_L a} \right)$ = over-all resistance to mass transfer or the reciprocal over-all liquid-phase mass transfer coefficient.

Obtaining a relationship for C_G from the stripping section mass balance and substituting in equation (6), we obtain :

$$\int_{C_{L2}}^{C_{L1}} \frac{dC_L}{C_L - \frac{R\,T_{avg}}{H}\left[C_{G2} + \frac{Q_L}{Q_G}(C_L - C_{L2})\right]} = \frac{AK_L a}{Q_L} \int_o^L dL \tag{7}$$

After integration, it is found that

$$\mathrm{Ln}\left[\frac{C_{L1} - \frac{R\,T_{avg}}{H}\left[C_{G2} + \frac{Q_L}{Q_G}(C_{L1} - C_{L2})\right]}{C_{L2} - \frac{R\,T_{avg}}{H} C_{G2}} \right] = \frac{K_L aAL \left(1 - \frac{R\,T_{avg}}{H}\frac{Q_L}{Q_G}\right)}{Q_L} \tag{8}$$

Noting that

$$C_{G1} = C_{G2} + \frac{Q_L}{Q_G} (C_{L1} - C_{L2}) \quad (9)$$

where:

C_{G1} = exit sweep gas carbon dioxide concentration,

and rearranging equation (8) we can determine

$$\frac{C_{L1} - \frac{R\,T_{avg}}{H} C_{G1}}{C_{L2} \quad \frac{R\,T_{avg}}{H} C_{G2}} = \exp \frac{K_L aAL \left(1 - \frac{R\,T_{avg}}{H} \frac{Q_L}{Q_G}\right)}{Q_L}, \quad (10)$$

Equation (10) can then be solved for C_{L2} to give

$$C_{L2} = e^{-N/Q_L} \left(C_{L1} - \frac{R\,T_{avg}}{H} C_{G1}\right) + \frac{R\,T_{avg}}{H} C_{G2} \quad (11)$$

where:

$$N = K_L a\, V_s \left(1 - \frac{R\,T_{avg}\, Q_L}{H\, Q_G}\right)$$

$$V_s = AL.$$

Replacing C_{G1} in equation (11) with its equivalent from the mass balance on the stripping section, we obtain after algebraic manipulation:

$$C_{L2} = F\, C_{G2} + (B + 1)\, C_{L1} \quad (12)$$

where:

$$F = \frac{\frac{R\,T_{avg}}{H} \left(1 - e^{-N/Q_L}\right)}{1 - e^{-N/Q_L \left(\frac{R\,T_{avg}}{H}\frac{Q_L}{Q_G}\right)}}$$

$$B = \frac{e^{-N/Q_L}\left(1 - \frac{R\,T_{avg}\,Q_L}{H\,Q_G}\right)}{1 - e^{-N/Q_L}\left(\frac{R\,T_{avg}\,Q_L}{H\,Q_G}\right)} - 1$$

Substituting equation (12) into equation (2) and integrating the carbon dioxide concentration in the water reservoir over stripping time, t, we obtain:

$$\int_{C_{L10}}^{C_{L1}} \frac{dC_{L1}}{C_{L1}B + FC_{G2}} = \frac{Q_L}{V_L}\int_o^t dt \qquad (13)$$

and

$$\text{Ln}\left[\frac{C_{L1}B + FC_{G2}}{C_{L10}B + FC_{G2}}\right] = \frac{Q_L B t}{V_L}. \qquad (14)$$

Solving for the carbon dioxide concentration in normalized form, we obtain:

$$\frac{C_{L1}}{C_{L10}} = e^{Q_L B t/V_L}\left(1 + \frac{F}{B}\frac{C_{G2}}{C_{L10}}\right) - \frac{F}{B}\frac{C_{G2}}{C_{L10}}. \qquad (15)$$

Since,

$$\frac{F}{B} = -\frac{R\,T_{avg}}{H}$$

and

$$\frac{R\,T_{avg}}{H}\;C_{G2} = C_{LF}$$

where:

C_{LF} = final liquid concentration in equilibrium with

the sweep air stream;

equation (15) takes the form:

$$Y(t) = (1 - Z_2)\, e^{Q_L Bt/V_L} + Z_2 \qquad (16)$$

where:

$$Y = \frac{C_{L1}}{C_{L10}}$$

$$Z_2 = \frac{C_{LF}}{C_{L10}} .$$

To plot Y as a function of stripping time, the values of C_{L10} and C_{LF} were taken from experimental ph measurements. For this reason the theoretical and experimental plots of concentration versus time always coincided at time = 0 and time = ∞ . The constant, B, is theoretically negative and the value, Z_2, is very small so that, initially, the depletion of the normalized carbon dioxide concentration in water is nearly an exponential decay. At large stripping times the value of Z_2 becomes significant as the plot levels off to this asymptotic value.

To analyze experimental data on carbon dioxide concentrations in the exit sweep gas stream as a function of time, the mathematical model was used to theoretically obtain $C_{G1}(t)$. Thus, by combining the material balance on the stripping section,

$$C_{G1} = C_{G2} + \frac{Q_L}{Q_G} (C_{L1} - C_{L2}), \qquad (9)$$

with the final form of the liquid concentration leaving the stripping section,

$$C_{L2} = FC_{G2} + (B + 1) C_{L1}, \quad (12)$$

we can solve for the exit sweep gas concentration as a function of stripping time:

$$C_{G1}(t) = C_{G2} - \frac{Q_L B}{Q_G} e^{Q_L B\, t/V_L} \left(C_{L10} + \frac{F}{B} C_{G2}\right) . \quad (17)$$

Substituting

$$Z = \frac{R T_{avg}}{H} \frac{C_G}{C_{L10}} ,$$

we obtain the normalized sweep gas concentration as a function of time:

$$Z(t) = \frac{Q_L B}{Q_G} \frac{R T_{avg}}{H} (Z_2 - 1) e^{Q_L B t/V_L} + Z_2 . \quad (18)$$

Mathematical Model for Large Spray Ring Contactor

The representative flow diagram for analysis of stripping using the larger spray ring is depicted in Figure 4.

Since there were no baffles mounted with the larger spray ring which would inhibit the free circulation of gas, the outer pool or stripping volume was assumed to be a well-mixed gas space. Similarly, the well-mixed assumption was also applied to the water reservoir.

The mass transfer rate equation for transfer of carbon dioxide from the liquid spray to the surrounding gas is

$$Q_L\, dC_L = K_L a\, dV \left(\frac{R T_{avg}}{H} C_G - C_L\right) \quad (19)$$

where:

$K_L a$ = over-all liquid-phase mass transfer coefficient;

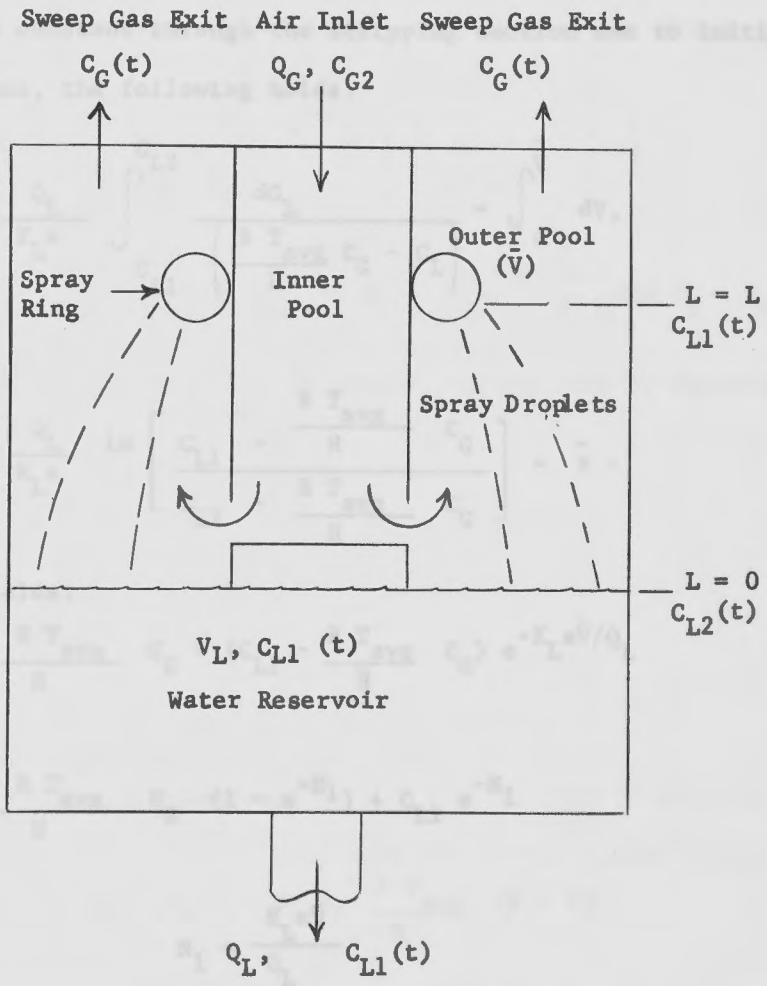

Figure 4. Flow Diagram to Represent the Stripping System Employing the Large Spray Ring.

dV = differential stripping volume.

The carbon dioxide concentration in water can be integrated over time since C_G remains constant through the stripping section due to initial assumptions. Thus, the following holds:

$$\frac{Q_L}{K_L a} \int_{C_{L1}}^{C_{L2}} \frac{dC_L}{\left(\frac{R\,T_{avg}}{H} C_G - C_L \right)} = \int_0^{\bar{V}} dV, \qquad (20)$$

$$\frac{Q_L}{K_L a} \; Ln \left[\frac{C_{L1} - \frac{R\,T_{avg}}{H} C_G}{C_{L2} - \frac{R\,T_{avg}}{H} C_G} \right] = \bar{V} . \qquad (21)$$

Equation (21) yields:

$$C_{L2} = \frac{R\,T_{avg}}{H} C_G + \left(C_{L1} - \frac{R\,T_{avg}}{H} C_G \right) e^{-K_L a \bar{V}/Q_L} \qquad (22)$$

or

$$C_{L2} = \frac{R\,T_{avg}}{H} C_G \left(1 - e^{-N_1} \right) + C_{L1} e^{-N_1} \qquad (23)$$

where:

$$N_1 = \frac{K_L a \bar{V}}{Q_L}$$

Carbon dioxide concentration in the water reservoir is

$$V_L \frac{dC_{L1}}{dt} = Q_L C_{L2} - Q_L C_{L1} . \qquad (24)$$

A carbon dioxide material balance on the gas volume above the water is

$$V_G \frac{dC_G}{dt} = Q_G C_{G2} - Q_G C_G - Q_L \left(C_{L2} - C_{L1} \right) \qquad (25)$$

where:

V_G = total gas volume above the liquid pool.

Substituting for C_{L2} in both conservation relationships, we obtain

$$V_L \frac{dC_{L1}}{dt} = Q_L (1 - e^{-N_1}) \left(\frac{R T_{avg}}{H} C_G - C_{L1} \right) \quad (26)$$

and

$$V_G \frac{dC_G}{dt} = Q_G C_{G2} - Q_G C_G - Q_L \left(1 - e^{-N_1}\right) \left(\frac{R T_{avg}}{H} C_G - C_{L1} \right) \quad (27)$$

Equations (26) and (27) can be put in dimensionless form by defining:

$$Z = \frac{R T_{avg}}{H} \frac{C_G}{C_{L10}} ;$$

$$Y = \frac{C_{L1}}{C_{L10}} ;$$

$$T = \frac{Q_L}{V_L} \cdot t ;$$

which gives the following equations:

$$\frac{dZ}{dT} = G_t Z_2 - G_t Z - G_v A_1 \frac{R T_{avg}}{H} (Z - Y) \quad (28)$$

and

$$\frac{dY}{dT} = A_1 (Z - Y) \quad (29)$$

where:

$$A_1 = 1 - e^{-N_1}$$

$$G_t = \frac{Q_G}{Q_L} \cdot \frac{V_L}{V_G}$$

$$G_V = \frac{V_L}{V_G} .$$

The variable Y can be eliminated by differentiating equation (28) with respect to time and adding the result to equation (29). Further algebraic manipulation affords the second order differential equation in Z:

$$\left[D^2 + (A_1 + G_t + G_V A_1 \frac{R T_{avg}}{H}) D + A_1 G_t \right] Z = A_1 G_t Z_2 . \qquad (30)$$

Simplification of equation (30) leads to the following result:

$$[D^2 + M_1 D + M_2] Z = M_3 \qquad (31)$$

where:

$$M_1 = A_1 + G_t + G_v A_1 \frac{R T_{avg}}{H} ;$$

$$M_2 = A_1 G_t ;$$

$$M_3 = A_1 G_t Z_2 .$$

For a 25 per cent carbon dioxide - 75 per cent air mixture initially in equilibrium with the water reservoir, the following initial conditions can be applied to equation (31):

at T = 0, (1) $Z = 1$

(2) $Y = 1$

(3) $\frac{dZ}{dT} = G_t Z_2 - G_t .$

Solving for Z, we obtain:

$$Z = C_1 e^{r_1 T} + C_2 e^{r_2 T} + \frac{M_3}{M_2} \qquad (32)$$

where:

$$r_1 = -\frac{M_1}{2} + \frac{1}{2}\sqrt{M_1^2 - 4M_2} \; ;$$

$$r_2 = -\frac{M_1}{2} - \frac{1}{2}\sqrt{M_1^2 - 4M_2} \; .$$

Constants C_1 and C_2 can be determined for this gas concentration equation by applying initial conditions to equation (32):

$$C_2 = \left(1 - \frac{M_3}{M_2}\right) - \frac{G_t\,(Z_2 - 1) + r_1\left(1 - \frac{M_3}{M_2}\right)}{r_2 - r_1} \; ;$$

$$C_1 = \frac{r_2\left(1 - \frac{M_3}{M_2}\right) - G_t\,(Z_2 - 1)}{r_2 - r_1}$$

The carbon dioxide concentration in water can be determined by rearranging equation (28) to give:

$$Y = \frac{\left(D + G_t + G_v A_1 \frac{R\,T_{avg}}{H}\right) Z - G_t Z_2}{G_v A_1 \frac{R\,T_{avg}}{H}} \; . \qquad (33)$$

Substituting for DZ and Z in equation (33), we obtain the desired result:

$$Y = \frac{C_3}{C_5}\,(r_1 C_6 + C_7)e^{r_1 T} + \frac{C_4}{C_5}\,(r_2 C_6 + C_7)e^{r_2 T} + Z_2 \qquad (34)$$

where:

$$C_3 = r_2\,(1 - Z_2) - G_t\,(Z_2 - 1) \; ;$$

$$C_4 = G_t\,(Z_2 - 1) - r_1\,(1 - Z_2) \; ;$$

$$C_5 = r_2 - r_1 \quad ;$$

$$C_6 = \frac{1}{G_v A_1 \frac{R T_{avg}}{H}} \quad ;$$

$$C_7 = \frac{G_t}{G_v A_1 \frac{R T_{avg}}{H}} + 1 \quad .$$

The result can be presented in the following manner:

$$Y = P_1 e^{r_1 T} + P_2 e^{r_2 T} + E_2 \tag{35}$$

where:

$$P_1 = \frac{C_3}{C_5} (r_1 C_6 + C_7) \quad ;$$

$$P_2 = \frac{C_4}{C_5} (r_2 C_6 + C_7) \quad .$$

Constants r_1 and r_2 are both negative and P_2 is negative so that Y is actually the difference between two exponential decay terms. Again, E_2 is the asymptotic value of Y at large stripping times. As before, the maximum concentration of carbon dioxide in water, C_{L10}, and the final concentration in water, $\frac{R T_{avg}}{H} C_{G2}$, are experimentally determined for substitution in equation (35). The over-all liquid-phase mass transfer coefficient is contained in all four constants as the exponential term, $e^{-K_L a \bar{V}/Q_L}$.

If the gas volume initially contained air instead of a carbon dioxide-air mixture, the same mathematical representation would apply to solve analytically for Y as a function of stripping time. The derivation is the same until initial conditions are applied to equation (32). If

air is contained initially in the spray chamber,

at T = 0, (1) $Y = 1$

(2) $Z = Z_2$

(3) $\frac{dZ}{dT} = G_v A_1 \frac{R T_{avg}}{H} (1 - Z_2)$.

Solving for C_1 and C_2, we obtain:

$$C_1 = \frac{1}{r_2 - r_1} \left[G_v A_1 \frac{R T_{avg}}{H} (Z_2 - 1) \right] ;$$

$$C_2 = \frac{1}{r_2 - r_1} \left[G_v A_1 \frac{R T_{avg}}{H} (1 - Z_2) \right] .$$

Referring to equation (33) and solving for Y, we obtain:

$$Y = E_1 E_2 (E_4 + E_3) e^{r_2 T} - E_1 E_2 (E_5 + E_3) e^{r_2 T} + Z_2 \qquad (36)$$

where:

$$E_1 = \frac{1}{r_2 - r_1}$$

$$E_2 = G_v A_1 \frac{R T_{avg}}{H} (1 - Z_2) ;$$

$$E_3 = \frac{G_t}{G_v A_1 \frac{R T_{avg}}{H}} + 1 ;$$

$$E_4 = \frac{r_2}{G_v A_1 \frac{R T_{avg}}{H}} ;$$

$$E_5 = \frac{r_1}{G_v A_1 \frac{R T_{avg}}{H}} .$$

Again, the final form can be presented in the following manner:

$$Y = P_3 e^{r_2 T} - P_4 e^{r_1 T} + E_2 \qquad (37)$$

where:

$$P_3 = E_1 E_2 (E_4 + E_3) \; ;$$

$$P_4 = E_1 E_2 (E_5 + E_3) \; .$$

At time = 0 the exponential terms become one and Y is the sum of P_3, P_4 and E_2, which is Y = 1.0. Again, the mass transfer coefficient in exponential form is contained in all four equation constants.

CHAPTER III

APPARATUS AND EXPERIMENTAL PROCEDURE

I. THE STRIPPING SYSTEM AND EXPERIMENTAL TECHNIQUES

Carbon Dioxide-Air-Water Stripping System

The stripping system, depicted schematically in Figure 5 was furnished by the Oak Ridge National Laboratory and was assembled for use in the Engineering Mechanics Laboratory at Estabrook Hall. The spray chamber containing the small spray ring system is shown in Figure 6 along with liquid and gas concentration measuring equipment. The sprinkler head is not visible in the picture since it is mounted inside the vertical splash baffle. Water entered the spray chamber through the tygon tubing on the right side of the tank and exited through the Plexiglas tube beneath the tank. The valve employed for obtaining liquid samples is visible at the 90^{o} turn in the exit water line.

The thermal conductivity gas analyzer and recording equipment are shown to the left of the iron stand which supports the stripping tank. The ph meter employed for liquid concentration measurements is shown above the recorder.

A Plexiglas tank, 36 inches in diameter and 21-3/4 inches high, served as a reservoir for distilled water. The water was routed from the bottom of the tank through the pump suction leg, a 67 inch length of 2-inch O.D. stainless steel tubing which was jacketed with a small countercurrent heat exchanger. Building water was used in the heat exchanger to maintain a constant system temperature. After passing through a 146 GPM. capacity liquid rotameter on the downstream side of the pump,

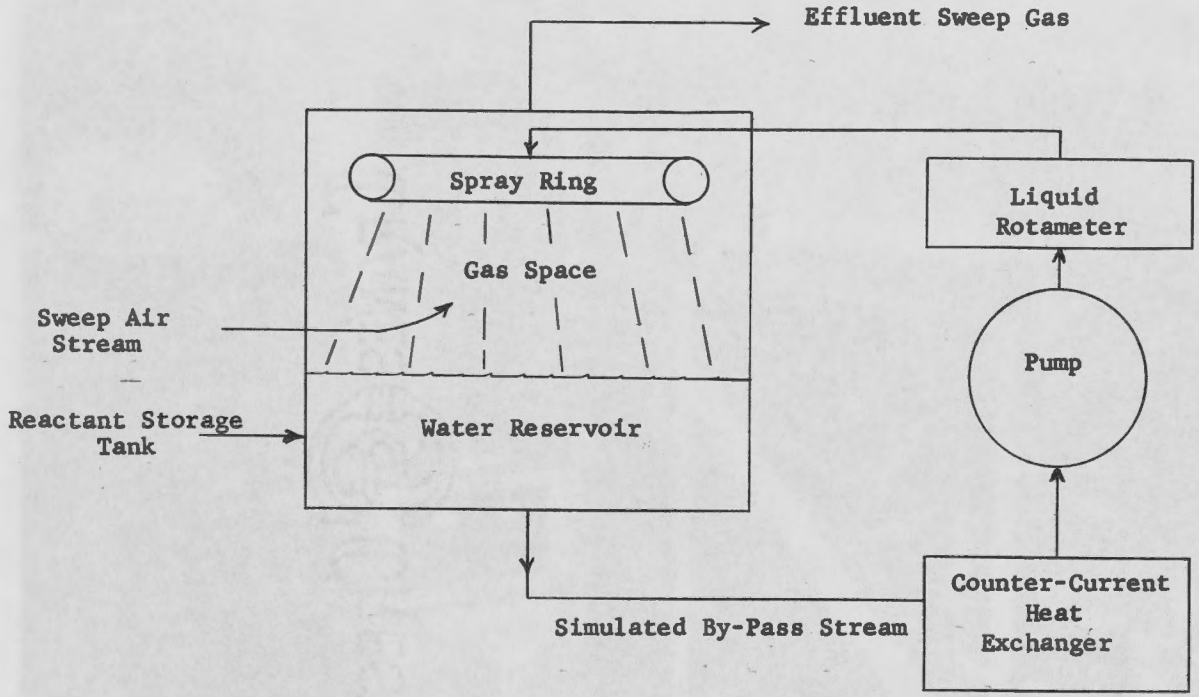

Figure 5. Schematic Representation of Stripping System.

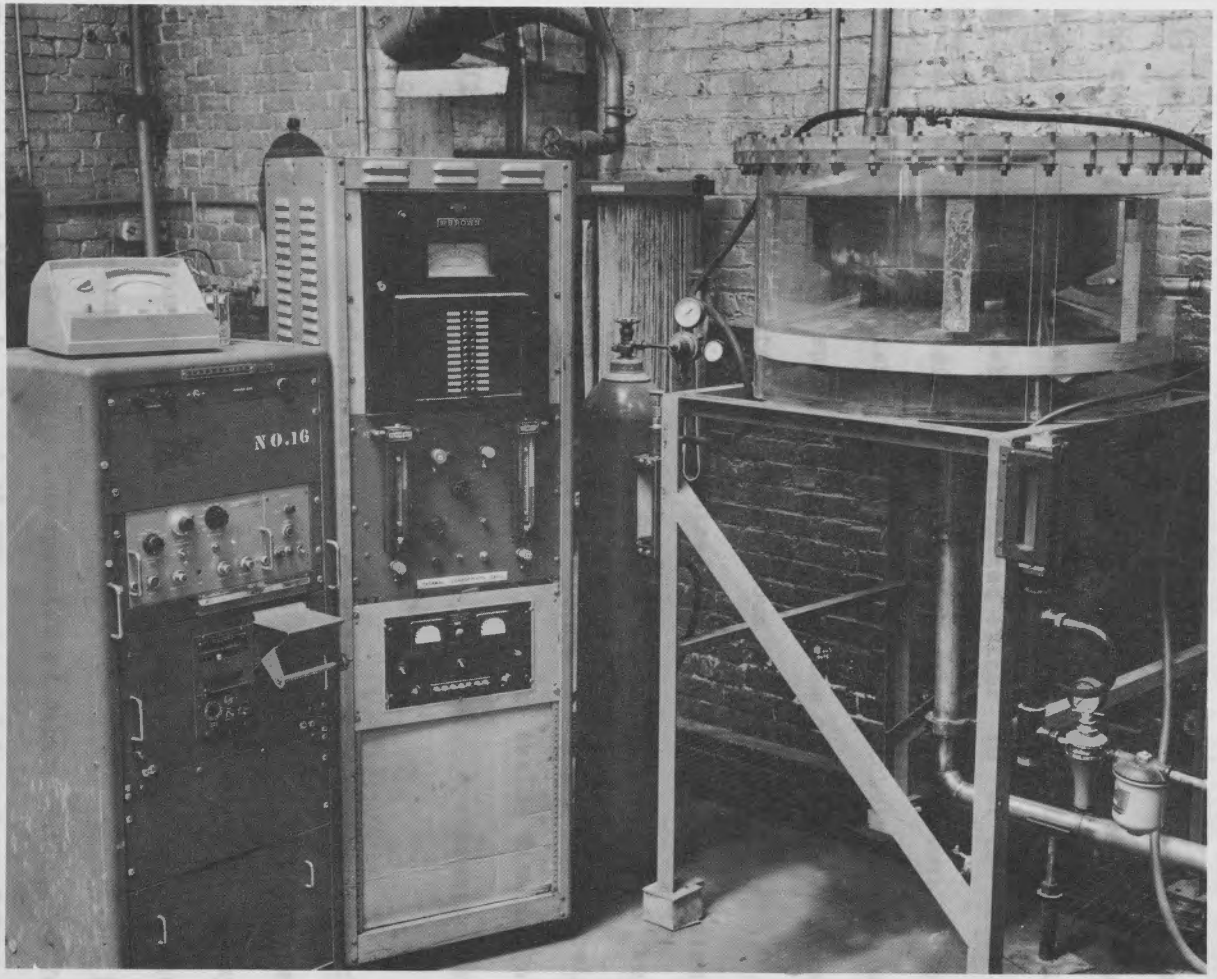

Figure 6. Experimental Stripping System with Concentration Measuring Equipment.

the test water was returned through a 64 inch section of 1-inch I.D. tygon tubing to a spray ring mounted inside the Plexiglas storage tank.

An analysis of the rate of carbon dioxide transfer from water to air was made for each of two stainless steel spray rings. The smaller of the two rings had an inside diameter of 14-1/2 inches and a 2-inch inside tube diameter. The small spray ring contained 138 1/16-inch drill through diameter holes, with each hole staggered either 10° or 20° below horizontal and spaced equi-distanced around the ring. A network of splash and guide baffles was furnished by Oak Ridge National Laboratory for use with this spray ring. The spray ring and its system of baffles were mounted inside the Plexiglas storage tank as shown in Figure 1.

The larger spray ring contained 150 1/8-inch diameter holes and 150 1/16-inch diameter holes, the smaller holes being about 15° below a horizontal radius and the larger holes being approximately 20° below the horizontal radius. The larger spray ring had an inside diameter of 29-1/2 inches and a 1-5/8-inch inside tube diameter. A schematic representation of its mounting is shown in Figure 2.

A 75 GPM. stainless steel centrifugal pump purchased from the Yeomans Bros. Company in Chicago was used to circulate distilled water through the stripping system. A 1.5 horsepower, three phase, 60 cycle motor furnished power to this pump. To obtain increased liquid flow rates for later experimental runs, a larger stainless steel centrifugal pump was purchased from Goulds Pump Incorporated of Seneca Falls, New York. The pump, model 3196, developed 75 GPM. and was driven by a 5 horsepower, 60 cycle, three phase, model ABDP Westinghouse motor.

Compressed building air, which served as the sweep gas during stripping, entered the inner gas pool near the center of the cover flange for the Plexiglas tank. A 1/4-inch brass type T fitting was mounted above the 1/4-inch drilled and tapped gas entrance hole. A pet cock valve was placed before one entrance to the type T fitting to control the flow of air into the system. Another pet cock valve was placed at the other entrance to the fitting to control the flow of carbon dioxide into the system. Therefore, it was possible to inject any carbon dioxide-air mixture into the Plexiglas test tank through the simulated two way valve.

Before entering the system, air was filtered with a model FB4 Fulflo filter made by Commercial Filters Corporation in Lebanon, Indiana. Air flow was regulated by a type No. 1118 rotameter made by Brooks Rotameter Company in Landsdale, Pennsylvania. The rotameter was mounted to a leg of the stand supporting the spray chamber. After passing through the liquid-gas contacting section of the test tank, the sweep gas exited from the outer gas pool at two holes placed 180° from each other in the tank cover.

Welding grade carbon dioxide, which is bone dry and the highest grade of purity, was purchased in pressurized cylinders from The Welding Gas Products Company in Knoxville. A standard pressure regulator was mounted on the cylinder and gas flow was metered by a Type 8-1110-VV rotameter made by Brooks Instrument Company in Hatfield, Pennsylvania.

Measurement of Carbon Dioxide Concentration in Water

A Beckman Expanded Scale Model 76 PH Meter was used to determine

the concentration of carbon dioxide in water. Electrodes used with the ph meter, were made by the Scientific Instruments Division of Beckman Instruments, Incorporated in Fullerton, California. A type 41263 general purpose glass electrode with silver-silver chloride internals was employed. This glass electrode is applicable for temperatures from -5°C. to 80°C. and is accurate for ph values from 0 to 11. A fiber junction reference electrode was used with the glass electrode. The reference electrode contained a mercury-mercurous chloride or calomel internal element surrounded by a saturated potassium chloride solution. A detailed analysis of the glass electrode, describing its function during ph measurement, its advantages over other types of electrodes and its range of usefulness is presented by M. Dole in The Glass Electrode (1). Operating procedures and maintenance of the ph meter are described in the instruction manual published by The Beckman Company (7).

To encompass the range of ph values taken during experimentation, the ph meter was standardized with buffers furnished by The Macbeth Corporation of ph = 7 and ph = 4. Standardization procedures are also described in the instruction manual (7).

Carbon dioxide in water either remains as a linear molecule attached physically to water molecules or it forms carbonic acid, H_2CO_3, a weak acid which has not been isolated and is therefore completely unstable. A saturated solution of carbonic acid in water at atmospheric pressure and 25°C. is approximately .04 molar and gives a ph measurement of approximately 4.00. This ph value was verified experimentally by bubbling carbon dioxide through distilled water at 25°C. until a constant

ph of 4.00 was attained. The concentration of carbonic acid in water and therefore the amount of carbon dioxide present as carbonic acid was determined from this ph measurement. The amount of carbon dioxide that did not react chemically with the water but still dissolved in molecular form could not be determined using the ph technique. The maximum concentration of carbon dioxide in water that reacted chemically to form carbonic acid was 0.984 grams/liter.

The maximum concentration of carbon dioxide in water that can be attained at 25°C. and atmospheric pressure is 1.449 grams/liter of water (5). Therefore, assuming complete saturation, .984/1.449 x 100 or 68 per cent of the carbon dioxide in water formed carbonic acid, while the remaining carbon dioxide retained its molecular form in solution.

A similar analogy can be made for distilled water in equilibrium with air. Assuming air contains 0.031 per cent carbon dioxide by volume (4) and Henry's law holds at 25°C. and atmospheric pressure, the concentration of carbon dioxide in distilled water in equilibrium with air is 0.000466 grams/liter. The ph of distilled water in equilibrium with air was determined experimentally to be 5.75 or in other words, distilled water is actually very weak carbonic acid. The weight of carbon dioxide present in distilled water as carbonic acid was then calculated from a ph of 5.75 to be 0.000390 grams/liter. For this situation 83.5 per cent of the total amount of carbon dioxide in water was in the form of carbonic acid. Since comparable weight per cents of carbon dioxide in water were present as carbonic acid for both the maximum and minimum concentration cases, it was assumed that this percentage remained essentially constant

throughout the range of concentrations measured.

An examination of theoretical results from both mathematical models:

$$Y = P_1 e^{r_1 T} + P_2 e^{r_2 T} + Z_2 \tag{35}$$

and

$$Y = (1 - Z_2) \exp (Q_L BT/V_L) + Z_2 \tag{16}$$

revealed that the normalized concentrations, Y, depended only on ratios of experimental concentrations and not on any absolute experimental concentration. Thus, the calculated mass transfer coefficients were also not dependent upon the accurate measurement of an absolute carbon dioxide concentration in water. Errors incurred in the measurement of absolute carbon dioxide concentrations were canceled when the equations were normalized.

For the above reasons the amount of carbon dioxide present in water as carbonic acid was assumed to be the total weight of carbon dioxide present in solution. In other words the concentrations calculated from ph measurements were assumed to represent the total weight of carbon dioxide in solution.

Carbonic acid dissociates initially to form the bicarbonate ion according to the reaction,

$$H_2CO_3 \rightleftharpoons H^+ + HCO_3^- .$$

The bicarbonate ion, which is amphoteric, can then act as a weak acid to dissociate and form the carbonate ion according to the following reaction:

$$HCO_3^- \rightleftharpoons H^+ + CO_3^= .$$

The degree of dissociation of an acid in water can be determined if its dissociation or ionization constant is known. For an acid, HA, which dissociates according to:

$$HA \rightleftharpoons H^+ + A^-,$$

the ionization constant, K, determines the equilibrium relationship between acid molecules and their ions and is defined as

$$K = \frac{[H^+][A^-]}{[HA]}.$$

[HA] is the amount of unionized acid present in the water. The ionization constant for the formation of basic bicarbonate ion is approximately 4.4×10^{-7} at room temperature (5). Similarly, the dissociation of HCO_3^- to form $CO_3^=$ has an ionization constant of 5.6×10^{-11}. Since the bicarbonate ion acting as an acid is more than ten thousand times weaker than carbonic acid, its dissociation to form the carbonate ion was neglected.

If C represents the molar concentration of acid present in solution and X is the concentration of hydrogen ion, then the acid-ion equilibrium relation can be expressed as

$$K = \frac{X^2}{C - X}.$$

Solving for C, we obtain:

$$C = \frac{X^2}{K} + X,$$

which is the molar concentration of carbonic acid present in solution. Since one mole of carbon dioxide reacts with water to form one mole of

carbonic acid:

$$CO_2 + H_2O \rightleftharpoons H_2CO_3 ,$$

C is also the molar concentration of carbon dioxide in water.

Measurement of Carbon Dioxide Concentration in Air

The concentration of carbon dioxide in the exit air stream was measured with a thermal conductivity gas analyzer and recorded on a dual channel model 152-100B Sanborn recorder. A model 150-1500 low level A.C. preamplifier and a model 150-200B driver amplifier and power supply both from Sanborn were used with the recorder. A detailed description of the thermal conductivity gas analyzer with its operating procedure was presented by Hardwick (3).

A continuous sampling of the exit air stream was accomplished by placing a hypodermic probe just inside the spray chamber at one of the two air stream exits. A section of 1/8-in. I.D. tygon tubing connected the probe with the inlet side of the thermal conductivity cell. To prevent moisture from reaching the cell, a small drying tube filled with $CaSO_4$ was placed in the tubing between the probe and the gas analyzer.

Ambient air was drawn into the thermal conductivity cell through another hypodermic probe and used as the reference gas for the system. The thermal conductivity of carbon dioxide is 1.5 times less than the thermal conductivity of air and, therefore, detection of concentration changes was not too difficult.

A very slight vacuum was applied to the cell by a vacuum pump placed at the end of the gas analyzing system. The cell temperature and gas

stream temperatures were maintained at 125°F. by a constant temperature bath surrounding the cell. The wheatstone bridge current in the cell was set at 24 milliamperes for each run.

The detailed operating procedure and maintenance requirements for the a.c. preamplifier and dual channel recorder are available in manuals published by the Sanborn Company (9) and by Hardwick (3). The attenuator on the preamplifier was set at Xl to give a maximum stylus deflection for the voltage signal from the thermal conductivity cell.

To calibrate the gas analyzer system, the stylus was first positioned on the base line of the Sanborn permapaper by the "position control" knob on the preamplifier. This was done before any voltage signal from the thermal conductivity cell reached the recorder. Using Hardwick's technique (3) to set the thermal conductivity cell in operation, air was then allowed to flow through both sides of the wheatstone bridge circuit. The stylus was then returned to the base line on the recording paper by adjusting first the "coarse" adjustment potentiometer and then the "fine" adjustment potentiometer. Both knobs were located on the front of the gas analyzer housing. This stylus position provided a basis for detecting concentration changes and was considered a zero per cent concentration of carbon dioxide in air.

A known carbon dioxide-air mixture was then placed in the test tank by utilizing the type T fitting at the gas entrance. For example, to obtain a 25 per cent carbon dioxide - 75 per cent air mixture, gas flow rates into the tank were adjusted to give 1.0 CFM. of carbon dioxide and 3.0 CFM. of air. The sample hypodermic probe was then placed in the

sweep gas exit of the tank and the stylus deflection was noted. When the deflection remained constant, indicating a completely mixed gas space, the stylus position represented a 25 per cent by volume of carbon dioxide in air. The stylus base position or zero per cent carbon dioxide concentration was checked again by removing the probe from the sweep gas exit and allowing only air to flow through the cell. The base position of the stylus drifted noticeably and had to be reset frequently by readjusting the "fine" adjustment potentiometer. Calibration of the recorder for other carbon dioxide-air mixtures could be determined, similarly.

In addition to calibrating the recorder to determine absolute concentrations of carbon dioxide in air, it was also necessary to determine the speed of the paper before each run and the time delay required by the cell to detect a concentration change in the tank. Lag time in concentration measurements was determined by removing the probe from the tank exit, where it had been recording a certain carbon dioxide concentration, and measuring the time required for the stylus to return to its base or zero carbon dioxide concentration position. Depending on the vacuum pulled through the system, this lag time varied from 30 to 45 seconds.

Experimental Procedure

Experimental operating procedure was basically the same for all runs except for the initial conditions applied to the water reservoir and the gas space above the reservoir. Experimental runs were made using one of two sets of initial conditions depending upon which spray ring was

being analyzed.

For experimental runs employing the smaller spray ring system, distilled water, stored in a 55 gallon capacity stainless steel drum, was saturated with carbon dioxide before being transferred to the spray chamber. Saturation of the water was accomplished by placing a section of stainless steel tubing through an opening in the top of the storage drum and bubbling carbon dioxide through the water from a line connecting the tubing with a pressurized cylinder of carbon dioxide. Saturation was completed when the ph of the water reached a constant value which was usually around 4.00 depending on the water temperature.

The thermal conductivity gas analyzer was calibrated for zero per cent carbon dioxide concentration and twenty-five volume per cent carbon dioxide concentration in air before each run. Calibrations were made before every run, since it was impossible to attain exactly the same settings each time the gas analyzing system was turned on.

After calibration of the gas analyzer, the test tank was flushed with air to remove all carbon dioxide. Then the carbonated water was transferred to the stripping tank from a valve at the bottom of the 55 gallon drum to a 1/4-inch drilled and tapped hole in the side of the tank. A section of tygon tubing connected the drum valve with the reservoir in the stripping tank. To guard against unnecessary agitation of the carbonated water during transfer to the spray reservoir, water was released to the reservoir through a section of stainless steel tubing which reached the bottom of the Plexiglas tank. When water reached the desired level inside the spray chamber, which took approximately thirty minutes, flow

was stopped and the probe from the gas analyzer was inserted in the outer gas pool to determine how much carbon dioxide had escaped from the water while being transferred. This concentration was usually 2-3 volume per cent carbon dioxide. A very small stream of air was then used to displace the dilute carbon dioxide-air mixture above the water reservoir. Air at approximately 0.5 CFM entered the 1/4-inch hole used for carbonated water transfer in the side of the tank and exited at another 1/4-inch drilled hole placed opposite this air entrance. When the gas analyzer could detect no carbon dioxide in the space above the water, the system was ready for stripping.

Simultaneously, the sweep air was turned on at 3.0 CFM and the pump started to circulate the carbonated water. A ph measurement was taken about five seconds after the beginning of stripping to determine the initial carbon dioxide concentration in water. A ph value between 4.15 and 4.20 was recorded initially for this type run. Water samples were extracted from a pet cock valve placed under the tank in the pump suction leg. Ph measurements were recorded at two minute intervals for the first ten minutes, once every three minutes for the next ten minutes of stripping and finally once every five minutes until the run terminated. An experimental run terminated when ph measurements became identical.

Approximately 200 ml. of water were collected in a 400 ml. beaker for each ph measurement. A plastic cover was placed over the beaker to prevent carbon dioxide from leaving the water while transferring the sample from the pet cock valve to the ph meter. Approximately thirty seconds elapsed between the time the sample was taken until the electrodes

were immersed in the solution.

After recording the ph for a sample, the water was returned to the reservoir through a funnel that could be placed in one of the sweep gas exits. In this way the volume of test water in the system remained essentially constant. The same beaker was used to collect each sample and, therefore, only 200 ml. of water were taken from the stripping system at any one time.

For each run the tank was filled with water to a level even with the bottom of the openings connecting the inner and outer pools. The water level is illustrated in Figures 1 and 2. At this level the stripping tank contained 4.02 $ft.^3$ of water and 6.40 $ft.^3$ of gas space.

While ph measurements were being taken, a continuous sample of the exit air stream was being sent to the thermal conductivity gas analyzer. The base or zero per cent carbon dioxide concentration in air was checked every three to four minutes by removing the probe from the sweep gas exit.

The water temperature was checked periodically by measuring the temperature of ph samples. By adjusting the flow of water through the counter-current heat exchanger, the system temperature never varied more than $3^{\circ}F.$ for a single run. For all runs the temperature ranged from $74^{\circ}F.$ to $80^{\circ}F.$

Fresh distilled water was used for each experimental run to insure against slow outside contamination. Grease from the pump packing was the major contributor to contamination of the test water.

To vary the water flow rate between runs, a screw clamp was placed on the section of 1-inch I.D. tygon tubing leading from the downstream

side of the pump to the spray ring inside the stripping chamber.

For experimental runs employing the large spray ring, distilled water was transferred to the stripping tank and the pump turned on before saturation with carbon dioxide. To saturate the water a 25 per cent carbon dioxide - 75 per cent air mixture was passed through the gas-liquid contacting section until equilibrium was established between the spray droplets and the saturating gas. Equilibrium conditions were evident when ph measurements of the water reservoir became constant. These experimental runs initiated from ph values between 4.41 and 4.50.

With the system at equilibrium the beginning of a run was noted by stopping the flow of carbon dioxide into the spray chamber. Since for water saturation purposes the flow of air into the system was 3.0 CFM, the sweep air flow rate did not have to be adjusted at the beginning of stripping. The ph measurement at zero stripping time was the value recorded at gas mixture-water equilibrium.

Again, gas concentration data was recorded on the previously calibrated gas analyzer. For these runs with the large spray ring, gas concentration data began at 25 volume per cent carbon dioxide and dropped to nondetectable amounts of carbon dioxide in air.

CHAPTER IV

RESULTS AND DISCUSSION

Experimental concentration data are presented in Figures 7 and 8 to depict the effect of increased liquid flow on desorption of carbon dioxide from water. Each curve begins at a normalized maximum liquid concentration of one, and indicates that essentially a straight line depletion of Log C_{L1}/C_{L10} was observed with time; slopes of the straight line segments being more negative as the liquid flow rate was increased. Toward the end of stripping runs, the rate of mass transfer from the liquid to the gas space tapered to zero as the carbon dioxide liquid concentration approached its asymptotic air-water equilibrium value.

Over-all stripping rate coefficients were evaluated for both liquid-gas contacting systems by physically choosing the value of the parameter which provided a theoretical "best fit" of experimental stripping curves. The desired parameter was chosen taking into account physical observations during the experimental runs rather than from a method to mathematically minimize deviations, since it was felt that the model described the dynamics in the spray chamber more accurately at certain stripping times than at other stripping times. Most careful fitting was applied from the end of the straight line portion of the curve to the equilibrium asymptote for two reasons. Experimentally, assumptions that the gas and liquid volumes were well-mixed spaces were probably less in error through this region than at the beginning of stripping. Theoreti-

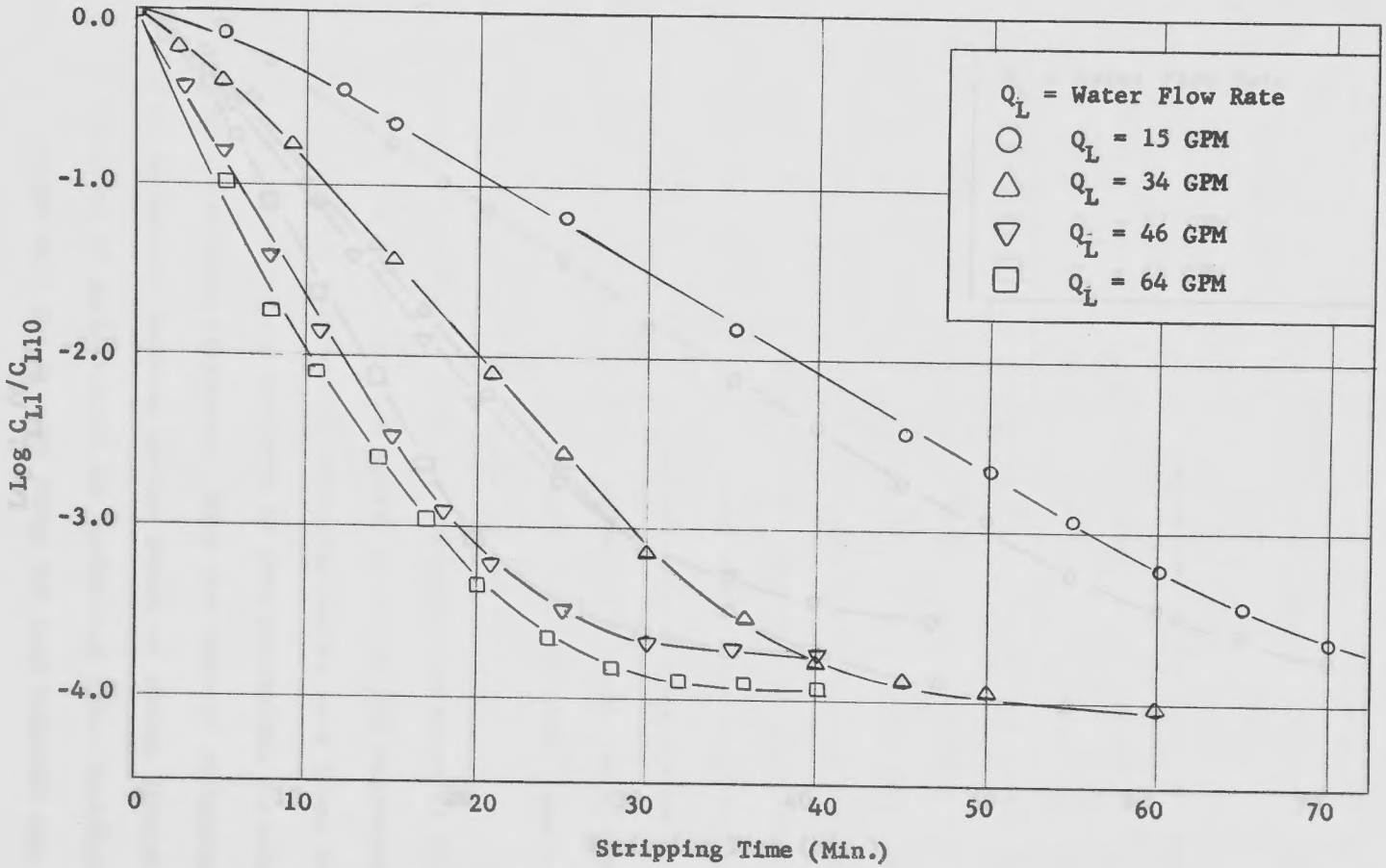

Figure 7. Experimental Stripping Curves for the Small Spray Ring.

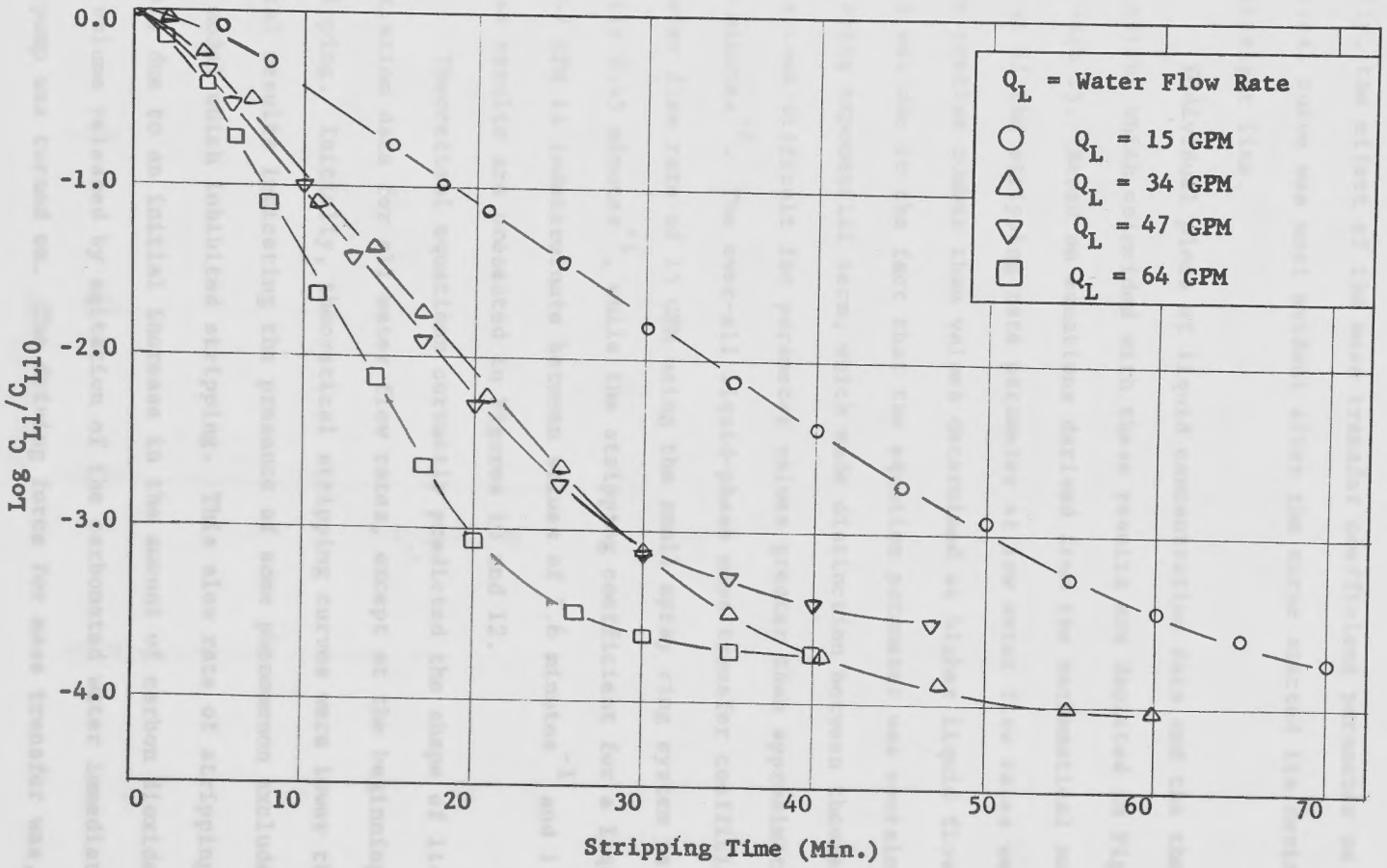

Figure 8. Experimental Stripping Curves for the Large Spray Ring.

cally, the effect of the mass transfer coefficient parameter on the theoretical curve was most evident after the curve started its deviation from a straight line.

Individual plots of liquid concentration data and the theoretical equations which coincided with these results are depicted in Figures 9 through 15. Based on equations derived from the mathematical models, the value of the stripping rate parameter at low water flow rates was a much more precise number than values determined at higher liquid flow rates. This was due to the fact that the equation parameter was contained in a decaying exponential term, which made distinction between theoretical equations difficult for parameter values greater than approximately 1.0 minutes^{-1}. The over-all liquid-phase mass transfer coefficient for a water flow rate of 15 GPM using the small spray ring system is essentially 0.45 minutes^{-1}, while the stripping coefficient for a liquid flow of 47 GPM is indeterminate between values of 1.6 minutes^{-1} and 1.8 minutes^{-1}. These results are presented in Figures 10 and 12.

Theoretical equations correctly predicted the shape of liquid concentration data for all water flow rates, except at the beginning of stripping. Initially, theoretical stripping curves were lower than experimental results indicating the presence of some phenomenon excluded from the model which inhibited stripping. This slow rate of stripping was most likely due to an initial increase in the amount of carbon dioxide in the gas volume released by agitation of the carbonated water immediately after the pump was turned on. The driving force for mass transfer was, there-

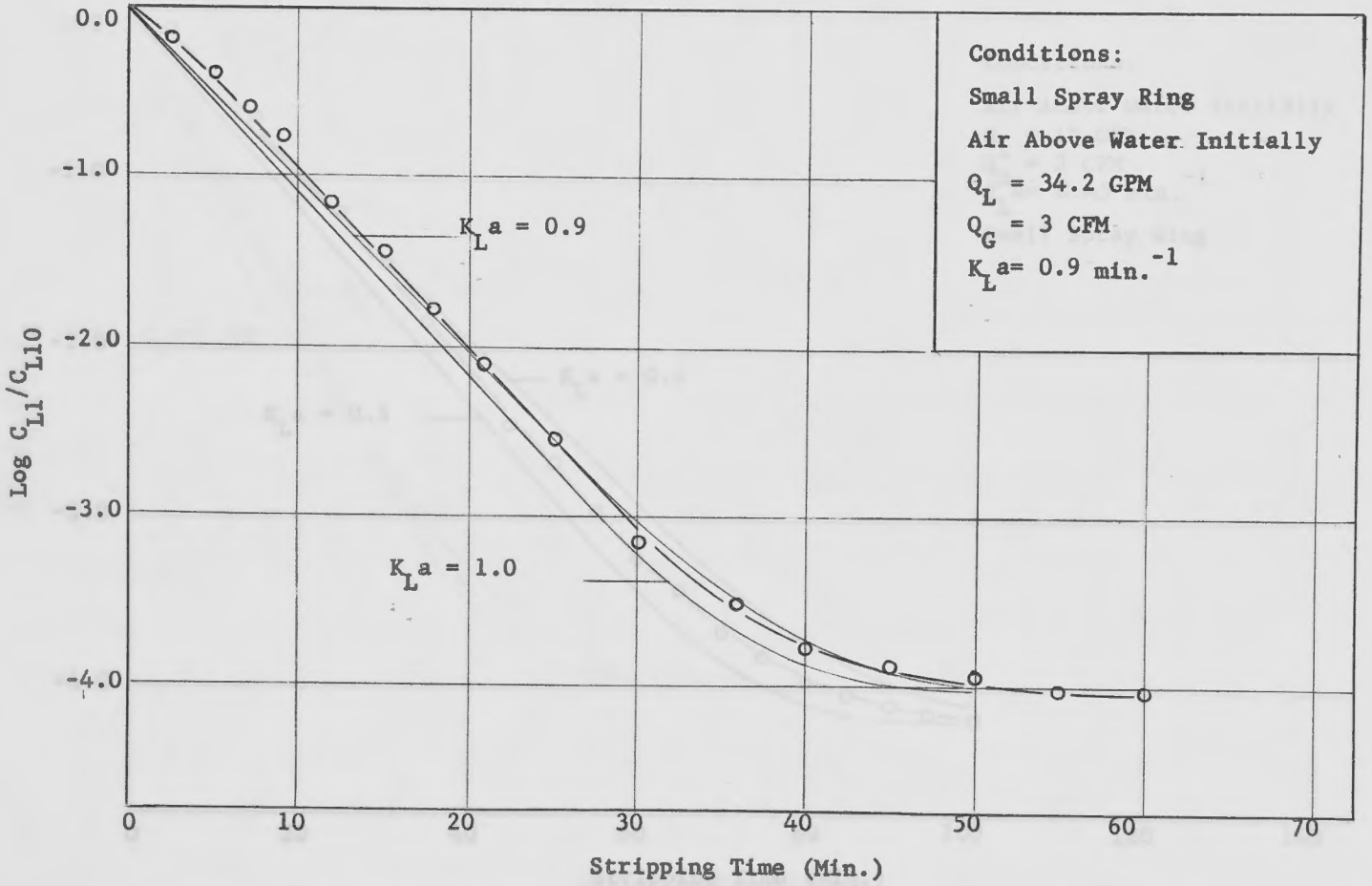

Figure 9. Fitting Experimental Data with Theoretical Curve - Run 34.

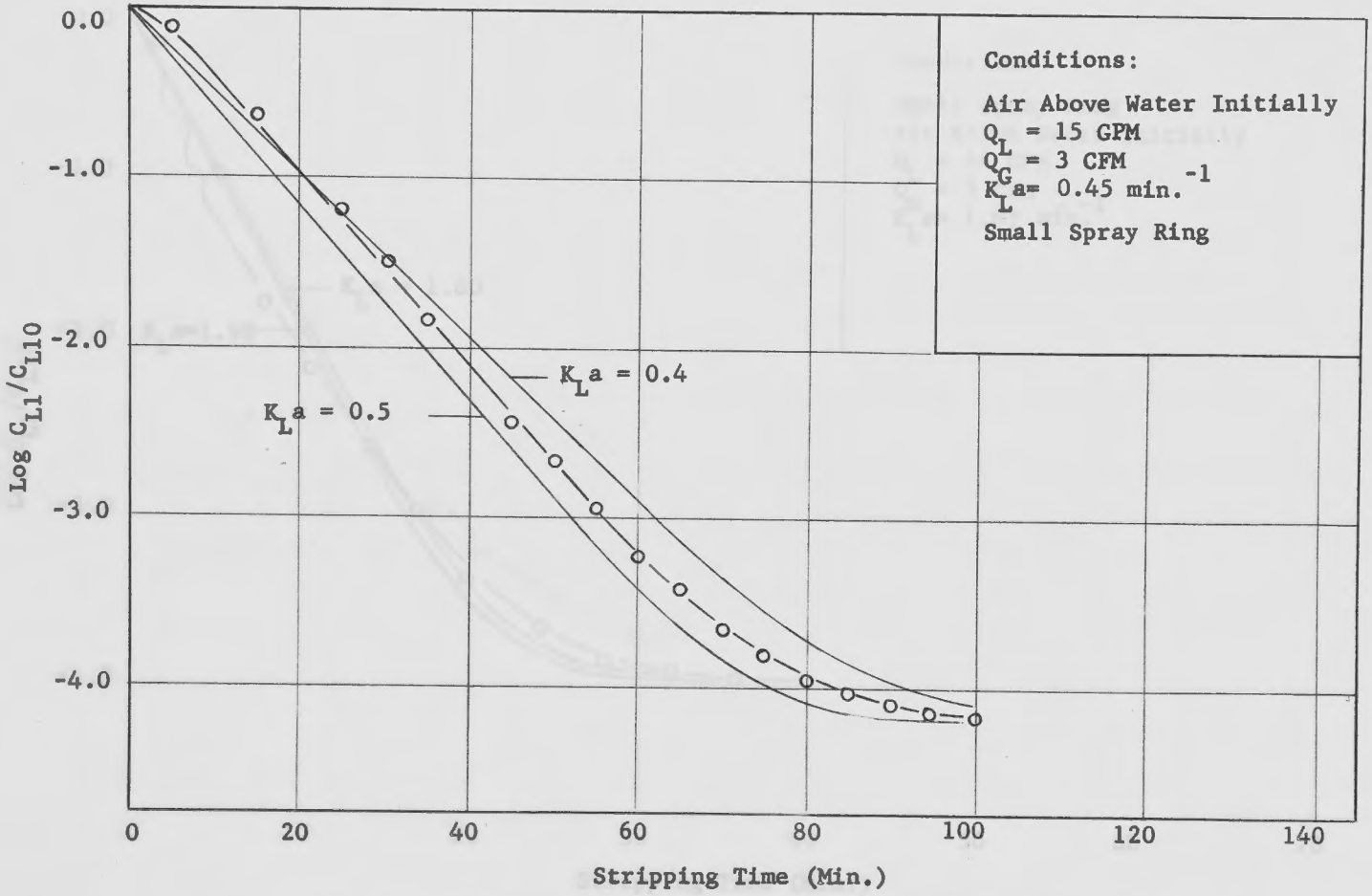

Figure 10. Fitting Experimental Data with Theoretical Curve - Run 36.

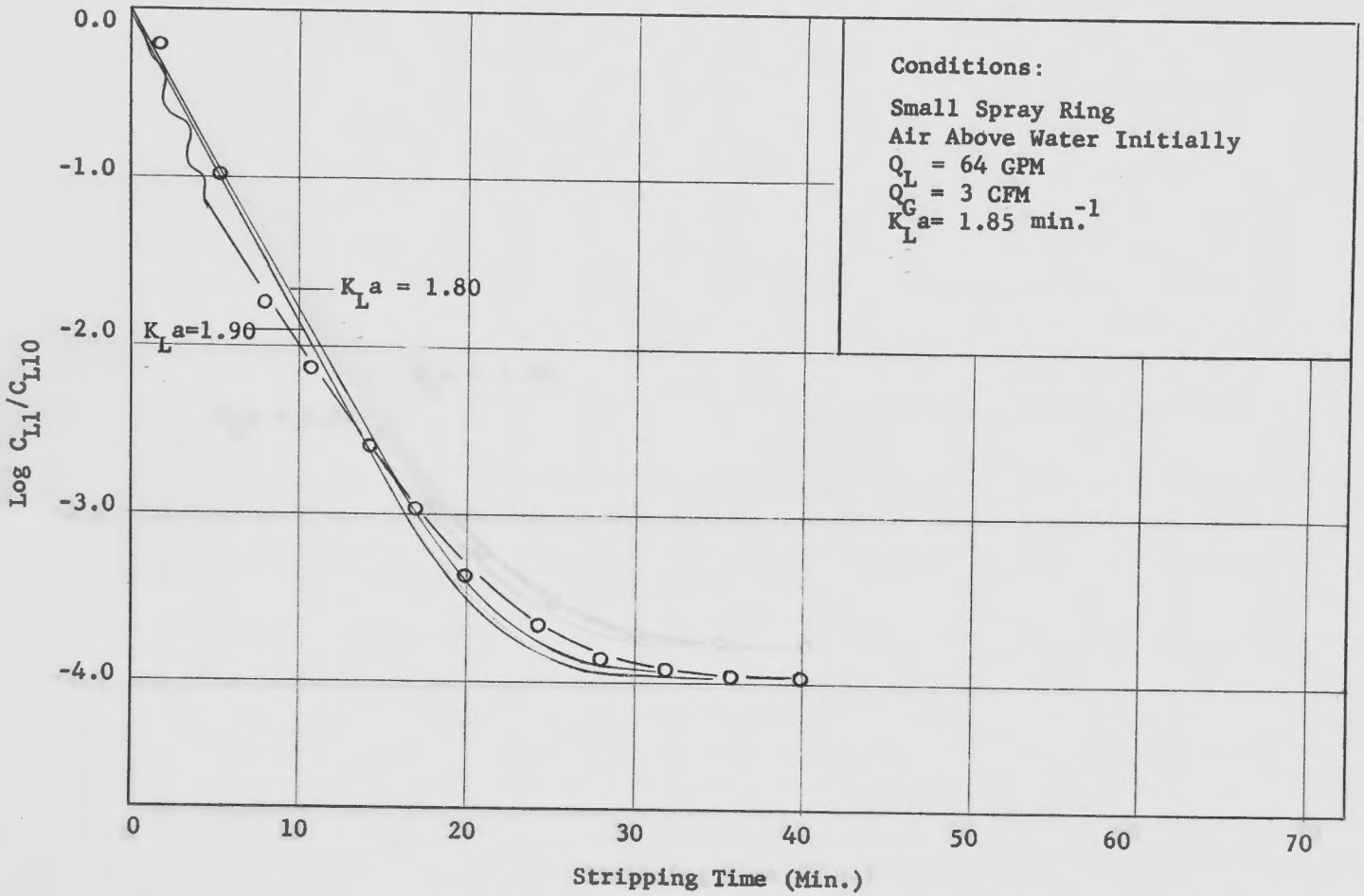

Figure 11. Fitting Experimental Data with Theoretical Curve - Run 47.

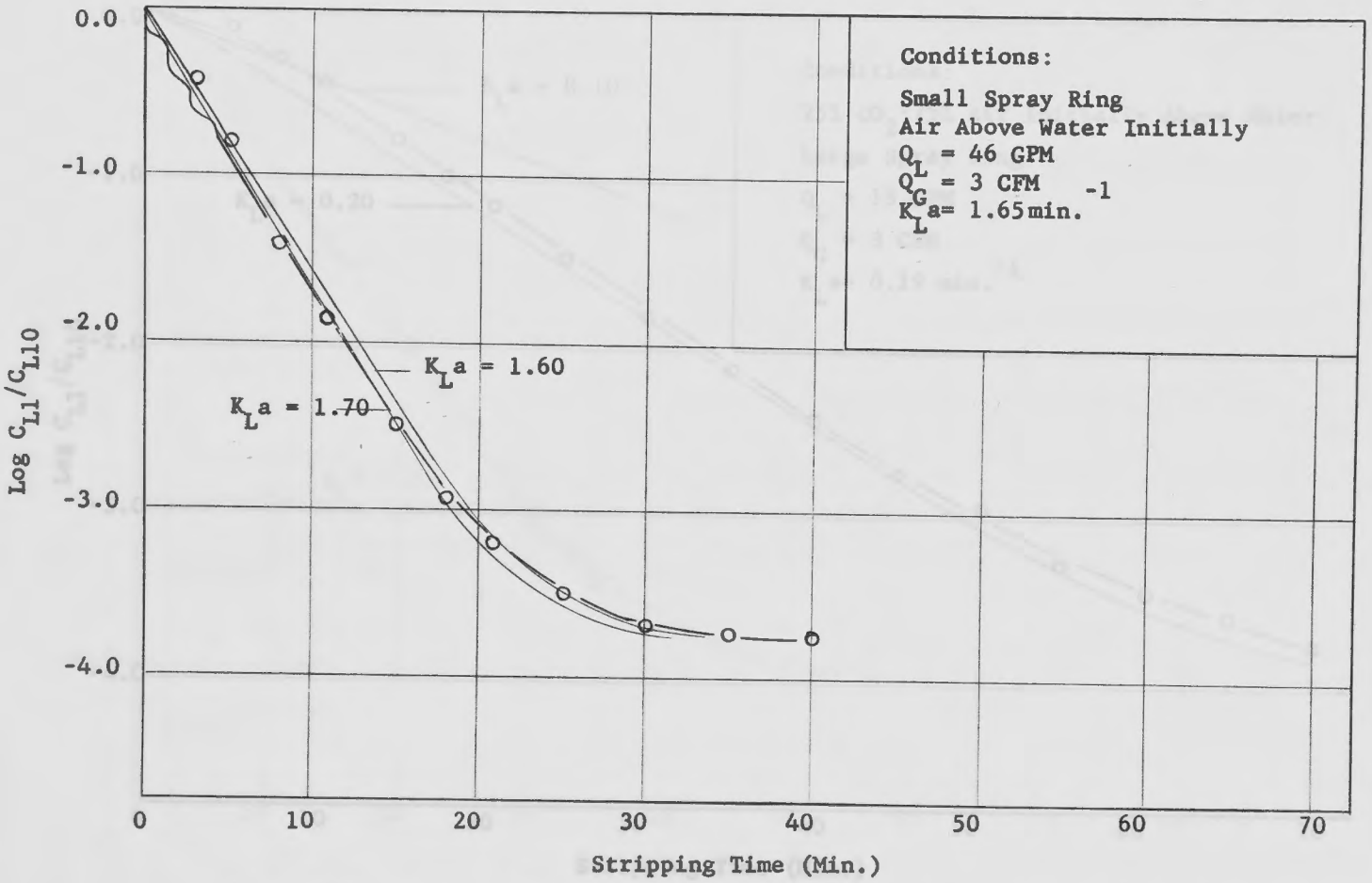

Figure 12. Fitting Experimental Data with Theoretical Curve - Run 48.

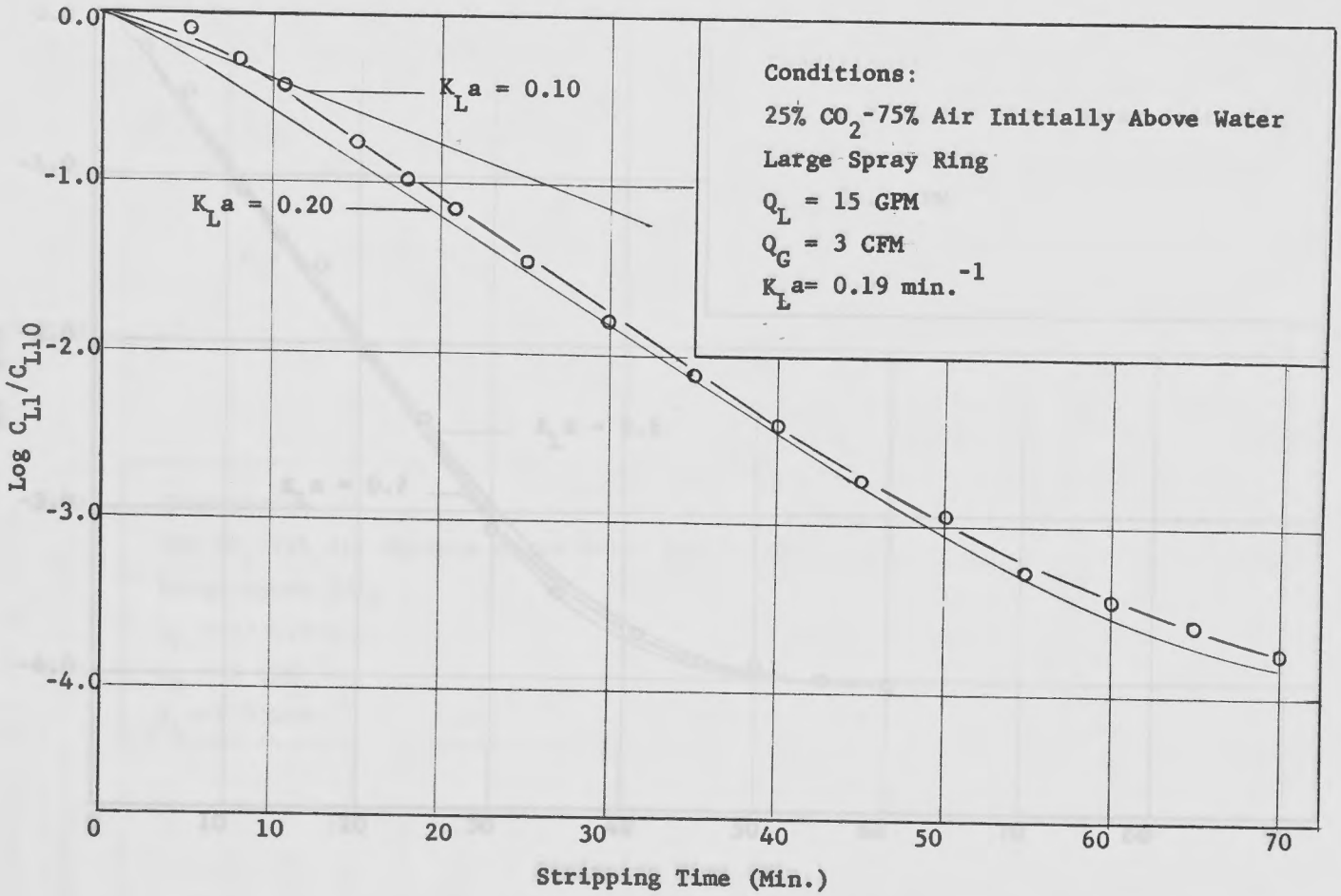

Figure 13. Fitting Experimental Data with Theoretical Curve - Run 40.

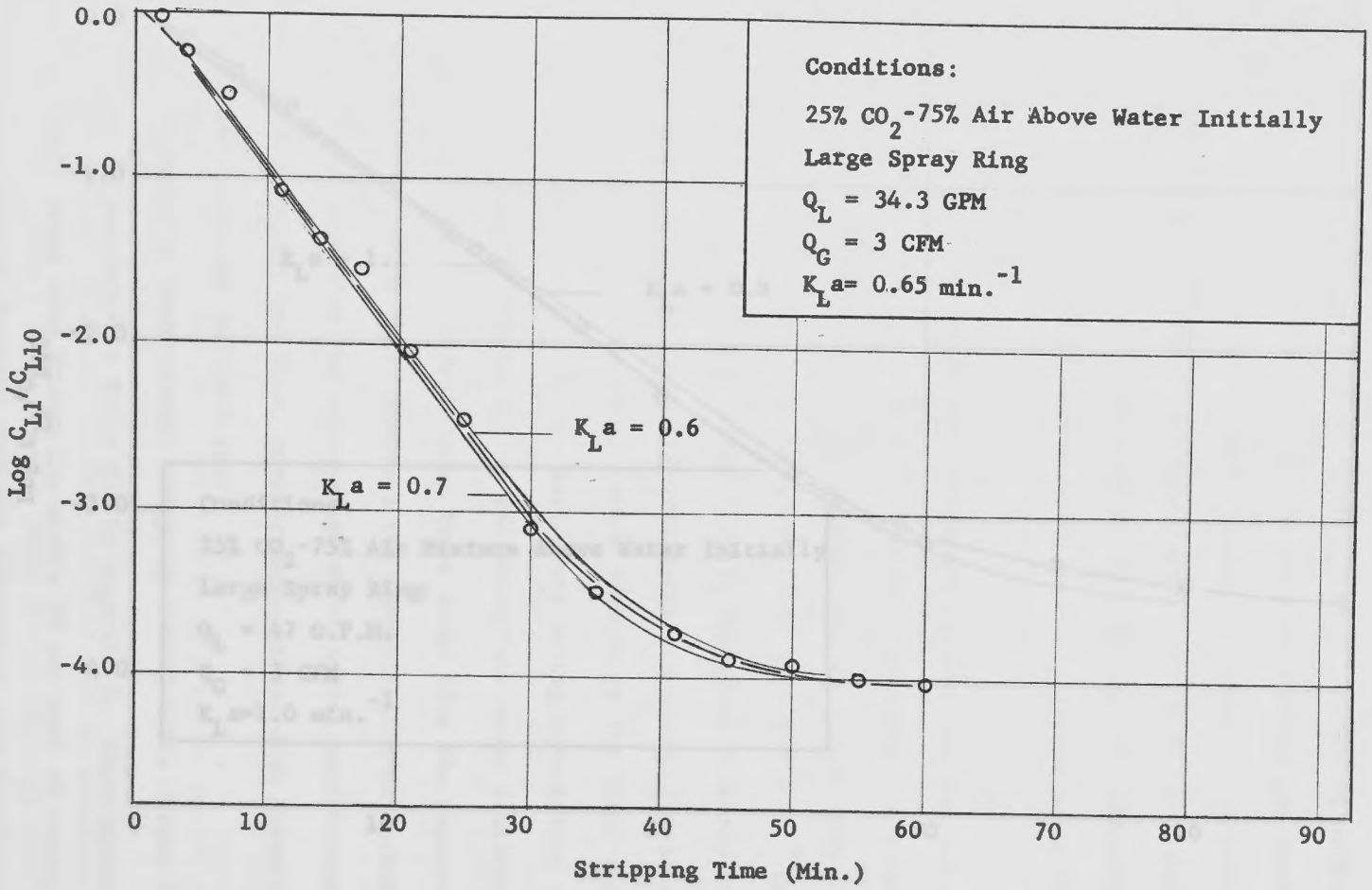

Figure 14. Fitting Experimental Data to Theoretical Curve - Run 42.

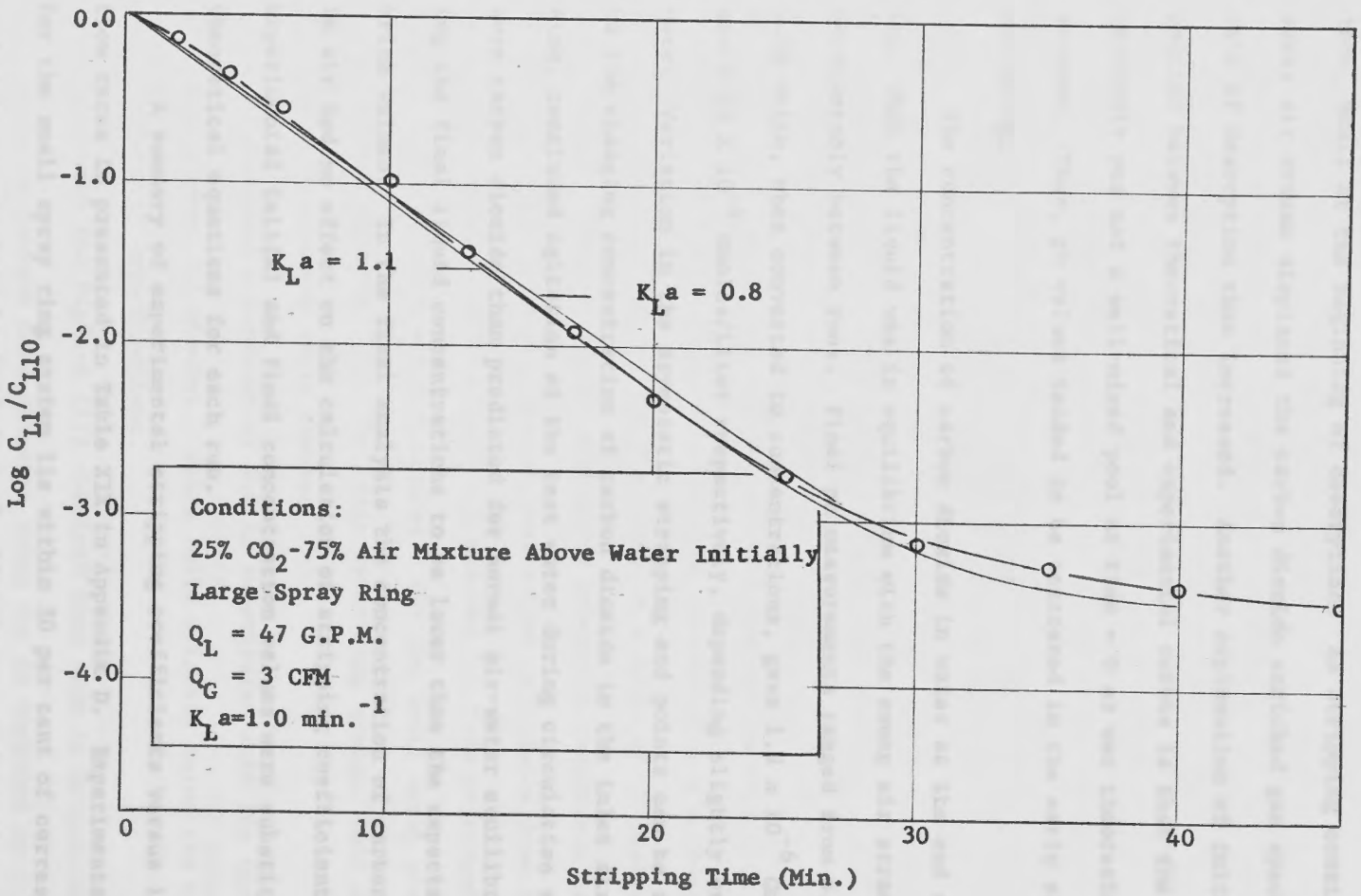

Figure 15. Fitting Experimental Data with Theoretical Curve - Run 45.

fore, small at the beginning of desorption. As stripping continued, the sweep air stream displaced the carbon dioxide enriched gas space and the rate of desorption then increased. Another explanation of initial descrepancies between theoretical and experimental curves is that the water reservoir was not a well-mixed pool at time = 0 as was theoretically assumed. Thus, ph values tended to be scattered in the early stages of stripping.

The concentration of carbon dioxide in water at the end of stripping, when the liquid was in equilibrium with the sweep air stream, varied considerably between runs. Final ph measurements ranged from 6.14 to 6.70 which, when converted to concentrations, gave 1.9×10^{-6} Gmoles/Liter and 0.29×10^{-6} Gmoles/Liter respectively, depending slightly on temperature. Variation in the asymptotic stripping end points can be attributed to the changing concentration of carbon dioxide in the inlet air stream. Also, continued agitation of the test water during circulation released more carbon dioxide than predicted for normal air-water equilibrium causing the final liquid concentrations to be lower than the expected equilibrium values. In the final analysis the concentration of carbon dioxide in air had no effect on the calculation of stripping coefficients, since experimental initial and final concentration values were substituted into theoretical equations for each run.

A summary of experimental stripping coefficients versus liquid flow rates is presented in Table XIX in Appendix D. Experimental values for the small spray ring system lie within 30 per cent of corresponding packed tower results obtained from the literature, and coefficients for

the large spray ring system lie within 67 per cent of the same literature values. Koch (6) used 1/2-inch and 3/4-inch raschig rings in a 10-inch pipe packed to a heighth of 4 feet to study carbon dioxide desorption from water with air. He determined that the liquid film coefficient was independent of gas velocity and packing size and varied with water flow rate according to the relationship:

$$K_L a = 0.25\ L^{0.96}$$

where:

$K_L a$ = liquid-film coefficient, 1/hour

L = lb moles/hr-ft.^{2}

Koch also makes reference to similar work done by Sherwood (10) who obtained an exponent of 0.8 instead of 0.96 by employing a 2.05-inch I.D. tower packed with 3/8-inch raschig rings to a depth of 12 inches.

When the assumption of negligible gas-phase resistance is made, the over-all liquid-phase transfer coefficient calculated from Koch's equation for Q_L = 34 GPM is $K_L a$ = 1.3 minutes^{-1}. This corresponds to experimental values of $K_L a$ = 0.9 minutes^{-1} for the small spray ring system and $K_L a$ = 0.65 minutes^{-1} for the large spray ring system, both obtained without packing in the spray chamber.

If Sherwood's exponent of 0.8 is substituted into the above equation, $K_L a$ becomes 0.5 minutes^{-1} which falls slightly below the corresponding experimental determinations.

Sherwood and Pigford (11) obtained data from an oxygen-water absorption system to compare mass transfer rates for an unpacked spray absorber

with those of a packed tower. They concluded that the spray chamber closely approached the performance of a packed tower for very short packed heights, both for liquid-phase and gas-phase controlled systems. Their analysis substantiates the validity of the comparisons made between this investigation and work done by Koch.

Since stripping was initiated differently for each liquid-gas contacting system, it was necessary to determine whether or not initial stripping conditions inside the spray chamber had an effect on the value of the over-all stripping rate coefficient. Runs carried out at identical liquid and sweep gas flow rates and distinguishable only by the method of saturating the test water were made using the larger spray ring system.

In the first investigation a 25 per cent carbon dioxide - 75 per cent air mixture was used to saturate water in the liquid pool and stripping began with this gas composition above the carbonated water. Secondly, water was transferred to the test tank after being saturated with carbon dioxide in a 55 gallon drum and, thus, stripping began with essentially air contained in the gas volume, V_G. By utilization of the appropriate mathematical model, stripping coefficients were determined by fitting experimental results with theoretical predictions. Values obtained are presented in Figures 14 and 16. Theoretical equations in Figure 16 do not coincide with experimental concentrations until the stripping time reached twenty minutes due to the previously discussed excess of carbon dioxide initially in the gas space. After twenty minutes, comparison can be made which leads to a stripping rate coefficient of 0.5 minutes^{-1}. This value compares favorably with the coefficient, 0.65 minutes^{-1}, deter-

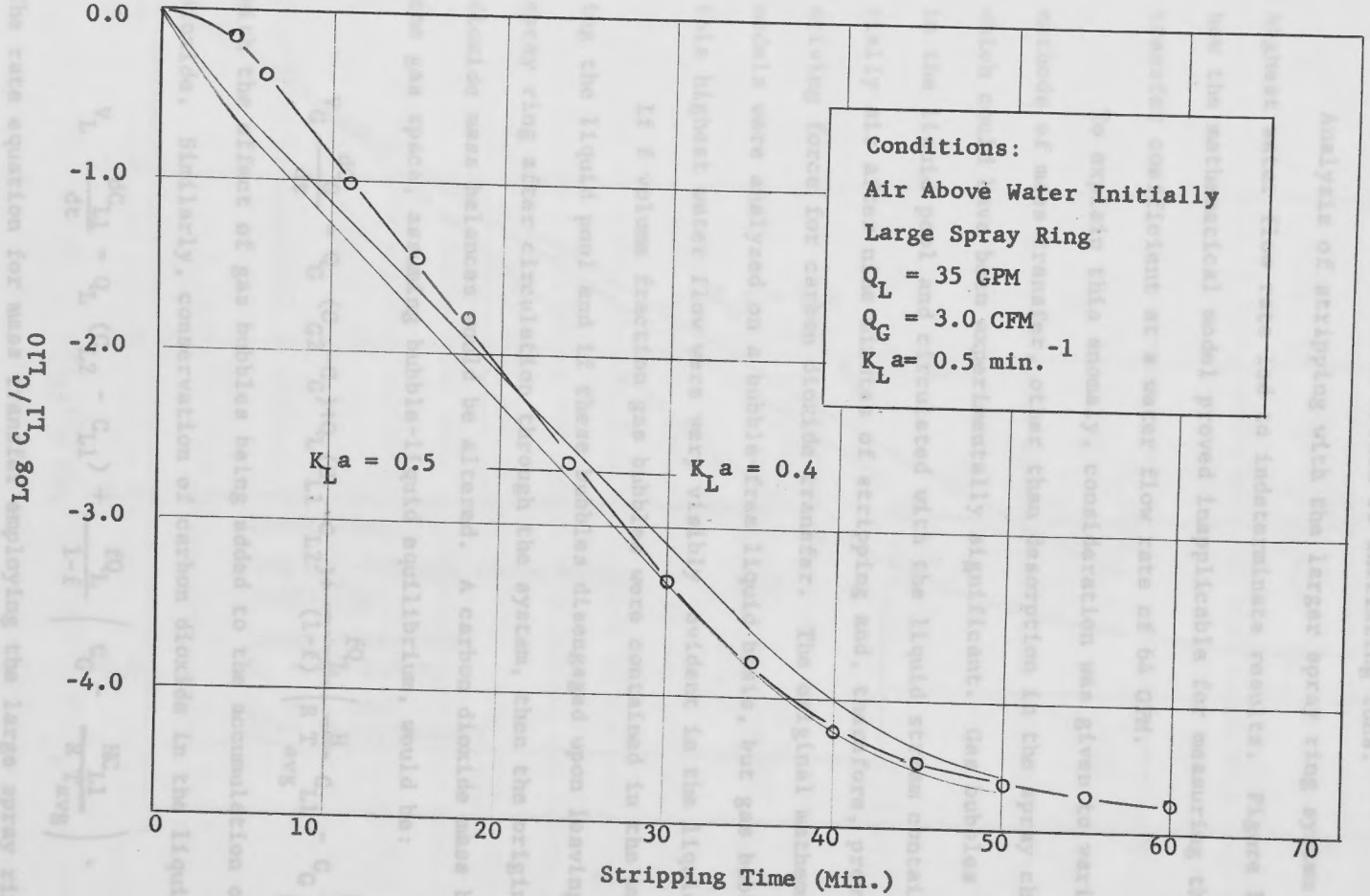

Figure 16. Fitting Experimental Data with Theoretical Curve - Run 38.

mined from the alternative method of initiating runs.

Analysis of stripping with the larger spray ring system at the highest water flow rate led to indeterminate results. Figure 17 depicts how the mathematical model proved inapplicable for measuring the mass transfer coefficient at a water flow rate of 64 GPM.

To explain this anomaly, consideration was given to various methods of mass transfer, other than desorption in the spray chamber, which could have been experimentally significant. Gas bubbles entrapped in the liquid pool and circulated with the liquid stream contained essentially air after nine minutes of stripping and, therefore, provided a driving force for carbon dioxide transfer. The original mathematical models were analyzed on a bubble-free liquid basis, but gas bubbles at this highest water flow were very visibly evident in the liquid stream.

If f volume fraction gas bubbles were contained in the water entering the liquid pool and if these bubbles disengaged upon leaving the spray ring after circulation through the system, then the original carbon dioxide mass balances would be altered. A carbon dioxide mass balance on the gas space, assuming bubble-liquid equilibrium, would be:

$$V_G \frac{dC_G}{dt} = Q_G (C_{G2}-C_G)+Q_L(C_{L1}-C_{L2})+ \frac{fQ_L}{(1-f)}\left(\frac{H}{R T_{avg}} C_{L1} - C_G\right) \qquad (38)$$

with the effect of gas bubbles being added to the accumulation of carbon dioxide. Similarly, conservation of carbon dioxide in the liquid pool is

$$V_L \frac{dC_{L1}}{dt} = Q_L (C_{L2} - C_{L1}) + \frac{fQ_L}{1-f}\left(C_G - \frac{HC_{L1}}{R T_{avg}}\right). \qquad (39)$$

The rate equation for mass transfer employing the large spray ring system

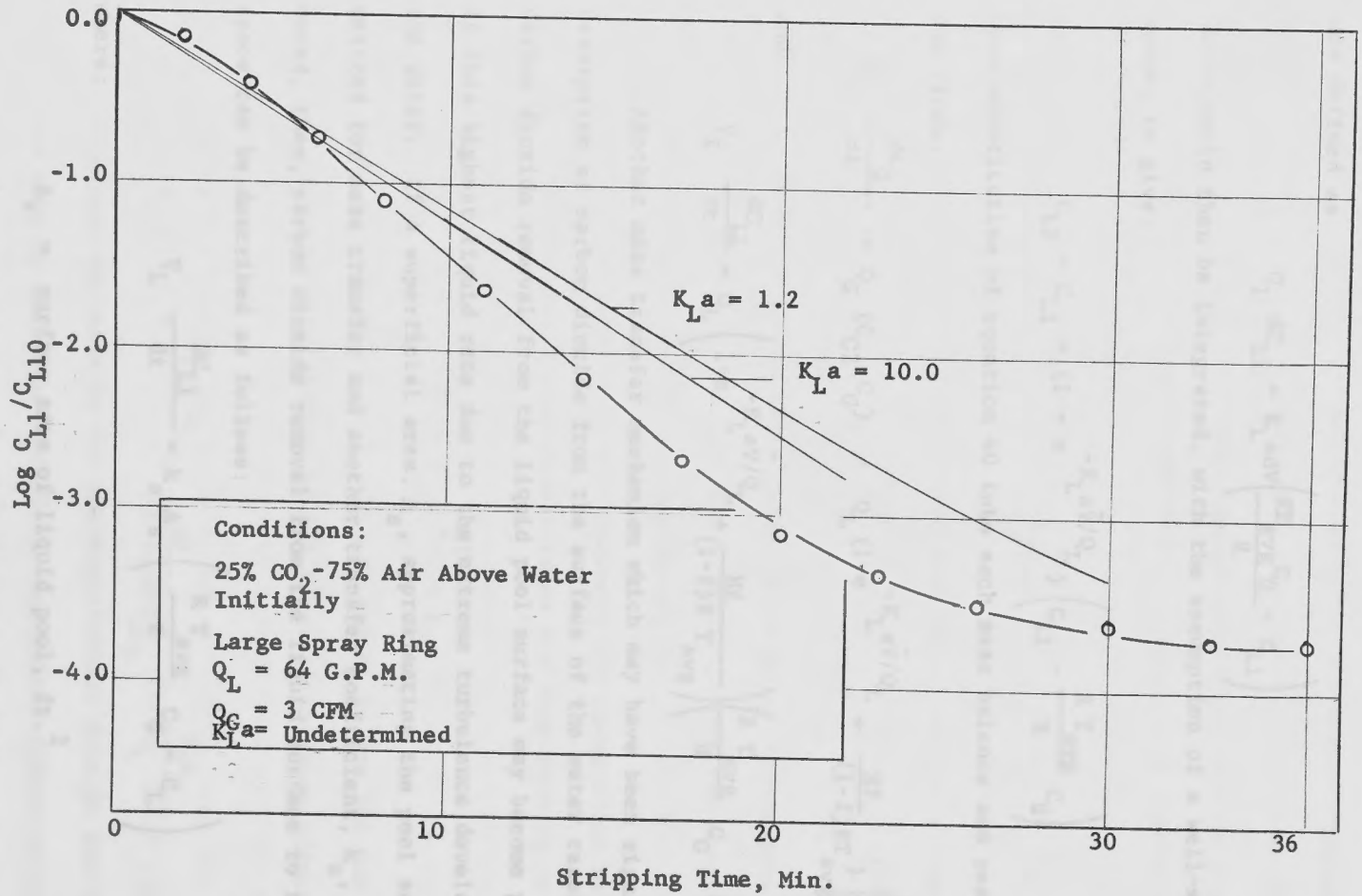

Figure 17. Fitting Experimental Data to Theoretical Curve - Run 44.

was defined as

$$Q_L \, dC_{L1} = K_L a dV \left(\frac{RT_{avg} C_G}{H} - C_{L1} \right) \tag{19}$$

which could then be integrated, with the assumption of a well-mixed gas space, to give:

$$C_{L2} - C_{L1} = (1 - e^{-K_L a \bar{V}/Q_L}) \left(C_{L1} - \frac{R T_{avg}}{H} C_G \right) \tag{40}$$

Upon substitution of equation 40 into each mass balance and rearranging, one finds:

$$V_G \frac{dC_G}{dt} = Q_G (C_{G2} - C_G) - Q_L (1 - e^{-K_L a \bar{V}/Q_L} + \frac{Hf}{(1-f)RT_{avg}}) \left(\frac{RT_{avg}}{H} C_G - C_{L1} \right) \tag{41}$$

and

$$V_L \frac{dC_{L1}}{dt} = Q_L \left(1 - e^{-K_L a \bar{V}/Q_L} + \frac{Hf}{(1-f) R T_{avg}} \right) \left(\frac{R T_{avg}}{H} C_G - C_{L1} \right) \tag{42}$$

Another mass transfer mechanism which may have been significant was desorption of carbon dioxide from the surface of the water reservoir. Carbon dioxide removal from the liquid pool surface may become pronounced at this highest liquid rate due to the extreme turbulence developed in the water. If a superficial area, A_s, approximating the pool surface is defined for mass transfer and another transfer coefficient, k_s, is introduced, then, carbon dioxide removal from the liquid surface to the gas space can be described as follows:

$$V_L \frac{dC_{L1}}{dt} = k_s A_s \left(\frac{R T_{avg}}{H} C_G - C_{L1} \right) \tag{43}$$

where:

A_s = surface area of liquid pool, $ft.^2$

k_s = mass transfer coefficient, ft./min.

These combined mass transfer effects, desorption from spray droplets, the entrapped gas bubble effect and mass transfer from the liquid pool surface constitute the total removal of carbon dioxide from the water reservoir. Thus, the conservation statement for carbon dioxide in the liquid pool becomes:

$$V_L \frac{dC_{L1}}{dt} = Q_L \left(1-e^{-K_L a\bar{V}/Q_L} + \frac{Hf}{(1-f)\ R\ T_{avg}} + \frac{K_s A_s}{Q_L} \right) \left(\frac{R\ T_{avg}}{H}\ C_G - C_{L1} \right) \quad (44)$$

Similarly, the conservation of carbon dioxide in the gas stream becomes:

$$V_G \frac{dC_G}{dt} = Q_G(C_{G2}-C_G) - Q_L \left(1-e^{-K_L a\bar{V}/Q_L} + \frac{Hf}{(1-f)R\ T_{avg}} + \frac{k_s A_s}{Q_L} \right) \left(\frac{R\ T_{avg}}{H}\ C_G - C_{L1} \right) \quad (45)$$

These mass balances are identical with the original bubble-free conservation statements in equations (26) and (27) except for the constant term which is multiplied times the driving force.

If these "total effect" mass balances are combined as before and integrated to determine Y, the result takes the same form as in the bubble-free derivation:

$$Y = P_1 e^{r_1 T} + P_2 e^{r_2 T} + Z_2 . \quad (35)$$

The constant, A_1, contained in P_1, P_2, r_1 and r_2 is now the sum of three mass transfer mechanisms instead of the single desorption effect, and is defined as:

$$A_1 = 1 - e^{-K_L a\bar{V}/Q_L} + \frac{Hf}{(1-f)\ R\ T_{avg}} + \frac{k_s A_s}{Q_L} . \quad (46)$$

An attempt was made to fit the experimental data at the highest liquid flow rate by using this additive theoretical effect on carbon dioxide desorption. It was discovered, however, that regardless of the

magnitude of A_1 above a value of 1.0, the theoretical stripping curve retained the same slope. At $A_1 = 1$, $k_L a$ is ∞ and the other mass transfer effects are negligible or some combination of the three effects is 1.0. The effect of increasing A_1 on the theoretical equation was possibly hidden due to the fact that the driving force for mass transfer from the liquid to the gas was always very small for the experimental conditions of this investigation.

The sweep air stream entering the outer gas pool or spray chamber comes into this liquid-gas contacting volume directly above the liquid pool surface. If air displaces the carbon dioxide enriched gas near the water before diffusing to all parts of the chamber, a large driving force for mass transfer may exist at the pool surface. This phenomenon is more apt to be significant at the high liquid flow rates due to the "dragging" effect of spray droplets returning to the water reservoir. As a result, the well-mixed gas space assumption may involve quite a large error at the highest liquid flow. The above consideration is another possible explanation for failure of the large spray ring model at the highest liquid flow rate, but studies to correct this erroneous assumption would be a major problem and the work was not undertaken here.

Plots of reciprocal over-all liquid-phase mass transfer coefficient versus reciprocal water flow rate for each spray ring are presented in Figure 18 and Figure 19. From these graphs insight as to the magnitude of individual liquid-phase and gas-phase coefficients can be determined. By assuming that the individual liquid-phase mass transfer coefficient is proportional to liquid flow rate raised to a power, the

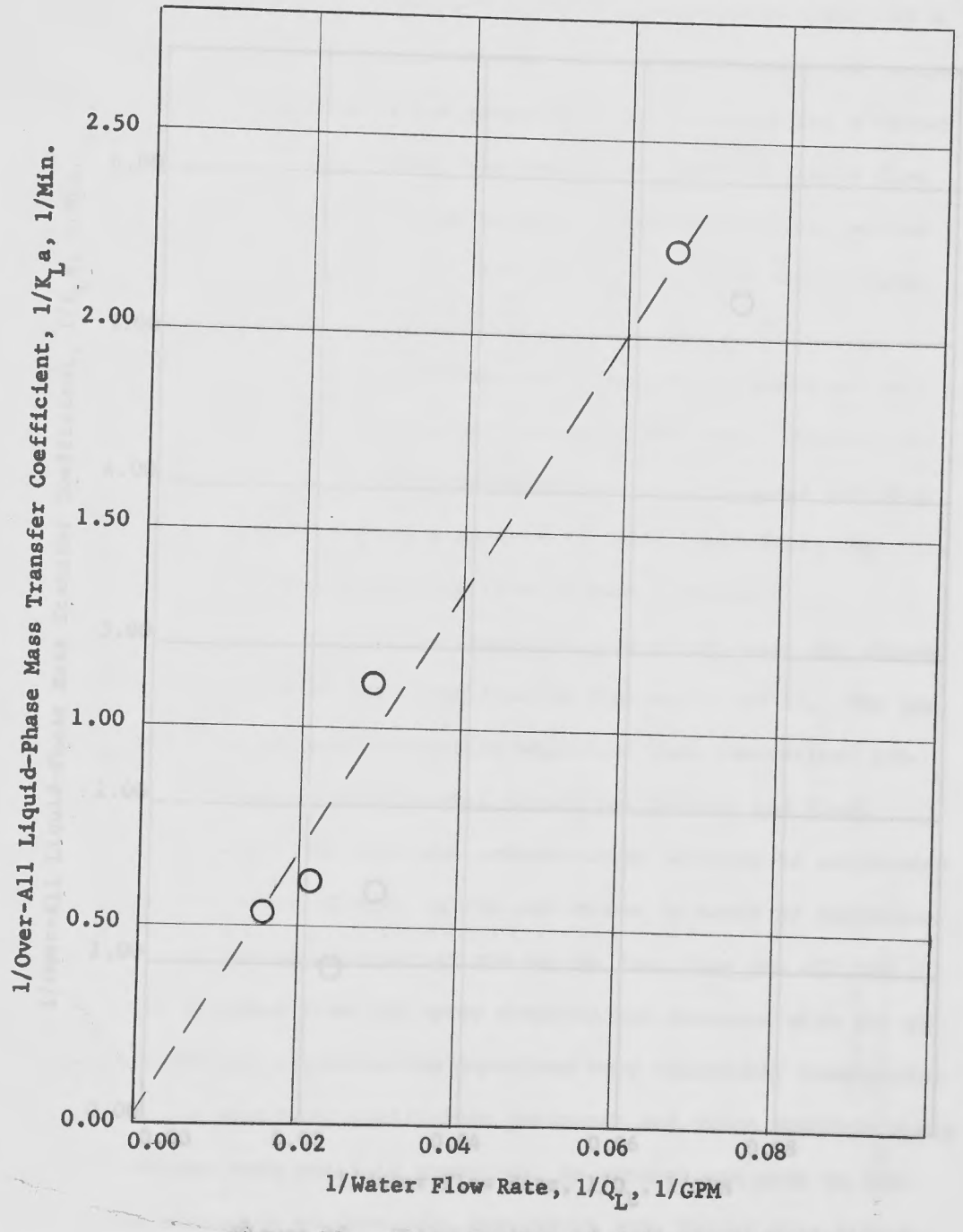

Figure 18. Determination of Individual Mass Transfer Coefficients for the Small Spray Ring.

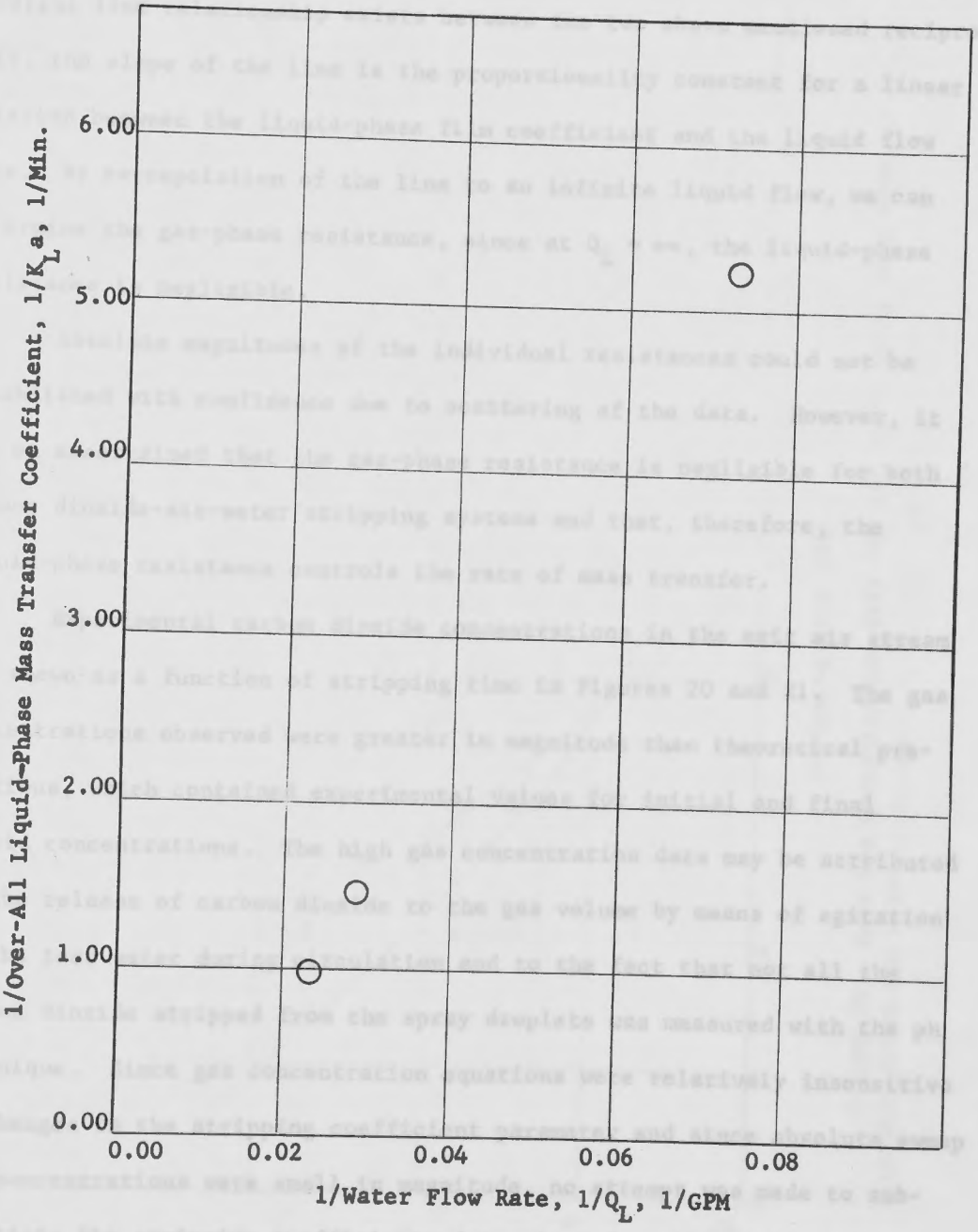

Figure 19. Determination of Individual Mass Transfer Coefficients for the Large Spray Ring.

intercept and slope of the plots have mass transfer explanations. If a straight line relationship exists between the two above mentioned reciprocals, the slope of the line is the proportionality constant for a linear relation between the liquid-phase film coefficient and the liquid flow rate. By extrapolation of the line to an infinite liquid flow, we can determine the gas-phase resistance, since at $Q_L = \infty$, the liquid-phase resistance is negligible.

Absolute magnitudes of the individual resistances could not be established with confidence due to scattering of the data. However, it can be ascertained that the gas-phase resistance is negligible for both carbon dioxide-air-water stripping systems and that, therefore, the liquid-phase resistance controls the rate of mass transfer.

Experimental carbon dioxide concentrations in the exit air stream are shown as a function of stripping time in Figures 20 and 21. The gas concentrations observed were greater in magnitude than theoretical predictions, which contained experimental values for initial and final liquid concentrations. The high gas concentration data may be attributed to the release of carbon dioxide to the gas volume by means of agitation of the test water during circulation and to the fact that not all the carbon dioxide stripped from the spray droplets was measured with the ph technique. Since gas concentration equations were relatively insensitive to changes in the stripping coefficient parameter and since absolute sweep gas concentrations were small in magnitude, no attempt was made to substantiate the stripping coefficients determined from liquid data with a similar analysis employing gas data. However, theoretical plots of

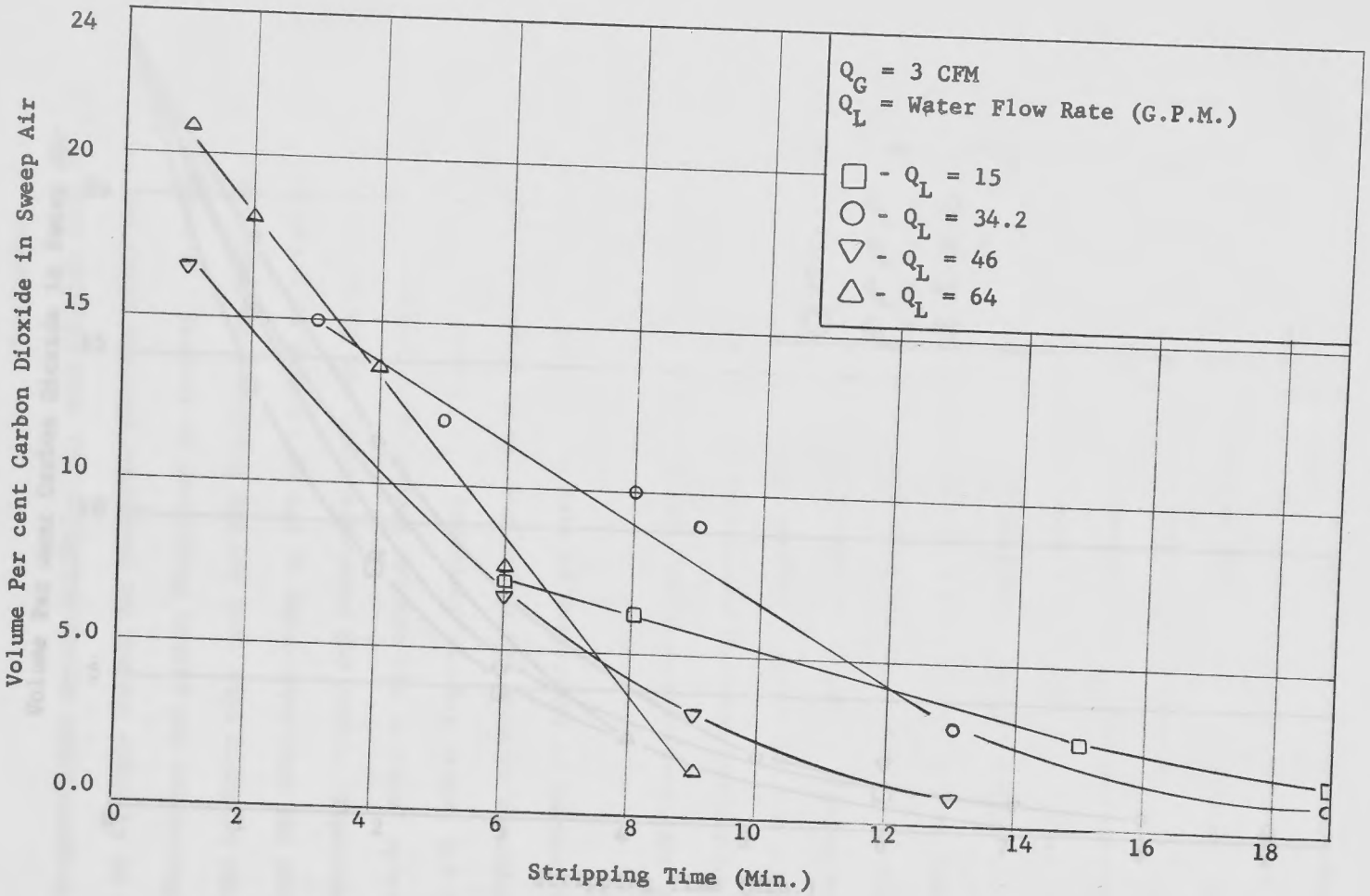

Figure 20. Exit Gas Concentration Data for the Small Spray Ring when Air is Initially Above the Water.

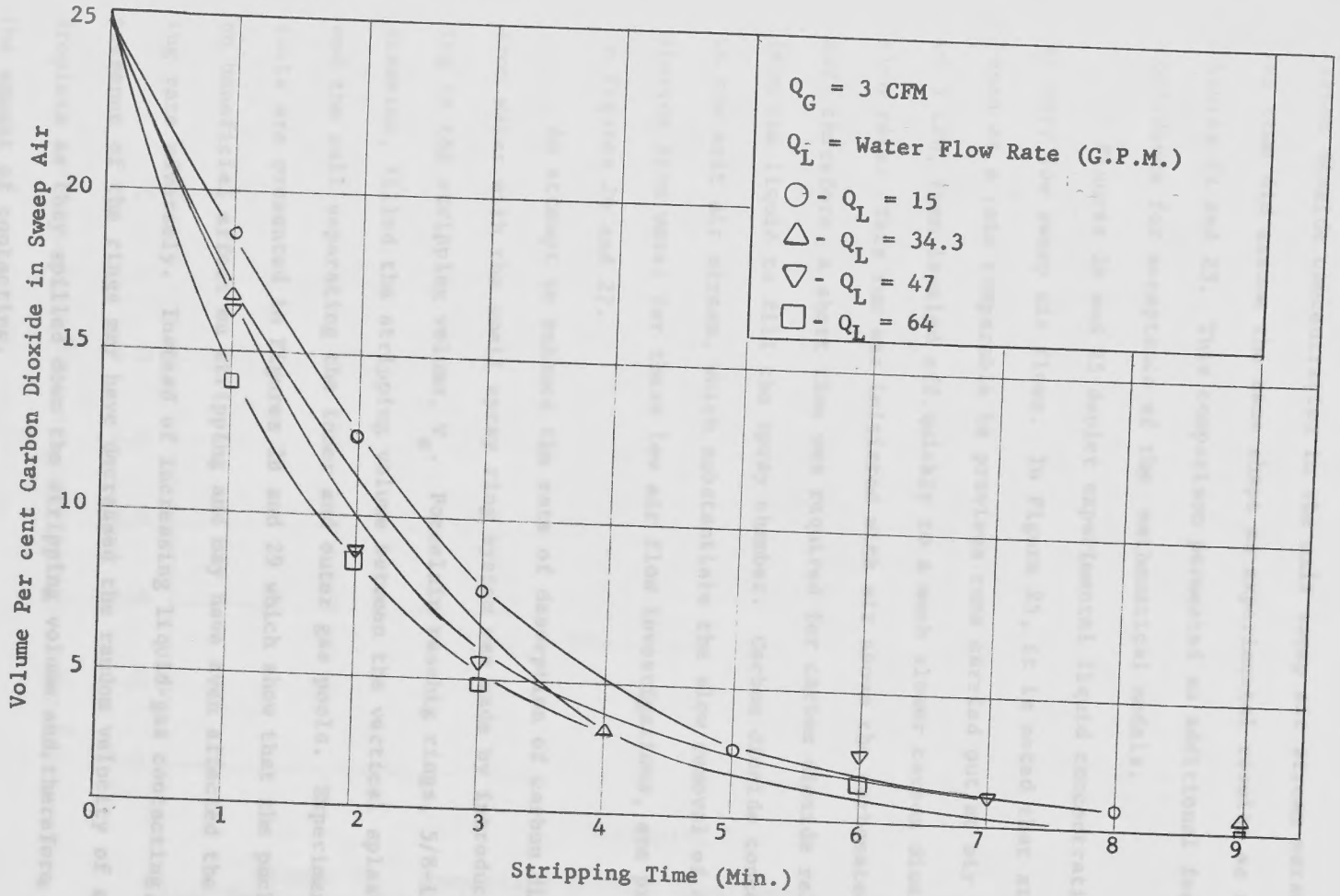

Figure 21. Exit Gas Concentration Data for the Larger Spray Ring when a 25 Per Cent Carbon Dioxide - 75 Per Cent Air Mixture is Initially Above the Water.

carbon dioxide concentration in the exit sweep air stream versus stripping time did assume the same shape as experimental results as shown in Figures 22 and 23. This comparison permeated an additional feeling of confidence for acceptance of the mathematical models.

Figures 24 and 25 depict experimental liquid concentration curves at very low sweep air flows. In Figure 25, it is noted that stripping began at a rate comparable to previous runs carried out at air flow rates of 3 CFM, then leveled off quickly to a much slower carbon dioxide desorption rate. This run was initiated with air above the carbonated water and, therefore, a short time was required for carbon dioxide released from the liquid to fill the spray chamber. Carbon dioxide concentrations in the exit air stream, which substantiate the slow removal of carbon dioxide from water for these low air flow investigations, are presented in Figures 26 and 27.

An attempt to enhance the rate of desorption of carbon dioxide from water with the small spray ring system was made by introducing packing in the stripping volume, V_s. Porcelain raschig rings, 5/8-inch in diameter, filled the stripping volume between the vertical splash baffle and the wall separating the inner and outer gas pools. Experimental results are presented in Figures 28 and 29 which show that the packing had no beneficial effect on stripping and may have even affected the stripping rate adversely. Instead of increasing liquid-gas contacting, the presence of the rings may have decreased the random velocity of spray droplets as they spilled down the stripping volume and, therefore, decreased the amount of contacting.

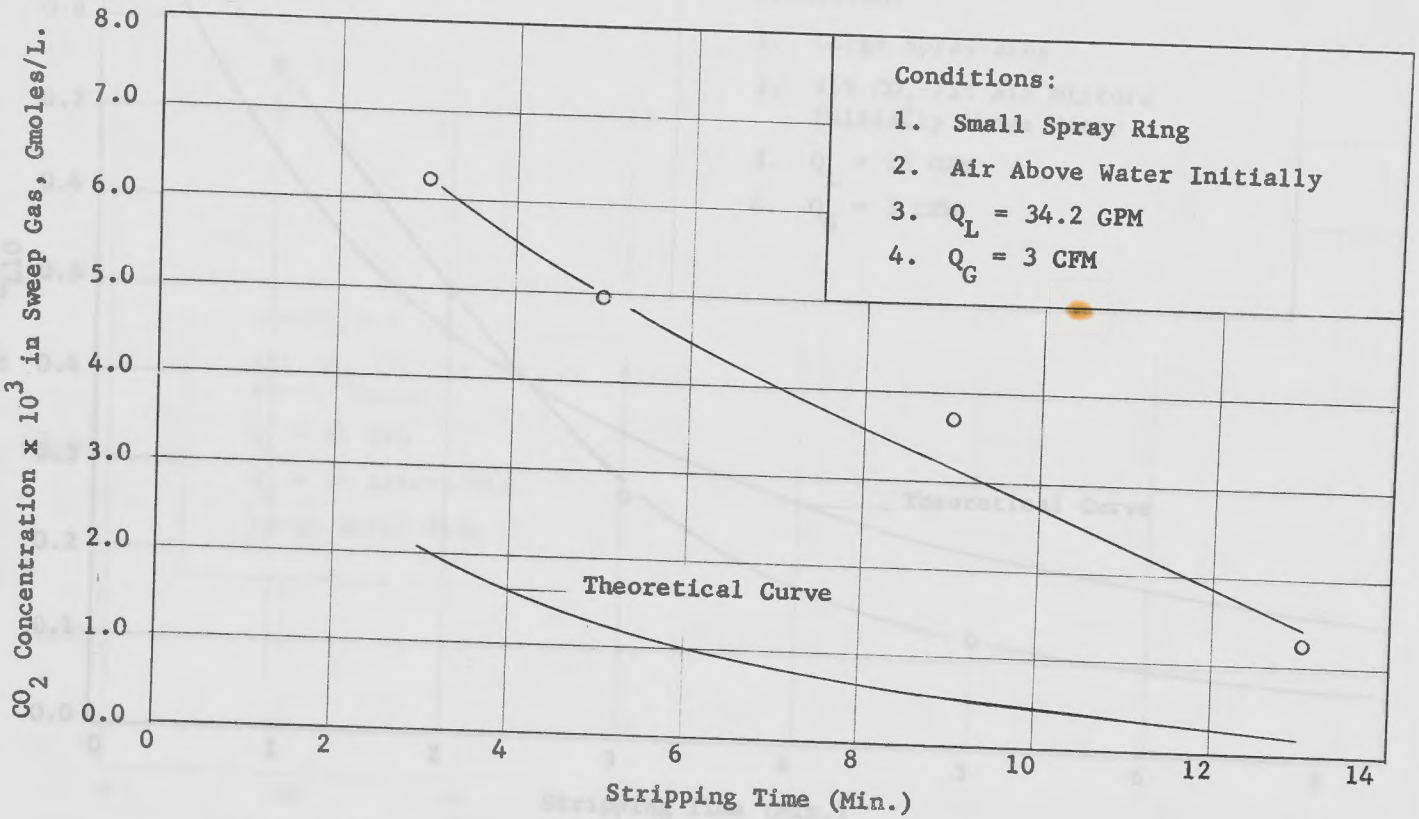

Figure 22. Comparison Between Experimental Gas Concentrations and Theoretical Predictions at $K_L a$ = 0.9 1/Min.

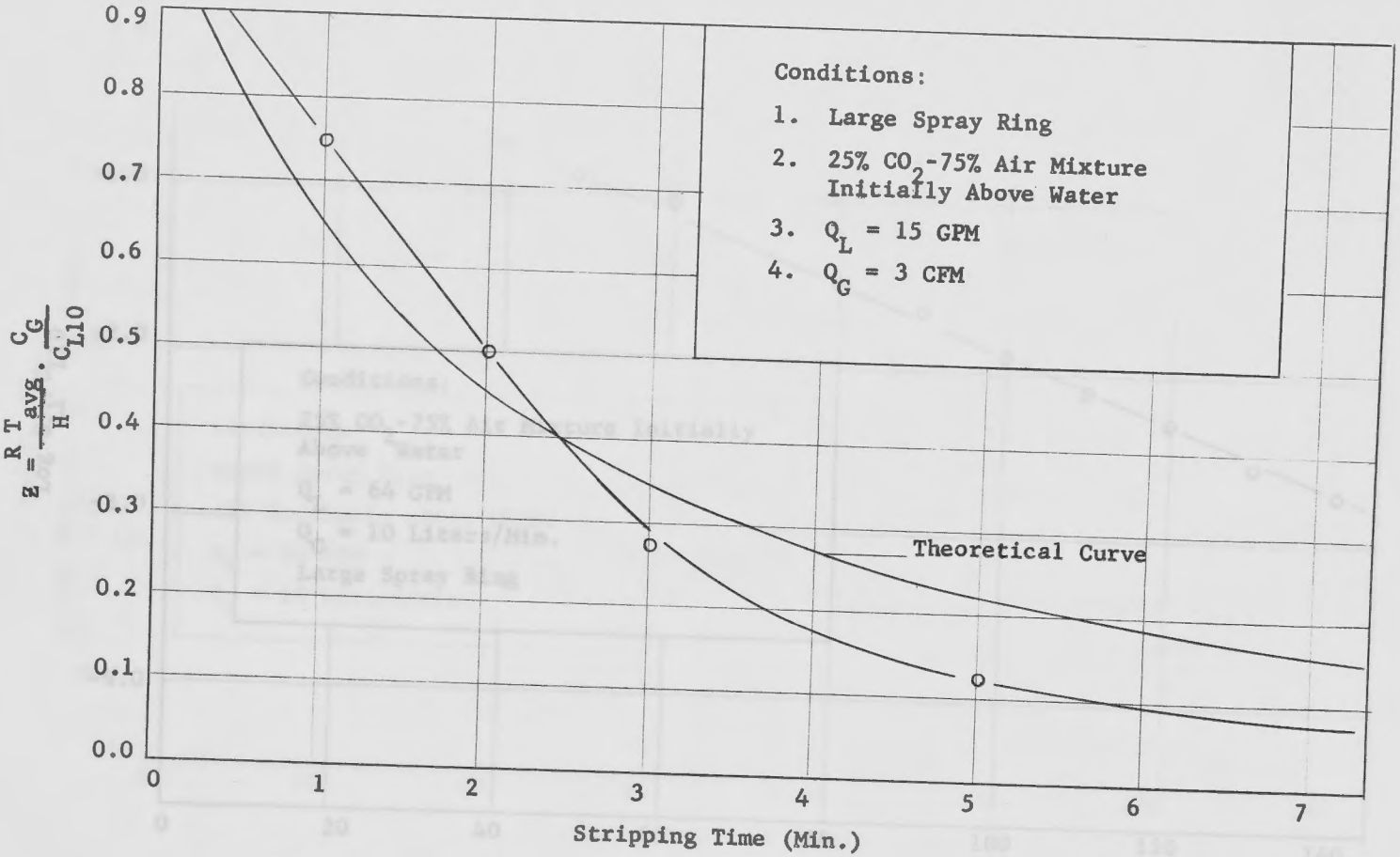

Figure 23. Comparison Between Experimental Gas Concentrations and Theoretical Predictions at $K_L a$ = 0.19 min.$^{-1}$.

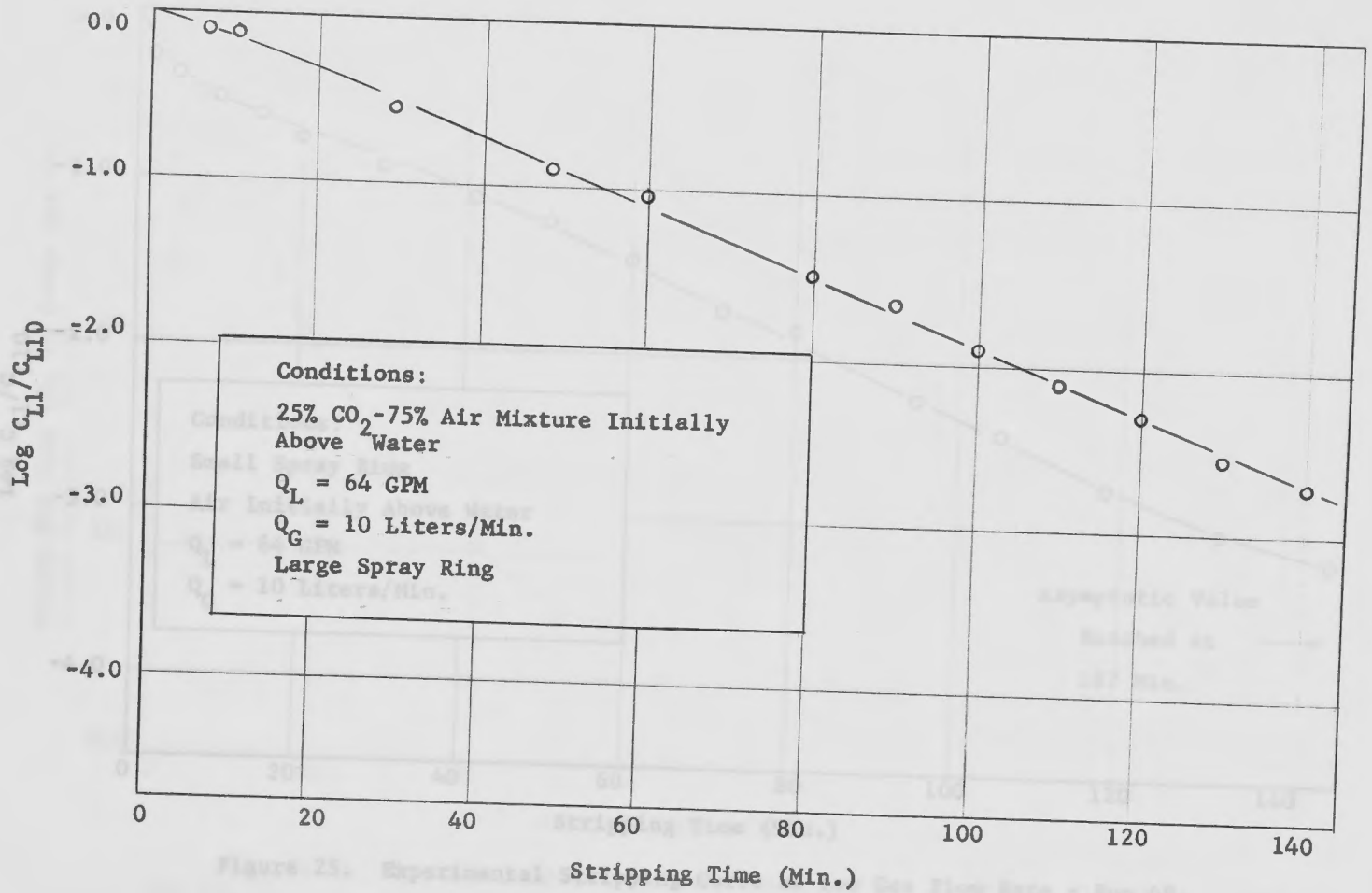

Figure 24. Experimental Stripping Curve at Low Gas Flow Rate - Run 46.

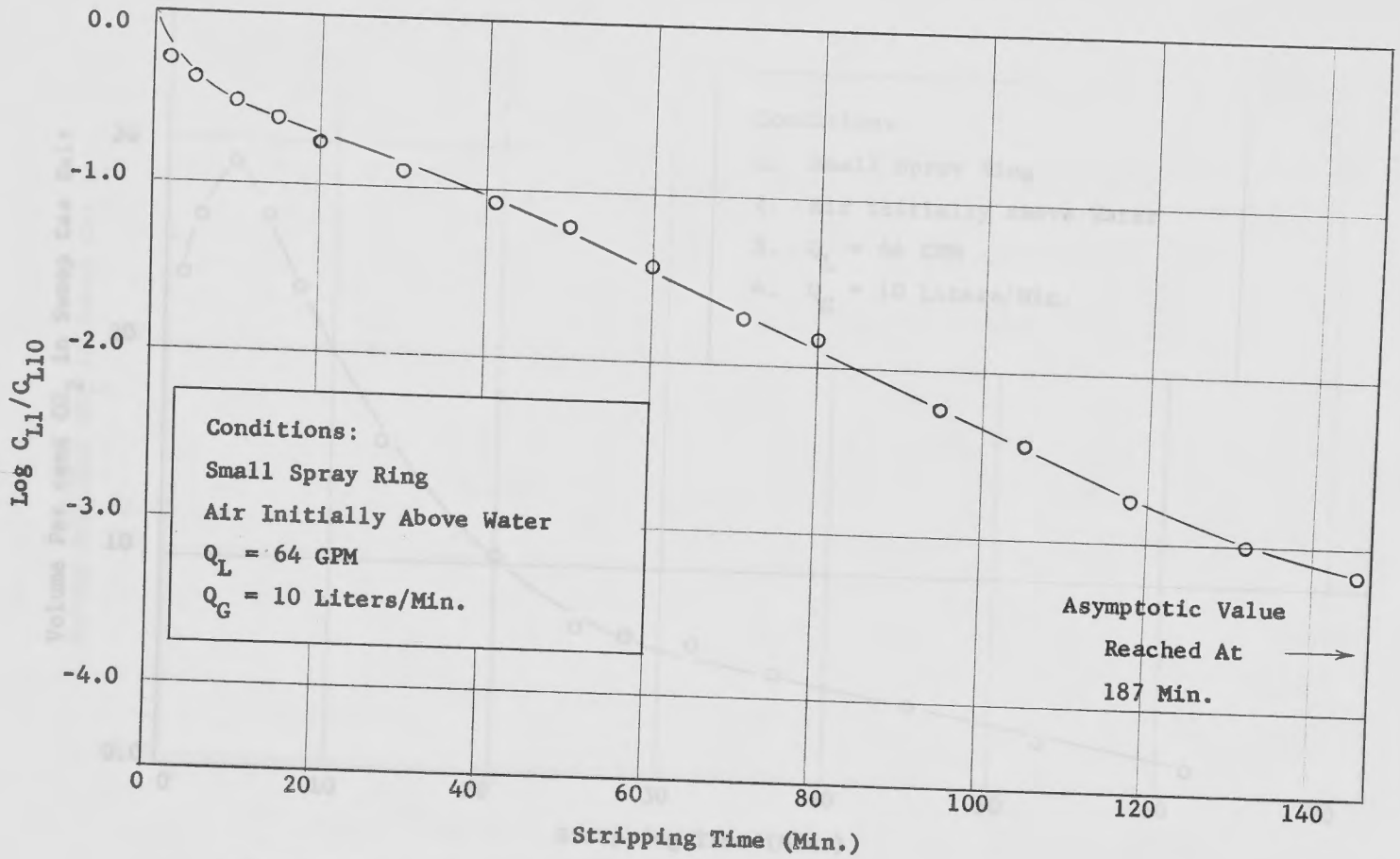

Figure 25. Experimental Stripping Curve at Low Gas Flow Rate - Run 49.

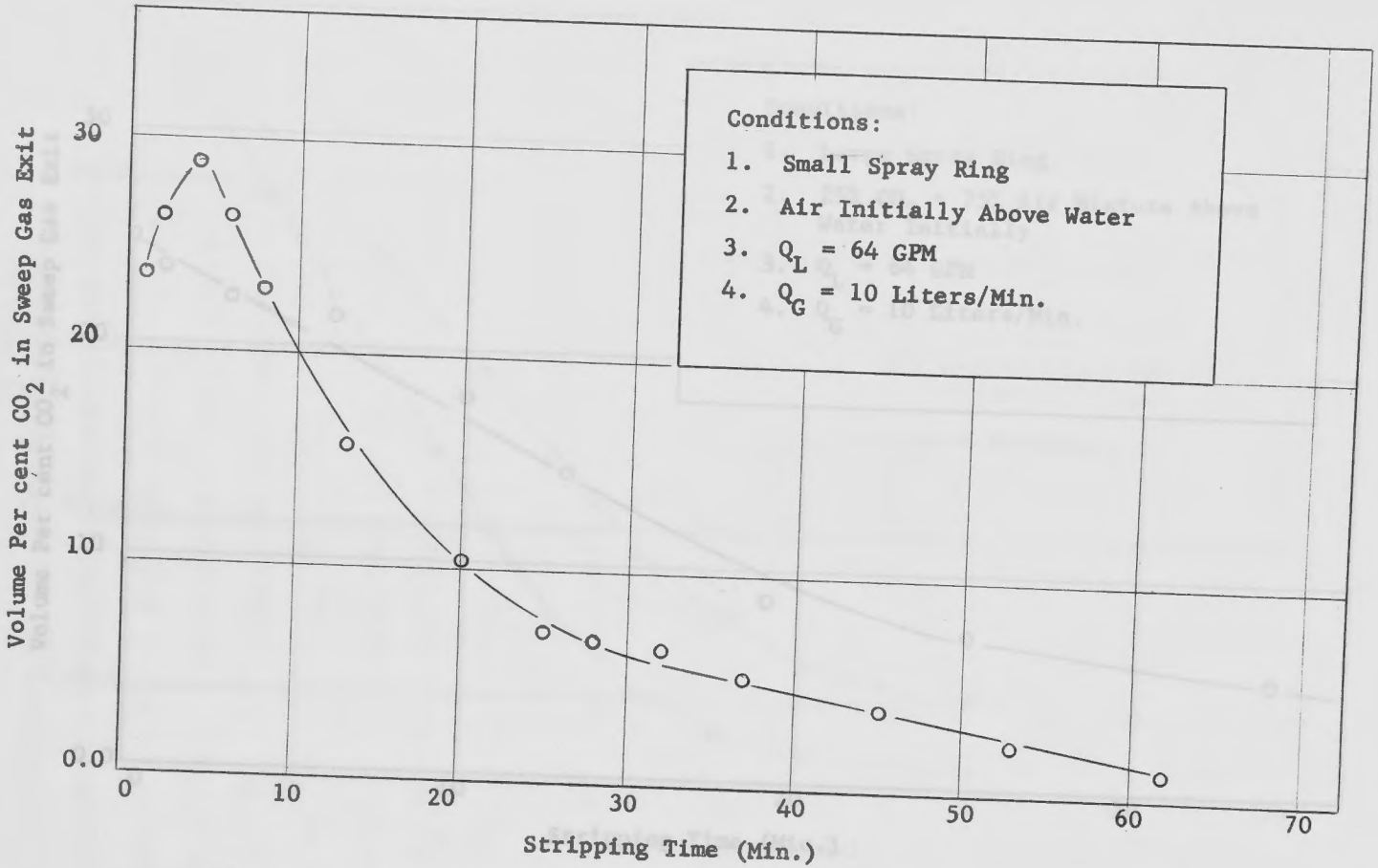

Figure 26. Experimental Gas Concentrations at Low Sweep Gas Flow Rate - Run 49.

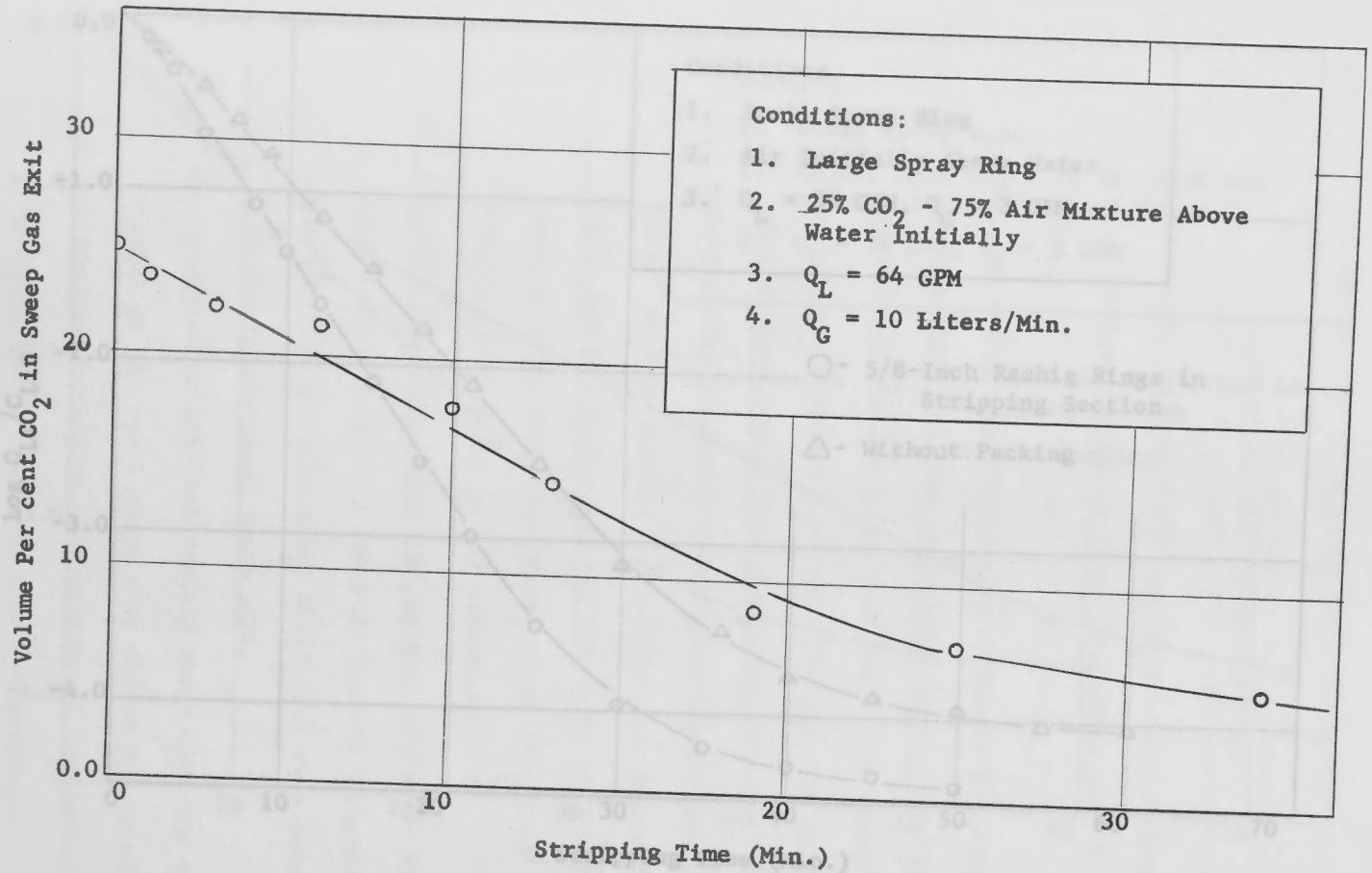

Figure 27. Experimental Gas Concentrations at Low Sweep Gas Flow Rate - Run 46.

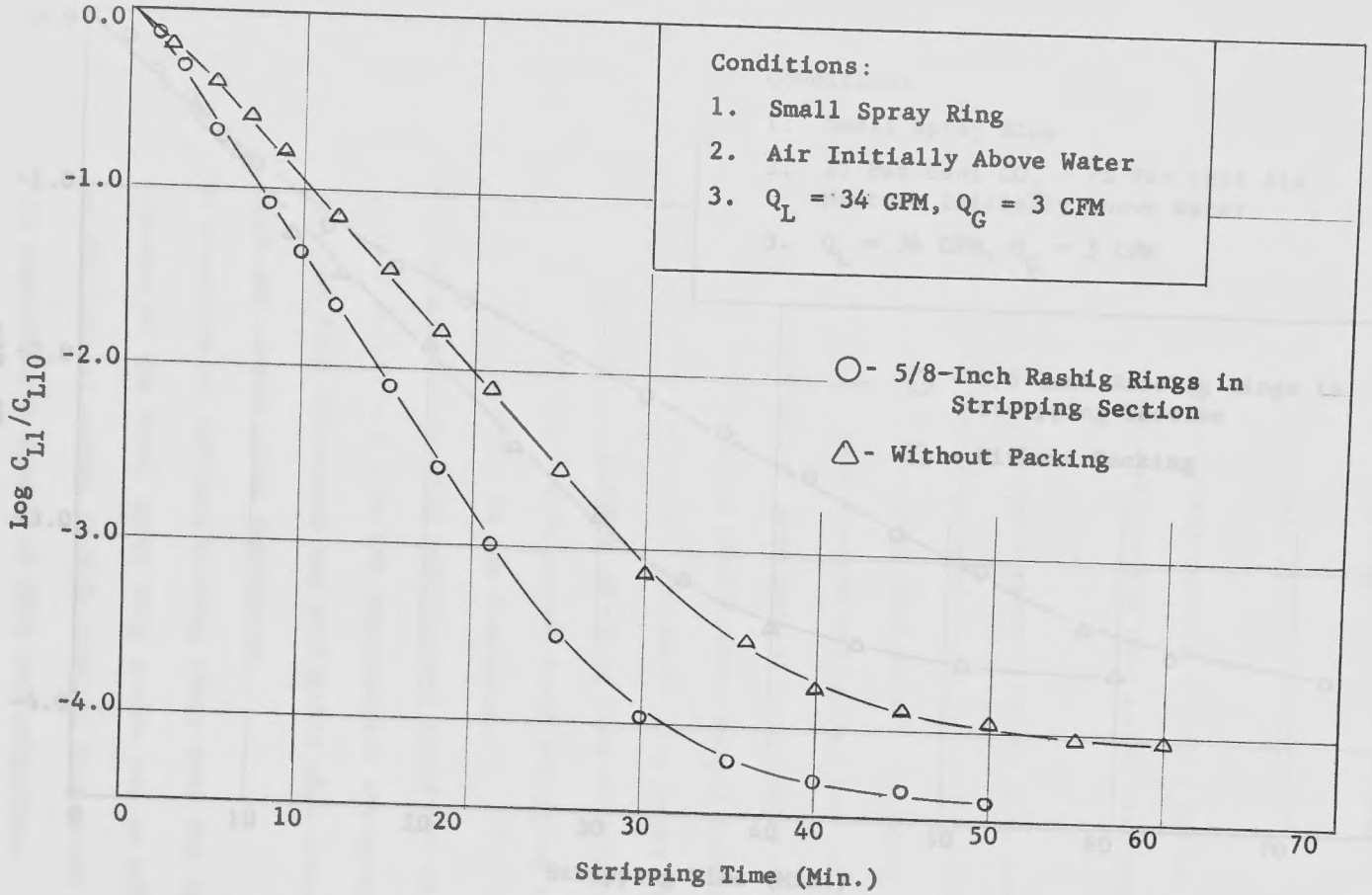

Figure 28. Experimental Data to Determine Effectiveness of 5/8-Inch Raschig Rings in Stripping Section - Air Above Water Initially.

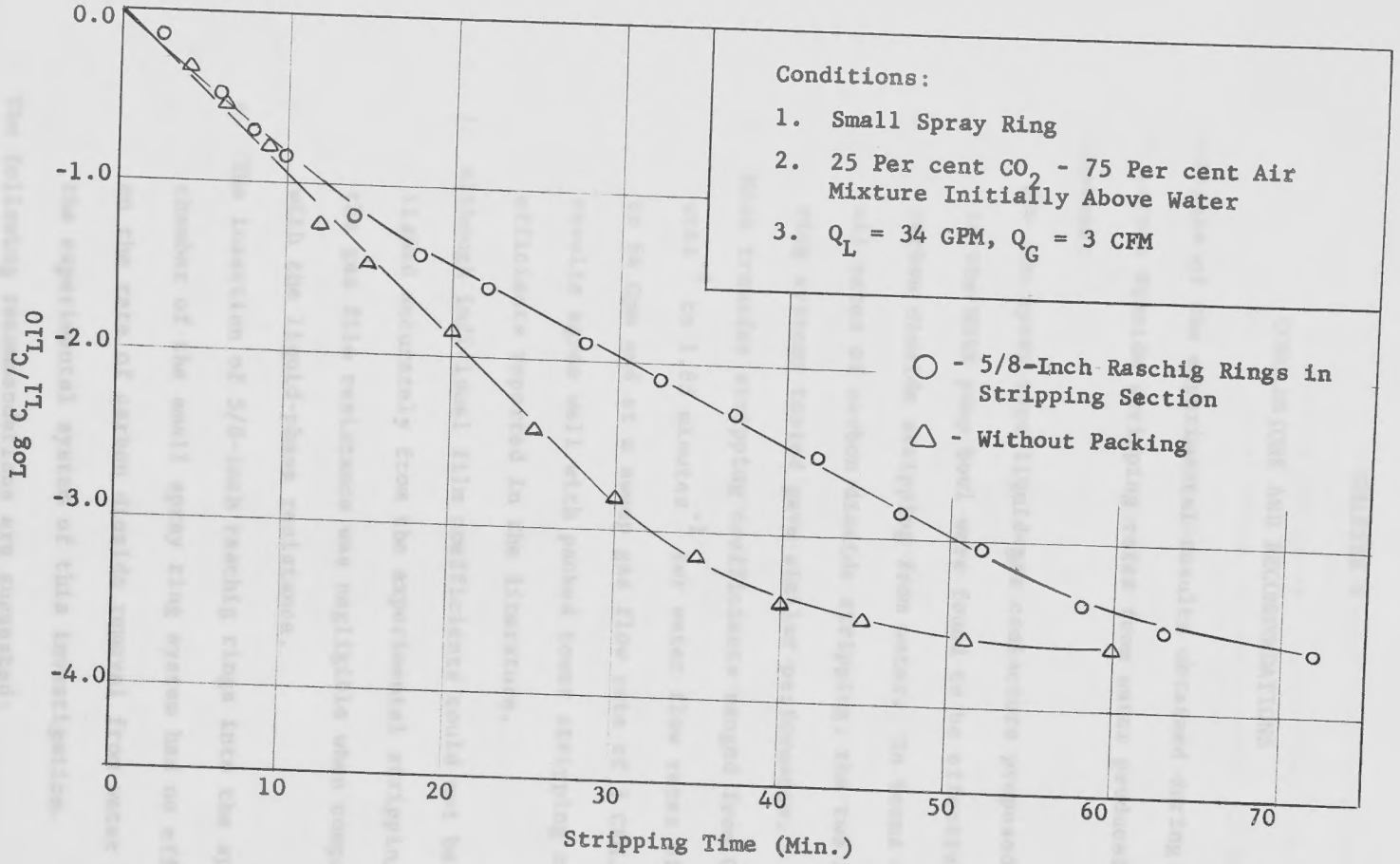

Figure 29. Experimental Results to Determine Effectiveness of 5/8-Inch Raschig Rings in Stripping Section - Gas Mixture Above Water Initially.

CHAPTER V

CONCLUSIONS AND RECOMMENDATIONS

Analysis of the experimental results obtained during this investigation of carbon dioxide stripping rates from water produced the following conclusions:

1. The two spray type liquid-gas contactors proposed for use in the MSRE pump bowl were found to be effective for carbon dioxide stripping from water. In terms of overall rates of carbon dioxide stripping, the two spray ring systems tested gave similar performance.
2. Mass transfer stripping coefficients ranged from 0.19 minutes^{-1} to 1.85 minutes^{-1} for water flow rates of 15 GPM to 64 Gpm and at a sweep gas flow rate of 3 CFM. These results agree well with packed tower stripping coefficients reported in the literature.
3. Although individual film coefficients could not be established accurately from the experimental stripping data, the gas film resistance was negligible when compared with the liquid-phase resistance.
4. The insertion of 5/8-inch raschig rings into the spray chamber of the small spray ring system had no effect on the rate of carbon dioxide removal from water in the experimental system of this investigation.

The following recommendations are suggested:

1. The dynamics of steady-state desorption experiments employing the two stripping systems should be investigated by allowing carbonated water to make one pass through the spray chamber and not be recirculated, as in the experiments of this investigation.

2. The ph technique for measuring carbon dioxide concentrations in water is inapplicable for accurate determinations and, therefore, other methods to measure the carbon dioxide concentration in water should be employed in future work. One alternative method was presented by Sherwood and Holloway (10).

LIST OF REFERENCES

LIST OF REFERENCES

1. Dole, M., "The Glass Electrode," John Wiley and Sons, Inc., (1941).

2. Foust, A. S., L. A. Wenzel, C. W. Clump, L. Maus and L. B. Anderson, "Principles of Unit Operations," 208-212, New York: John Wiley and Sons, Inc. (1962).

3. Hardwick, D., "Mass Transport in a Two-Dimensional Turbulent Wall Jet," Master's Thesis, The University of Tennessee, 1964.

4. Henley, E. J. and H. Bieber, "Chemical Engineering Calculations," 397, New York: McGraw-Hill Book Company, Inc. (1959).

5. Hodgman, C. D., editor, "Handbook of Chemistry and Physics," 1708, 1746, Cleveland, Ohio: Chemical Rubber Publishing Company (1959).

6. Koch, H. A., Jr., L. F. Stutzman, H. A. Blum and L. E. Hutchings, "Liquid Transfer Coefficients for the Carbon Dioxide-Air-Water System," Chem. Eng. Progress 45, 677-682 (1949).

7. "Model 76 Expanded Scale ph Meter Operation, Service, Maintenance, Beckman Instruction Manual," Beckman Instruments Inc., Fullerton, California.

8. Perry, J. H., editor, "Chemical Engineers' Handbook," 14-4, New York: McGraw-Hill Book Company, Inc. (1963).

9. "Sanborn Recorder Models 152-100B, 154-100B, Instruction Manual IM-152-100B-3," Sanborn Company, Waltham, Massachusetts.

10. Sherwood, T. K. and F. A. L. Holloway, "Performance of Packed Towers-Liquid Film Data for Several Packings," Trans. Am. Inst. Chem. Engrs. 36, 39-70 (1941).

11. Sherwood, T. K. and R. L. Pigford, "Absorption and Extraction," New York: McGraw-Hill Book Company, Inc. (1952).

APPENDICES

APPENDIX A

GAS AND LIQUID ROTAMETER CALIBRATIONS

Rotameters employed to measure carbon dioxide and high air flow rates were calibrated with a Precision wet test meter. Resulting calibration curves are shown in Figures 30 and 31. Low sweep air flows were metered with a Precision Bore Flowrator Tube, number 2A-25-A, from the F and P Company. A calibration curve for this rotameter is presented in Figure 32.

The liquid rotameter was calibrated at The Oak Ridge National Laboratory and the resulting calibration curve is shown in Figure 33.

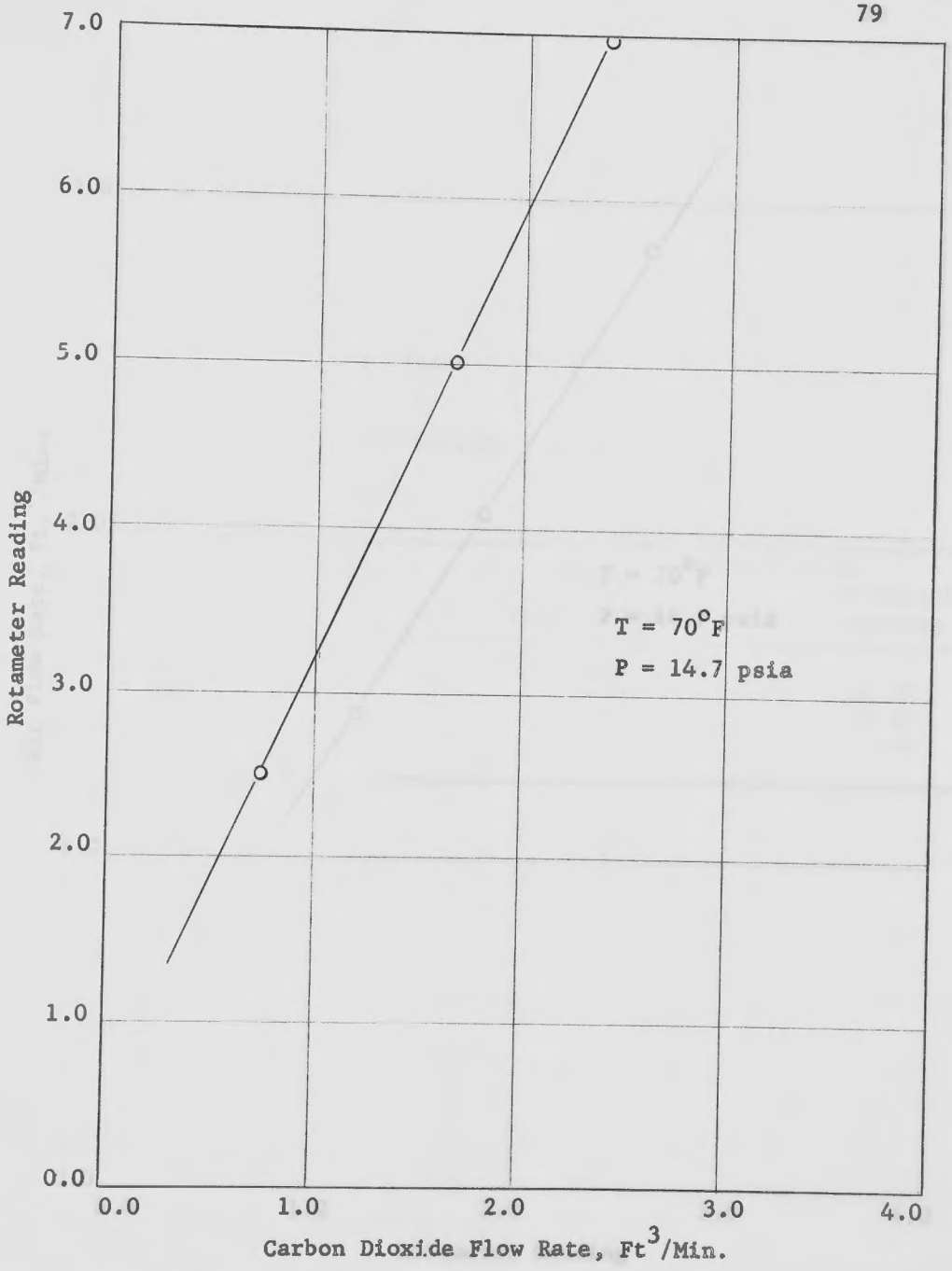

Figure 30. Rotameter Calibration for Carbon Dioxide.

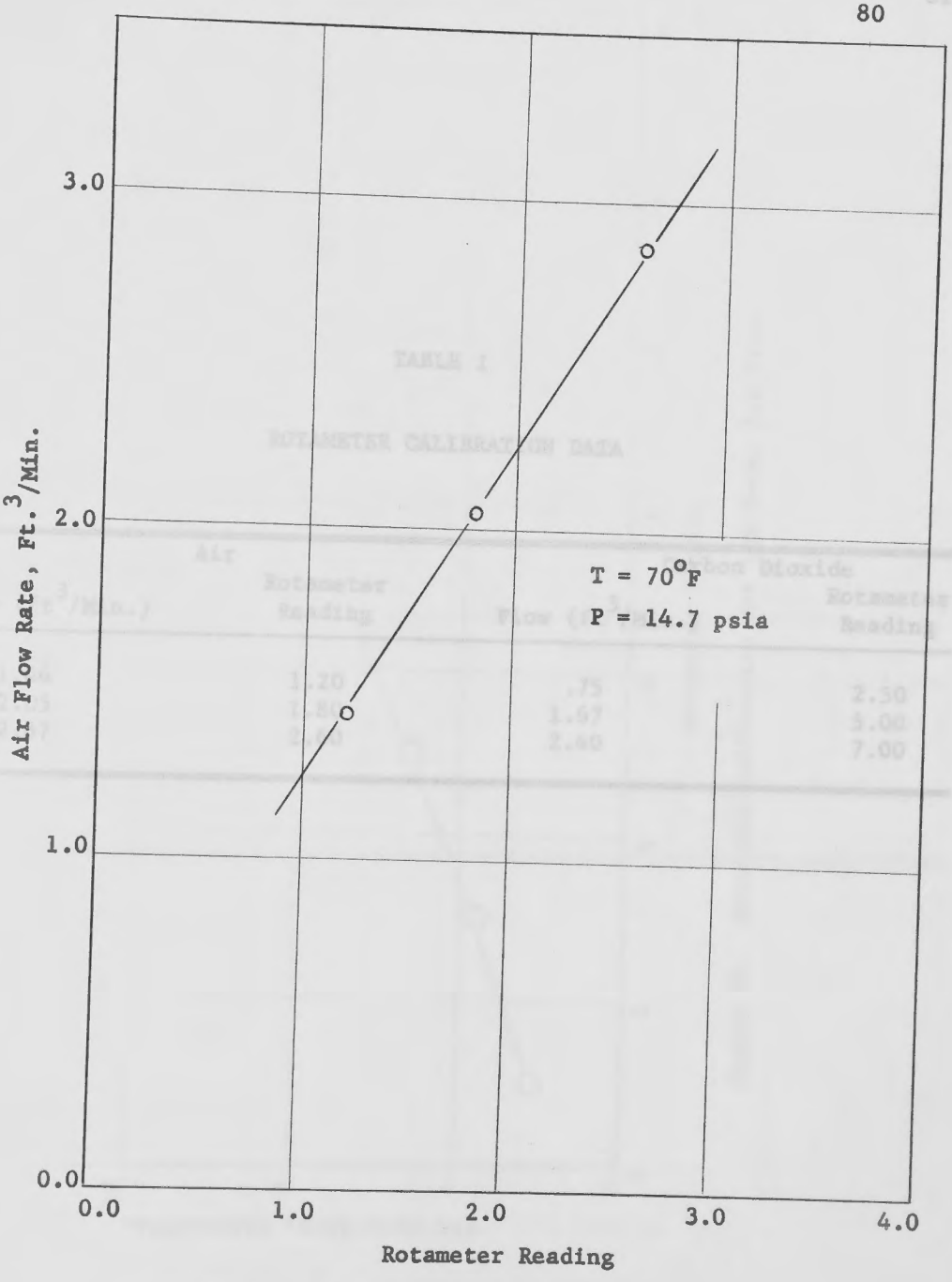

Figure 31. Rotameter Calibration for Air.

TABLE I

ROTAMETER CALIBRATION DATA

Air		Carbon Dioxide	
Flow (ft^3/Min.)	Rotameter Reading	Flow (ft^3/Min.)	Rotameter Reading
1.44	1.20	.75	2.50
2.05	1.80	1.67	5.00
2.87	2.60	2.40	7.00

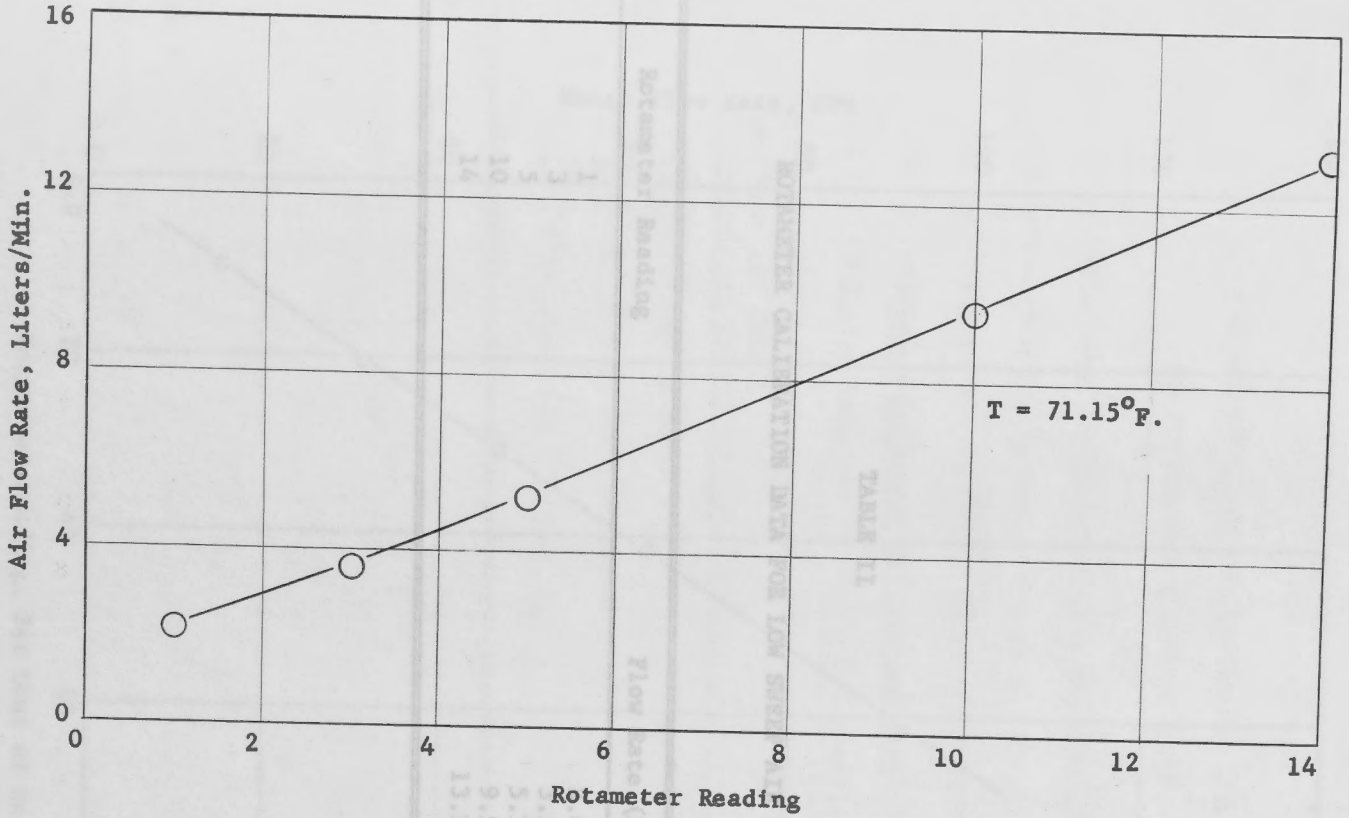

Figure 32. Rotameter Calibration for Low Sweep Air Flow.

TABLE II

ROTAMETER CALIBRATION DATA FOR LOW SWEEP AIR FLOW

Rotameter Reading	Flow Rate (Liters/Min.)
1	2.085
3	3.580
5	5.200
10	9.585
14	13.150

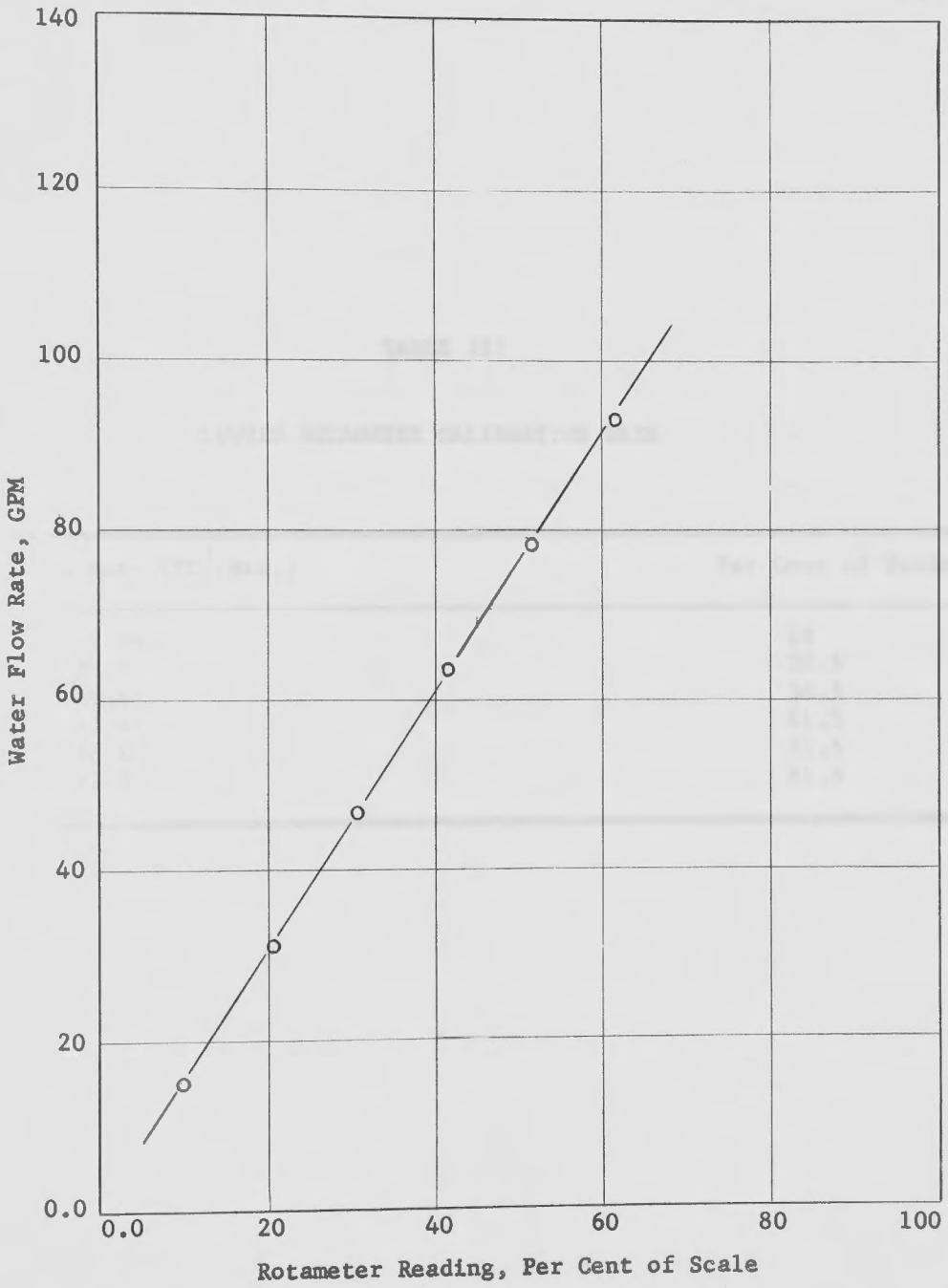

Figure 33. Rotameter Calibration for Water.

TABLE III

LIQUID ROTAMETER CALIBRATION DATA

Water Flow Rate (Ft^3/Min.)	Per Cent of Scale
15.04	10
31.0	20.5
46.8	30.5
63.4	41.5
78.1	51.5
93.0	61.5

APPENDIX B

CALIBRATION CHART FOR LIQUID AND GAS VOLUMES INSIDE THE STRIPPING TANK

The stripping tank was filled with a known weight of water to a level 11.19 inches from the bottom of the tank. Then, volumes of the liquid were taken out of the reservoir through the valve in the pump suction leg and weighed. Each successive water level was recorded on the outside of the Plexiglas tank for reference and results of these calibrations are shown in Table IV.

Corresponding gas volumes calculated from the dimensions of the tank are also presented in Table IV. The volume of baffles contained in the space above the liquid was subtracted from the total space above the liquid to determine these gas volumes.

TABLE IV

LIQUID AND GAS VOLUMES INSIDE STRIPPING TANK

Distance from Bottom of Tank, in.	V_L ft.^{3}	V_G ft.^{3}
5.50	2.196	8.223
5.81	2.350	8.069
6.12	2.517	7.902
6.44	2.686	7.733
6.75	2.860	7.559
7.12	3.035	7.384
7.38	3.198	7.221
7.69	3.371	7.048
8.00	3.536	6.883
8.34	3.700	6.719
8.62	3.859	6.560
8.88	4.018	6.401
9.31	4.235	6.184
9.94	4.579	5.840
10.56	4.916	5.503
11.19	5.252	5.167

APPENDIX C

SAMPLE CALCULATIONS

Computer Programs for Determination of Theoretical Concentration Data

Theoretical solutions of equations of carbon dioxide liquid concentration as a function of stripping time were obtained by programming the equations on an IBM 1620 digital computer. Fortran programs used for theoretical compilation are presented in Table V for the small spray ring system and Table VI for the large spray ring system. Concentrations were obtained from these programmed equations in logarithmic form.

Values of the mass transfer coefficient, TKLA (K), were chosen by first solving the equations in an approximate manner for two parameter values which clearly constituted an upper and lower bound to the "best fit" of experimental data. Computer input values for the mass transfer coefficient were obtained by adding 0.1 to this lower bound until the upper bound was attained. An error statement, which is the difference between the logarithmic theoretical concentration, VAR (I), and the logarithmic experimental concentration, YEXPT (I), at a certain stripping time, was inserted in the programs to facilitate determination of the correct parameter. For this reason theoretical stripping times were the same as experimental stripping times.

Preliminary Liquid Concentration Calculations for the Small Spray Ring System

To determine an upper and lower bound for the over-all stripping

TABLE V

FORTRAN PROGRAM FOR LIQUID DATA EMPLOYING THE SMALL SPRAY RING

```
      DIMENSION TAL(30),YTHEO(30),TKLA(15),YEXPT(30),
     1ERROR(30),VAR(30)
   50 READ 2,M,M1
      READ 1,(TAL(I),I=1,M),(YEXPT(I),I=1,M),
     1(TKLA(K),K=1,M1)
      READ 4,QL,H1,VL,QG,VS,Z2
    2 FORMAT(2I3)
    1 FORMAT(10F8.3)
    4 FORMAT(6F10.5)
      DO 40 K=1,M1
      X=TKLA(K)*VS*(1.0-H1*QL/QG)
      R=1.0-(1.0/EXPF(X/QL))*H1*QL/QG
      B=(1.0/EXPF(X/QL))*(1.0-H1*QL/QG)/R -1.0
      DO 10 I=1,M
      YTHEO(I)=EXPF(QL*B*TAL(I)/VL)*(1.0-Z2)+Z2
      VAR(I)=LOGF(YTHEO(I))/2.3026
      ERROR(I)=YEXPT(I)-VAR(I)
   10 PUNCH 30,I,TAL(I),YTHEO(I),VAR(I),ERROR(I)
   30 FORMAT (1X,I3,4(F15.5,1X))
   40 CONTINUE
      GO TO 50
      END
```

TABLE VI

FORTRAN PROGRAM FOR LIQUID DATA EMPLOYING THE LARGE SPRAY RING

```
      DIMENSION TAL(30),YTHEO(30),TKLA(15),YEXPT(30),
     1ERROR(30),VAR(30)
   50 READ 2,M,M1
      READ 1,(TAL(I),I=1,M),(YEXPT(I),I=1,M),
     1(TKLA(K),K=1,M1)
      READ 4,QL,H1,VL,QG,VG,Z2
    2 FORMAT(2I3)
    1 FORMAT(10F8.3)
    4 FORMAT(6F10.5)
      DO 40 K=1,M1
      A=1.0-EXPF(((-VG+.8463)/QL)*TKLA(K))
      ALPHAT=(QG/QL)*(VL/VG)
      ALPHAV=VL/VG
      RM1=A+ALPHAT+ALPHAV*H1*A
      RM2=A*ALPHAT
      R1=-RM1/2.0+(0.5)*SQRTF(RM1**2-4.0*RM2)
      R2=-RM1/2.0-(0.5)*SQRTF(RM1**2-4.0*RM2)
      C1=1.0/(ALPHAV*A*H1)
      C2=ALPHAT/(ALPHAV*A*H1)+1.0
      C3=R2*(1.0-Z2)-ALPHAT*(Z2-1.0)
      C4=ALPHAT*(Z2-1.0)-R1*(1.0-Z2)
      C5=R2-R1
      CONS1=(C3/C5)*(C1*R1+C2)
      CONS2=(C4/C5)*(C1*R2+C2)
      DO 10 I=1,M
      YTHEO(I)=CONS1*EXPF(R1*TAL(I))+CONS2*EXPF(R2*TAL(I))+Z2
      VAR(I)=LOGF(YTHEO(I))/2.3026
      ERROR(I)=YEXPT(I)-VAR(I)
   10 PUNCH 30,I,TAL(I),YTHEO(I),VAR(I),ERROR(I)
   30 FORMAT (1X,I3,4(F15.5,1X))
   40 CONTINUE
      GO TO 50
      END
```

coefficient, preliminary calculations were made for each run. One of these runs will be reproduced to present the calculation procedure employed.

The system temperature was obtained by averaging the initial and final temperatures of the test water. For this run T_{avg} was $74^{\circ}F$.

The value of Henry's law constant for $T = 74^{\circ}F$. is according to Perry (8):

$$H = 1.565 \times 10^{3} \text{ atm/mole fraction.}$$

After conversion to workable units:

$$H = 30.81 \text{ atm-liter/gmole.}$$

The ideal gas law constant in desired units is:

$$R = .04557 \text{ atm-liters/gmole-}^{\circ}R .$$

The liquid flow rate measured 34.2 GPM and was multiplied by 0.13368 $ft.^3$/gal. to obtain:

$$Q_L = 4.572 \text{ ft.}^3\text{/min.}$$

The liquid volume, V_L, was obtained from Table IV and was 4.018 $ft.^3$ The volume of the stripping section, $V_s = A \cdot L$, was the annular cross-sectional area of the spray chamber times the length of stripping, which was the vertical distance from holes in the sprinkler head to the water level inside the inner pool. Therefore,

$$V_s = 2.40 \text{ ft.}^2 \times .57 \text{ ft} = 1.368 \text{ ft.}^3$$

Other physical parameters include the sweep air flow rate, Q_G = 3 $ft.^3$/min., and the final normalized liquid concentration, C_{LF}/C_{L10} = .00009 gmoles/liter. Theoretical values of $Y = C_{L1}/C_{L10}$ were obtained by substituting these measured quantities into equation (15) and solving the equation for a range of stripping times in minutes with the mass transfer

coefficient as parameter.

Preliminary Liquid Concentration Calculations for the Large Spray Ring System

The only additional term needed for these calculations, that was not explained above, is the volume of the outer gas pool, $\bar{V}$, which was the stripping volume for these runs. This volume was determined by subtracting the volume of the inner gas pool, .8463 $ft.^3$, from the total gas volume obtained from Table IV.

Experimental Liquid Concentration Calculations

Experimental carbon dioxide concentrations in water were determined in the following manner. The measured ph value was converted to concentration of hydrogen ions, $[H^+]$, with the relationship:

$$[H^+] = 10^{-ph} .$$

Values of the first dissociation constant, K_1, of carbonic acid were obtained from the Handbook of Physics and Chemistry (5) and were chosen depending on the average water temperature. For $T_{avg} = 76^{\circ}F.$:

$$K_1 = 4.45 \times 10^{-7} .$$

Assuming that the concentration of hydrogen ions and bicarbonate ions were equal in solution, we can set up the following equilibrium relationship:

$$K_1 = \frac{[H^+] [H^+]}{[H_2CO_3]}$$

where:

$[H_2CO_3]$ = the amount of undissociated carbonic acid in solution, C-$[H^+]$, gmoles/liter.

and

C = total molar concentration of carbonic acid.

Therefore,

$$4.45 \times 10^{-7} = \frac{[H^+]^2}{C - [H^+]}$$

which can be solved for C to give:

$$C = \frac{[H^+]^2}{4.45 \times 10^{-7}} + [H^+] .$$

For a ph of 4.50:

$$[H^+] = 3.162 \times 10^{-5} \text{ gmoles/liter.}$$

Solving for C, the concentration of carbon dioxide dissolved in water as carbonic acid, we obtain:

$$C = 2.278 \times 10^{-3} \text{ gmoles/liter.}$$

Experimental Carbon Dioxide Concentrations in the Exit Gas Stream

Volume per cents of carbon dioxide contained in the exit gas stream were determined experimentally with a previously calibrated thermal conductivity gas analyzer. Conversion to C_{G1} involved multiplying volume per cent by the molecular weight and density of carbon dioxide at the system temperature.

For example, the density of carbon dioxide at 74°F. is 1.8214 grams/liter. A 25 volume per cent measurement of carbon dioxide in the exit gas stream would correspond to the following value of C_{G1}:

$$C_{G1} = .25 \times 1.8214 \times 1/44 = 0.0134 \text{ gmoles/liter.}$$

APPENDIX D

EXPERIMENTAL LIQUID AND GAS CONCENTRATION DATA

Table VII presents experimental runs with packing. Concentration data obtained by having air initially above the liquid pool is presented in Tables VIII through X. Liquid concentration data determined by initially saturating the water reservoir with a 25 per cent carbon dioxide - 75 per cent air mixture is presented in Table VIII and Tables XI and XII. Experimental liquid stripping data for the low gas flow investigation are presented in Table XIII.

Experimental gas concentration data corresponding to the liquid data already presented is shown in Tables XIV through XVIII.

Table XIX presents values of the stripping rate coefficient determined at each liquid flow rate for both liquid-gas contacting systems.

TABLE VII

LIQUID CONCENTRATIONS DURING STRIPPING

ph	Time (Min.)	$\frac{C_{L1}}{C_{L10}}$	ph	Time (Min.)	$\frac{C_{L1}}{C_{L10}}$
4.17	0	1.000	4.41	0	1.000
4.24	1.5	.727	4.42	1	.957
4.33	3	.481	4.49	2.5	.694
4.51	5	.2115	4.58	4	.459
4.72	8	.0824	4.67	6	.334
4.86	10	.0436	4.76	8	.202
5.01	12	.0218	4.83	10	.147
5.24	15	.00781	5.01	14	.0652
5.48	18	.00273	5.12	18	.0399
5.71	21	.00102	5.21	22	.0267
6.01	25	.000304	5.37	28	.0131
6.29	30	.000108	5.49	32.5	.00779
6.45	35	.0000625	5.60	37	.00487
6.52	40	.0000496	5.72	42	.00294
6.55	45	.0000450	5.90	47	.00141
6.59	50	.0000398	6.01	52	.000911
			6.21	58	.000430
			6.31	63	.000302
			6.33	67	.000281
			6.38	72	.000236
			6.42	77	.000206
			6.43	83	.000200

Q_L = 34.2 GPM, Q_G = 3 CFM

T_{avg} = 79°F

Small Spray Ring,

Air Initially Above Water,

5/8" Raschig Rings in Stripping Section.

C_{L10} = .01015 Gmoles/Liter

Run 20

Q_L = 34.2 GPM, Q_G = 3 CFM

T_{avg} = 79°F

Small Spray Ring,

25% CO_2 - 75% Air Mixture

Above Water Initially,

5/8" Raschig Rings in Stripping Section.

C_{L10} = .00339 Gmoles/Liter

Run 26

TABLE VIII

LIQUID CONCENTRATIONS DURING STRIPPING

ph	Time (Min.)	C_{L1}/C_{L10}	ph	Time (Min.)	C_{L1}/C_{L10}
4.44	0	1.000	4.21	0	1.000
4.49	2	.795	4.31	2.5	.630
4.61	4.25	.459	4.41	5	.398
4.72	6.5	.278	4.51	7	.252
4.85	9	.154	4.62	9	.165
5.01	12	.0748	4.79	12	.0704
5.18	15	.0349	4.93	15	.0373
5.39	20	.0138	5.11	18	.0166
5.69	25	.00381	5.28	21	.00778
5.91	30	.00154	5.51	25	.00284
6.11	35	.000710	5.84	30	.000710
6.28	40	.000381	6.06	36	.000298
6.33	45	.000319	6.21	40	.000170
6.40	51	.000251	6.29	45	.000127
6.40	56	.000251	6.33	50	.000111
6.43	60	.000227	6.38	55	.0000933
			6.39	60	.0000900

Q_L = 34 GPM, Q_G = 3 CFM
T_{avg} = 76°F
25% CO_2 - 75% Air Mixture
Initially Above Water,
Small Spray Ring.
C_{L10} = .00300 Gmoles/Liter
Run 31

Q_L = 34.2 GPM, Q_G = 3 CFM
T_{avg} = 74°F
Air Initially Above Water,
Small Spray Ring.
C_{L10} = .00870 Gmoles/Liter
Run 34

TABLE IX

LIQUID CONCENTRATIONS DURING STRIPPING

ph	Time (Min.)	C_{L1}/C_{L10}	ph	Time (Min.)	C_{L1}/C_{L10}
4.17	0	1.000	4.12	0	1.000
4.19	2.5	.910	4.21	4.25	.663
4.23	5	.759	4.31	6	.418
4.31	8	.525	4.63	11.25	.0966
4.41	12	.332	4.84	15	.0372
4.50	15	.220	5.02	18	.0165
4.56	18	.168	5.45	24	.00245
4.63	21	.122	5.64	27	.00109
4.77	25	.0650	5.83	30	.000492
4.92	30.5	.0326	6.11	35	.000164
5.09	35	.0151	6.37	40	.0000646
5.29	41	.00620	6.48	45	.0000447
5.41	45	.00366	6.58	50	.0000324
5.53	50	.00218	6.62	55	.0000283
5.69	55	.00111	6.65	60	.0000261
5.84	60	.000593			
5.95	65	.000382			
6.09	70	.000222			
6.18	75	.000159			
6.27	80	.000115			
6.32	85	.0000960			
6.37	90	.0000808			
6.41	95	.0000714			
6.44	100	.0000636			

Q_L = 15 GPM, Q_G = 3 CFM
T_{avg} = 76°F
Air Initially Above Water,
Small Spray Ring.
C_{L10} = .01036 Gmoles/Liter
Run 36

Q_L = 35 GPM, Q_G = 3 CFM
T_{avg} = 78.5°F
Air Initially Above Water,
Large Spray Ring.
C_{L10} = .01288 Gmoles/Liter
Run 38

TABLE X

LIQUID CONCENTRATION DURING STRIPPING

ph	Time (Min.)	C_{L1}/C_{L10}	ph	Time (Min.)	C_{L1}/C_{L10}
4.20	0	1.000	4.20	0	1.000
4.31	1.75	.615	4.22	1	.912
4.70	5.25	.102	4.42	3	.365
5.08	8	.0182	4.61	5	.153
5.27	11	.00779	4.91	8	.0391
5.52	14	.00261	5.13	11	.0145
5.72	17	.00112	5.47	15	.00324
5.94	20	.00456	5.70	18	.00121
6.12	24	.000228	5.86	21	.000628
6.24	28	.000147	6.03	25	.000321
6.27	32	.000132	6.14	30	.000211
6.29	36	.000123	6.17	35	.000189
6.30	40	.000118	6.18	40	.000182

Q_L = 64 GPM, Q_G = 3 CFM
T_{avg} = 76.5°F
Small Spray Ring,
Air Initially Above Water.
C_{L10} = .00899 Gmoles/Liter
Run 47

Q_L = 46 GPM, Q_G = 3 CFM
T_{avg} = 75.5°F
Small Spray Ring,
Air Initially Above Water.
C_{L10} = .00903 Gmoles/Liter
Run 48

TABLE XI

LIQUID CONCENTRATION DURING STRIPPING

ph	Time (Min.)	C_{L1}/C_{L10}	ph	Time (Min.)	C_{L1}/C_{L10}
4.47	0	1.000	4.44	0	1.000
4.47	2	1.000	4.46	2	.909
4.52	5	.797	4.57	4	.551
4.62	8	.504	4.71	7	.291
4.72	11	.358	4.99	11	.0815
4.86	15	.169	5.13	14	.0435
4.97	18	.103	5.33	17	.0179
5.06	21	.0686	5.59	21	.00579
5.21	25	.0351	5.82	25	.00221
5.39	30	.0158	6.09	30	.000763
5.55	35	.00791	6.32	35	.000330
5.72	40	.00385	6.49	41	.000185
5.90	45	.00185	6.60	45	.000130
6.02	50	.00115	6.63	50	.000119
6.22	55	.000544	6.69	55	.0000984
6.32	60	.000381	6.70	60	.0000955
6.43	65	.000261			
6.54	70	.000182			
6.61	75	.000146			
6.64	80	.000133			
6.71	85	.000108			

Q_L = 15 GPM, Q_G = 3 CFM
T_{avg} = 77°F.
25% CO_2 - 75% Air Mixture
Initially Above Water,
Large Spray Ring.
C_{L10} = .00260 Gmoles/Liter
Run 40

Q_L = 34.3 GPM, Q_G = 3 CFM
T_{avg} = 75°F.
25% CO_2 - 75% Air Mixture
Initially Above Water,
Large Spray Ring.
C_{L10} = .00303 Gmoles/Liter
Run 42

TABLE XII

LIQUID CONCENTRATION DURING STRIPPING

ph	Time (Min.)	C_{L1}/C_{L10}	ph	Time (Min.)	C_{L1}/C_{L10}
4.45	0	1.000	4.41	0	1.000
4.45	.33	1.000	4.41	.33	1.000
4.52	2	.726	4.48	2	.726
4.66	4	.383	4.59	4	.439
4.82	6	.185	4.69	6	.278
5.01	8	.0784	4.91	10	.102
5.28	11	.0235	5.12	13	.0398
5.55	14	.00723	5.37	17	.0131
5.82	17	.00234	5.58	20	.00528
6.08	20	.000839	5.83	25	.00186
6.23	23	.000481	6.07	30	.000721
6.34	26	.000326	6.19	35	.000540
6.42	30	.000249	6.23	40	.000398
6.49	35	.000197	6.31	47	.000299
6.50	40	.000191			

Q_L = 64 GPM, Q_G = 3 CFM
T_{avg} = 80°F
Large Spray Ring,
25% CO_2-75% Air Mixture
Above Water Initially.
C_{L10} = .00281 Gmoles/Liter
Run 44

Q_L = 47 GPM, Q_G = 3 CFM
T_{avg} = 76°F
Large Spray Ring,
25% CO_2-75% Air Mixture
Above Water Initially.
C_{L10} = .00344 Gmoles/Liter
Run 45

TABLE XIII

LIQUID CONCENTRATION DURING STRIPPING

ph	Time (Min.)	C_{L1}/C_{L10}	ph	Time (Min.)	C_{L1}/C_{L10}
4.44	0	1.000	4.20	0	1.000
4.46	3	.913	4.21	5	.955
4.50	10	.760	4.34	2	.526
4.61	17	.460	4.39	5	.418
4.62	23	.439	4.46	10	.303
4.71	29	.292	4.51	15	.242
4.75	36	.243	4.57	20	.184
4.85	43	.154	4.66	30	.122
4.90	48	.123	4.74	41	.0846
4.97	55	.0897	4.81	50	.0616
5.11	72	.0477	4.92	60	.0374
5.20	80	.0320	5.07	71	.0190
5.30	90	.0205	5.13	80	.0145
5.41	100	.0126	5.33	95	.00598
5.51	110	.00819	5.44	105	.00369
5.61	120	.00534	5.61	118	.00178
5.75	130	.00296	5.75	132	.000987
5.85	140	.00197	5.85	145	.000655
5.95	150	.00132	5.97	160	.000406
6.02	160	.00100	6.06	170	.000286
6.07	170	.000827	6.09	180	.000255
6.11	180	.000710	6.11	187	.000237
6.14	190	.000635			

Q_L = 64 GPM, Q_G = 10 Liters/Min.
T_{avg} = 76°F
Large Spray Ring,
25% CO_2 - 75% Air Mixture
Initially Above Water.
C_{L10} = .00300 Gmoles/Liter
Run 46

Q_L = 64 GPM, Q_G = 10 Liters/Min.
T_{avg} = 77°F
Small Spray Ring,
Air Initially Above Water.
C_{L10} = .00897 Gmoles/Liter
Run 49

TABLE XIV

EXIT GAS CONCENTRATIONS DURING STRIPPING

Time (Min.)	Volume % CO_2	Time (Min.)	Volume % CO_2
3	15	6	7.1
5	12	8	6.2
8	10	15	2.7
9	9	23	1.8
13	3		
19	9		
24	0		

Q_L = 34.2 GPM, Q_G = 3 CFM
T_{avg} = 74°F
Small Spray Ring,
Air Initially Above Liquid.
Run 34

Q_L = 15 GPM, Q_G = 3 CFM
T_{avg} = 76°F
Small Spray Ring,
Air Initially Above Liquid.
Run 36

TABLE XV

EXIT GAS CONCENTRATIONS DURING STRIPPING

Time (Min.)	Volume % CO_2	Time (Min.)	Volume % CO_2
0	25	0	25
1	18.7	1	16.7
2	12.5	4	3.5
3	6.8	9	1.4
5	3.1	10	0.8
8	1.6		
Q_L = 15 GPM, Q_G = 3 CFM		Q_L = 34.3 GPM, Q_G = 3 CFM	
T_{avg} = 77°F		T_{avg} = 75°F	
Large Spray Ring,		Large Spray Ring,	
25% CO_2-75% Air Mixture		25% CO_2-75% Air Mixture	
Initially Above Water.		Initially Above Water.	
Run 40		Run 42	

TABLE XVI

EXIT GAS CONCENTRATIONS DURING STRIPPING

Time (Min.)	Volume % CO_2	Time (Min.)	Volume % CO_2
1	20.8	1	16.6
2	18.1	3	15.0
3	15.3	6	6.7
4	13.7	9	3.2
6	7.6	13	0.8
9	1.4		
Q_L = 64 GPM, Q_G = 3 CFM T_{avg} = 76.5°F Small Spray Ring, Air Initially Above Water. Run 47		Q_L = 46 GPM, Q_G = 3 CFM T_{avg} = 75.5°F Small Spray Ring, Air Initially Above Water. Run 48	

TABLE XVII

EXIT GAS CONCENTRATIONS DURING STRIPPING

Time (Min.)	Volume % CO_2	Time (Min.)	Volume % CO_2
0	25	0	25
1	14.1	1	16.3
2	8.7	2	8.8
3	4.9	3	5.6
6	2.2	6	3.1
9	.98	7	1.9
Q_L = 64 GPM, Q_G = 3 CFM		Q_L = 47 GPM, Q_G = 3 CFM	
T_{avg} = 80°F		T_{avg} = 76°F	
Large Spray Ring,		Large Spray Ring,	
25% CO_2-75% Air Mixture		25% CO_2-75% Air Mixture	
Above Water Initially		Above Water Initially	
Run 44		Run 45	

TABLE XVIII

EXIT GAS CONCENTRATIONS DURING STRIPPING

Time (Min.)	Volume % CO_2	Time (Min.)	Volume % CO_2
0	25	1	23.7
1	23.7	2	26.3
3	22.4	4	28.9
6	21.7	6	26.3
10	17.8	8	23.0
13	14.5	13	15.8
19	8.5	20	10.5
25	7.2	25	7.2
34	5.3	28	6.8
		32	6.4
		37	5.3
		45	3.9
		53	2.4
		62	1.3

Q_L = 64 GPM, Q_G = 10 Liters/Min.
T_{avg} = 76°F
Large Spray Ring,
25% CO_2-75% Air Mixture
Initially Above Water.
Run 46

Q_L = 64 GPM, Q_G = 10 Liters/Min.
T_{avg} = 77°F
Small Spray Ring,
Air Initially Above Water.
Run 49

TABLE XIX

VARIATION OF THE OVER-ALL LIQUID-PHASE STRIPPING COEFFICIENT WITH LIQUID FLOW RATE

Q_L (GPM)	K_La (1/Min.)	$1/Q_L$	$1/K_La$
	Small Spray Ring System		
15	.45	.0667	2.222
34.2	.90	.0292	1.111
46	1.65	.0217	.606
64	1.85	.0156	.541
	Large Spray Ring System		
15	.19	.0667	5.263
34.3	.65	.0292	1.539
47	1.0	.0213	1.0

LIST OF SYMBOLS

LIST OF SYMBOLS

a - specific surface for mass transfer in spray chamber, $ft.^2/ft.^3$

A - cross-sectional area for mass transfer in spray chamber, $ft.^2$

A_1 - $1 - e^{-N_1}$

A_s - superficial area of liquid pool surface that is available for mass transfer, $ft.^2$

B - $e^{-N/Q_L}\left(\frac{1 + \frac{R\,T_{avg}}{H}\,\frac{Q_L}{Q_G}}{1 + e^{-N/Q_L}\,\frac{R\,T_{avg}}{H}\,\frac{Q_L}{Q_G}}\right) - 1$

C_G - carbon dioxide concentration in the gas stream flowing in the liquid-gas contacting section, gmoles/liter

$\overline{C}_G$ - concentration of carbon dioxide in outer gas pool for the small spray ring system, gmoles/liter

C_{Gi} - carbon dioxide interfacial concentration in the gas phase, gmoles/liter

C_{G1} - carbon dioxide concentration in sweep air stream at the gas exit of the spray chamber, gmoles/liter

C_{G2} - carbon dioxide concentration in air, gmoles/liter

C_L - carbon dioxide liquid concentration in droplets contained in the stripping section, gmoles/liter

C_{LF} - final carbon dioxide liquid concentration in equilibrium with air, gmoles/liter

C_{Li} - carbon dioxide interfacial concentration in the liquid-phase, gmoles/liter

C_{L1} - carbon dioxide concentration in the water reservoir, gmoles/liter

LIST OF SYMBOLS

a - specific surface for mass transfer in spray chamber, $ft.^2/ft.^3$

A - cross-sectional area for mass transfer in spray chamber, $ft.^2$

A_1 - $1 - e^{-N_1}$

A_s - superficial area of liquid pool surface that is available for mass transfer, $ft.^2$

B - $e^{-N/Q_L}\left(1 - \frac{R\,T_{avg}}{H}\,\frac{Q_L}{Q_G}\right) \Big/ \left(1 - e^{-N/Q_L}\,\frac{R\,T_{avg}}{H}\,\frac{Q_L}{Q_G}\right) - 1$

C_G - carbon dioxide concentration in the gas stream flowing in the liquid-gas contacting section, gmoles/liter

$\bar{C}_G$ - concentration of carbon dioxide in outer gas pool for the small spray ring system, gmoles/liter

C_{Gi} - carbon dioxide interfacial concentration in the gas phase, gmoles/liter

C_{G1} - carbon dioxide concentration in sweep air stream at the gas exit of the spray chamber, gmoles/liter

C_{G2} - carbon dioxide concentration in air, gmoles/liter

C_L - carbon dioxide liquid concentration in droplets contained in the stripping section, gmoles/liter

C_{LF} - final carbon dioxide liquid concentration in equilibrium with air, gmoles/liter

C_{Li} - carbon dioxide interfacial concentration in the liquid-phase, gmoles/liter

C_{L1} - carbon dioxide concentration in the water reservoir, gmoles/liter

C_{L10} - carbon dioxide concentration in the water reservoir at time = 0, gmoles/liter

C_{L2} - carbon dioxide concentration in the spray droplets as they return to the liquid pool, gmoles/liter

C_1, C_2 - coefficients of the exponential terms, $e^{r_1 T}$ and $e^{r_2 T}$, in the solution of the second order differential equation relating exit gas concentration to time for the large spray ring system

C_3 - $r_2 \left(1 - M_3/M_2 \right) - G_t \left(E_2 - 1 \right)$

C_4 - $G_t \left(E_2 - 1 \right) - r_1 \left(1 - M_3/M_2 \right)$

C_5 - $r_2 - r_1$

C_6 - $1/G_v A_1 H_1$

C_7 - $G_t/G_v A_1 H_1 + 1$

D - differentiation symbol

E_1 - $1/ \left(r_2 - r_1 \right)$

E_2 - $G_v A_1 H_1 \left(1 - E_2 \right)$

E_3 - $G_t/G_v A_1 H_1 + 1$

E_4 - $r_2/G_v A_1 H_1$

E_5 - $r_1/G_v A_1 H_1$

f - volume fraction of gas bubbles entrapped in the liquid pool

F - $$\frac{\left(1 - e^{-N/Q_L}\right) H_1}{1 - e^{-N/Q_L} \; H_1 \frac{Q_L}{Q_G}}$$

G_t - $Q_G/Q_L \cdot V_L/V_G$

G_v - V_L/V_G

H - Henry's law constant, atm/qmole/liter

H_1 - $R\,T_{avg}/H$

$k_G a$ - individual gas-phase mass transfer coefficient, 1/min.

$k_L a$ - individual liquid-phase mass transfer coefficient, 1/min.

$K_L a$ - over-all liquid-phase mass transfer coefficient, 1/min.

k_s - mass transfer coefficient for carbon dioxide removal from the liquid pool surface, ft./min.

K_1 - first dissociation constant of H_2CO_3

K_2 - second dissociation constant of H_2CO_3

L - length of stripping section for the small spray ring system

M_1 - $A_1 + G_t + G_v A_1 H_1$

M_2 - $A_1 G_t$

M_3 - $A_1 G_t Z_2$

n - gmoles of an ideal gas

N - $K_L a V_s \left(1 - H_1 \frac{Q_L}{Q_G}\right)$

N_1 - $K_L a\, V/Q_L$

P - partial pressure of carbon dioxide in the gas volume above the liquid pool, atm.

P_1 - $\frac{C_3}{C_5}\,(C_6 + C_7)$

P_2 - $\frac{C_4}{C_5}\,(C_6 + C_7)$

P_3 - $E_1 E_2 (E_4 + E_3)$

P_4 - $E_1 E_2 (E_5 + E_3)$

Q_G - volumetric sweep gas flow rate, $ft.^3/min.$

Q_L - volumetric liquid flow rate, $ft.^3/min.$

r_1 - $\frac{-M_1}{2} + \frac{1}{2}\sqrt{M_1^2 - 4M_2}$

r_2 - $\frac{-M_1}{2} - \frac{1}{2}\sqrt{M_1^2 - 4M_2}$

R - ideal gas law constant, atm-liters/gmole - ^{o}R

r - linear proportionality constant between $k_L a$ and Q_L, $1/ft.^3$

t - stripping time, min.

T - dimensionaless stripping time, $t\ Q_L/V_L$

T_{avg} - average stripping system temperature, $^{o}F.$

TAL - stripping time for fortran program, min. or dimensionaless depending on the spray ring system

TKLA - over-all liquid-phase mass transfer coefficient for use in the fortran programs, 1/min.

$\bar{V}$ - gaseous stripping volume for large spray ring system, $ft.^3$

$\bar{V}_1$ - volume of stagnant gas pool, outer pool, for the small spray ring system, $ft.^3$

V_G - total volume of gas space above the liquid pool, $ft.^3$

V_L - volume of liquid available for stripping, $ft.^3$

V_s - gaseous stripping volume for small spray ring system, $ft.^3$

Y - normalized carbon dioxide liquid concentration, C_{L1}/C_{L10}

YEXPT - experimental values of Log Y for use in the fortran programs which solve for Log Y as a function of stripping time

YTHEO - theoretical values of Y calculated as functions of time in the fortran programs

Z - dimensionaless carbon dioxide concentration in the sweep gas stream, $R\ T_{avg}\ C_G/HC_{L10}$

Z_2 - dimensionaless carbon dioxide concentration in the exit sweep gas at air-water equilibrium, $R\,T_{avg}\,C_{G2}/HC_{L1O}$

VITA

The author was born in Nashville, Tennessee on August 2, 1941 as the first son of Mr. and Mrs. Melburn J. Waggoner. He now has a brother, Tom, and a sister, Lucy.

After graduating from Goodlettsville High School, Goodlettsville, Tennessee in 1959, the author entered the Chemical Engineering program at Vanderbilt University. He received a Bachelor of Engineering degree in Chemical Engineering at Vanderbilt in June, 1963 and decided to continue his education at the University of Tennessee in Knoxville. The current Master of Science program was initiated in September, 1963 with financial support from the Department of Chemical and Metallurgical Engineering. In January, 1964 financial assistance was changed to a research assistantship sponsored jointly by the Engineering Mechanics Department and the Oak Ridge National Laboratory.

Upon completion of requirements for a Master of Science degree, the author plans to work with the Research and Development Laboratory in the Textile Fibers Division of E. I. DuPont de Nemours and Company in Old Hickory, Tennessee.